National Library of Canada
Bibliothèque nationale du Canada

Canadian Theses Service
Service des thèses canadiennes

Ottawa, Canada
K1A 0N4

NOTICE

The quality of this microform is heavily dependent upon the quality of the original thesis submitted for microfilming. Every effort has been made to ensure the highest quality of reproduction possible.

If pages are missing, contact the university which granted the degree.

Some pages may have indistinct print especially if the original pages were typed with a poor typewriter ribbon or if the university sent us an inferior photocopy.

Reproduction in full or in part of this microform is governed by the Canadian Copyright Act, R.S.C. 1970, c. C-30, and subsequent amendments.

AVIS

La qualité de cette microforme dépend grandement de la qualité de la thèse soumise au microfilmage. Nous avons tout fait pour assurer une qualité supérieure de reproduction.

S'il manque des pages, veuillez communiquer avec l'université qui a conféré le grade.

La qualité d'impression de certaines pages peut laisser à désirer, surtout si les pages originales ont été dactylographiées à l'aide d'un ruban usé ou si l'université nous a fait parvenir une photocopie de qualité inférieure.

La reproduction, même partielle, de cette microforme est soumise à la Loi canadienne sur le droit d'auteur, SRC 1970, c. C-30, et ses amendements subséquents.

NL-339 (r. 88/04) c

Canada

National Library of Canada
Bibliothèque nationale du Canada

Canadian Theses Service
Service des thèses canadiennes

Ottawa, Canada
K1A 0N4

The author has granted an irrevocable non-exclusive licence allowing the National Library of Canada to reproduce, loan, distribute or sell copies of his/her thesis by any means and in any form or format, making this thesis available to interested persons.

L'auteur a accordé une licence irrévocable et non exclusive permettant à la Bibliothèque nationale du Canada de reproduire, prêter, distribuer ou vendre des copies de sa thèse de quelque manière et sous quelque forme que ce soit pour mettre des exemplaires de cette thèse à la disposition des personnes intéressées.

The author retains ownership of the copyright in his/her thesis. Neither the thesis nor substantial extracts from it may be printed or otherwise reproduced without his/her permission.

L'auteur conserve la propriété du droit d'auteur qui protège sa thèse. Ni la thèse ni des extraits substantiels de celle-ci ne doivent être imprimés ou autrement reproduits sans son autorisation.

ISBN 0-315-55372-3

Canada

THE UNIVERSITY OF ALBERTA

AN EXPERIMENTAL AND NUMERICAL INVESTIGATION OF THE GROWTH OF SALINE ICICLES

by

(VICTOR) KWOK KEUNG CHUNG

(C)

A THESIS

SUBMITTED TO THE FACULTY OF GRADUATE STUDIES AND RESEARCH

IN PARTIAL FULFILMENT OF THE REQUIREMENTS FOR THE DEGREE

OF MASTER OF SCIENCE

IN

METEOROLOGY

DEPARTMENT OF GEOGRAPHY

EDMONTON, ALBERTA

FALL, 1989

THE UNIVERSITY OF ALBERTA

RELEASE FORM

NAME OF AUTHOR (VICTOR) KWOK KEUNG CHUNG

TITLE OF THESIS AN EXPERIMENTAL AND NUMERICAL INVESTIGATION OF THE GROWTH OF SALINE ICICLES

DEGREE FOR WHICH THESIS WAS PRESENTED MASTER OF SCIENCE

YEAR THIS DEGREE GRANTED FALL, 1989

Permission is hereby granted to THE UNIVERSITY OF ALBERTA LIBRARY to reproduce single copies of this thesis and to lend or sell such copies for private, scholarly or scientific research purposes only.

The author reserves other publication rights, and neither the thesis nor extensive extracts from it may be printed or otherwise reproduced without the author's written permission.

(SIGNED) Victor Kwok Keung Chung

PERMANENT ADDRESS:

5th Floor, 136

Shaukiwan Road

Hong Kong

DATED 4th Aug. 1989

THE UNIVERSITY OF ALBERTA

FACULTY OF GRADUATE STUDIES AND RESEARCH

The undersigned certify that they have read, and recommend to the Faculty of Graduate Studies and Research, for acceptance, a thesis entitled AN EXPERIMENTAL AND NUMERICAL INVESTIGATION OF THE GROWTH OF SALINE ICICLES submitted by (VICTOR) KWOK KEUNG CHUNG in partial fulfilment of the requirements for the degree of MASTER OF SCIENCE in METEOROLOGY.

J. R. Wilson for E. P. Lozowski

Supervisor

J. R. Wilson

Date 4th Aug. 1989

Abstract

The objective of this research is to develop a mathematical model to simulate the growth of pure and saline icicles. The growth mechanism of a pure icicle and the mathematical model developed by Makkonen (1988) to simulate its growth are first reviewed. Then, they are modified, extended, and applied to the growth mechanism of saline icicles. Finally, with the use of a finite element time step method, a mathematical model is developed to simulate the growth of saline icicles. This model can also be used to predict the growth of pure icicles. Some of the characteristics of the model are discussed. It is found that the model is very sensitive to the air temperature and wind speed, but insensitive to the relative humidity and air pressure. For the case of saline icicle growth, the model is sensitive to the supply rate, but, for the case of pure icicle growth, the model is insensitive to the supply rate, as far as the maximum length growth rate is concerned. Two sets of experiments with a temperature range from -7 °C to -15 °C and wind speed from 0.6 m/s to 0.7 m/s were performed in a coldroom in the Divison of Meteorology at the University of Alberta. The first set of experiments was performed to grow pure icicles while the second set of experiments was performed to grow saline icicles. The model's predictions were then compared with the results of these two sets of experiments, and the performance of the model was evaluated. It was found that the model generally overpredicts the icing rates, especially for the case of pure icicles. The growth termination time is generally underestimated. In addition, the model's predictions of the length, length growth rate, mean diameter, and mass do not agree with the experiments very well. However, the model does seem to give a good qualitative description of what is going on in nature for the growth of both pure and saline icicles. The model successfully predicts that the length growth rate of saline icicles will eventually stop, even with a continuous supply of brine to the tip.

Acknowledgements

Warm thanks to Dr. E.P. Lozowski for his supervision of this research, his encouragement and invaluable suggestions.

The author also gives thanks to J.D. Wilson and R. Gerard, who served on my examination committe.

Special thanks to Mr. Terry Thompson, who kindly prepared the coldroom and apparatus for the experiments, and to Lok Yan for his help with some of the coldroom experiments.

Table of Contents

Chapter		Page
1.	Introduction	1
2.	A review of pure icicle growth	5
	2.1 Growth mechanism of a pure icicle	5
	2.2 Growth in length	8
	2.3 Growth in diameter	15
3.	A qualitative description of the growth of a saline icicle	17
	3.1 Brine pockets	17
	3.2 Growth rate of a saline icicle	19
4.	A mathematical investigation of the growth of a saline icicle	22
	4.1 Introduction to the finite element time step method	22
	4.2 The effect of salinity on the thermodynamic properties	24
	4.3 Growth rate in diameter	31
	4.4 Growth rate in length	34
	4.5 Growth in mass	37
	4.6 Drip rate	38
	4.7 Discussion of assumptions	39
	4.7.1 Homogeneous liquid film thickness	39
	4.7.2 Circular cross section	39
	4.7.3 Vertical heat conduction	40
5.	Model implementation	41
6.	Model predictions	50
	6.1 Sensitivity of the model	50
	6.2 Model prediction of icicle length and growth rate	52
	6.3 Model prediction of diameter variation with length	53
	6.4 Predicted growth in mass	54
7.	Icicle growth experiments	67

7.1 Pure icicle growth experiments 68
7.1.1 Temperature and flowrate of the water supply 68
7.1.2 Air temperature, wind speed, relative humidity, and air pressure 70
7.1.3 Length of the pure icicle 73
7.1.4 Diameter of the pure icicle 73
7.1.5 Drip rate, mass of the pure icicle, and supply rate 73
7.2 Saline icicle growth experiments 74
7.3 Qualitative observations 75
7.3.1 Pure icicles 75
7.3.2 Saline icicles 78
8. Results and discussion 81
8.1 Length 82
8.2 Length growth rate 85
8.3 Length growth rate versus drip rate 87
8.4 Mean diameter and mass 89
9. Summary, discussion, and recommendations 140
9.1 Summary and discussion 140
9.2 Recommendations 141
Bibliography 143
Appendix A Calculation of the heat-transfer coefficient for the cylindrical sections of the icicle 146
Appendix B Calculation of the heat-transfer coefficient for the tip of the icicle 148
Appendix C A Fortran program to compute the growth of a pure or saline icicle. 149
Appendix D The experimental results of pure and saline icicle growth for thirteen different cases 158
Appendix E Calibration of the salinometer 171

List of Tables

Table		Page
5.1.	Pendant drop size for a pure icicle grown in an independent experiment	43
5.2.	The salinities of the pendant drops for various air conditions	48
7.1.2.	The measured wind speed at different heights	71
8.1.1.	Model and experiment growth termination time difference	83
8.1.2.	Final length of the pure and saline icicles	86
8.2.1.	Average length growth rates of pure and saline icicles	88
8.4.1.	Pure icicle mean diameter	90
8.4.2.	Saline icicle mean diameter	91
8.4.3.	Pure icicle mass	92
8.4.4.	Saline icicle mass	93
8.4.5.	A summary of the model and experimental results of pure and saline icicles growth	96

List of Figures

Figure		Page
1.1.	A simple sketch of a saline icicle	3
1.2.	Laboratory simulated saline icicles	4
2.1.	A schematic diagram of a pure icicle	7
3.1.1.	A schematic illustration of the formation of brine prockets	18
3.2.1.	Laboratory simulated pure and saline icicles	21
4.1.1.	A schematic illustration of the time step method	23
4.2.1.	A cylindrical section of a saline icicle	24
5.1.	Schematic illustration of how the simulation proceeds	42
5.2.	Schematic description of how a pendant drop falls	45
6.1.1.	The maximum length growth rate vs air temperature for both pure and saline icicle growth	55
6.1.2	The maximum length growth rate vs wind speed for both pure and saline icicle growth	56
6.1.3.	The maximum length growth rate vs relative humidity for both pure and saline growth	57
6.1.4.	The maximum length growth rate vs air pressure for both pure and saline icicle growth	58
6.1.5	The maximum growth rate vs supply rate for both pure and saline icicle growth	59
6.2.1.	The length vs time for a pure and saline icicle	60
6.2.2.	The length growth rate vs time for a pure and saline icicle	61
6.2.3.	The drip rate vs time for a pure and saline icicle	62
6.2.4	The length growth rate vs drip rate for a pure and saline icicle	63
6.3.1	The profiles of the diameters of the pure and saline icicles as a function of distance from the root	64
6.3.2.	The profiles of the diameters of the pure and saline icicles as a function of distance from the root	65
6.4.1.	The masses of pure and saline icicles as a function of time	66
7.1.1.	The apparatus used in the coldroom to grow pure icicles	69
7.1.2.	A schematic illustration of how the wind speed varies with height	72

Figure		Page
7.2.1.	The apparatus used in the coldroom to grow saline icicles	76
7.3.1.1.	Laboratory simulated pure icicles	77
7.3.2.1.	The cross-sections of a saline and a pure icicle	79
7.3.2.2.	The ribs of pure and saline icicles	80
8.1.	A schematic illustration of the circumferential variation of the Nusselt number for a cylinder	84
8.1.1.	Icicle length vs time for pure icicle growth, case #1 in Appendix D	97
8.1.2.	Icicle length vs time for pure icicle growth, case #2 in Appendix D	98
8.1.3.	Icicle length vs time for pure icicle growth, case #3 in Appendix D	99
8.1.4.	Icicle length vs time for pure icicle growth, case #4 in Appendix D	100
8.1.5	Icicle length vs time for pure icicle growth, case #5 in Appendix D	101
8.1.6	Icicle length vs time for pure icicle growth, case #6 in Appendix D	102
8.1.7	Icicle length vs time for saline icicle growth, case #7 in Appendix D	103
8.1.8	Icicle length vs time for saline icicle growth, case #8 in Appendix D	104
8.1.9	Icicle length vs time for saline icicle growth, case #9 in Appendix D	105
8.1.10	Icicle length vs time for saline icicle growth, case #10 in Appendix D	106
8.1.11	Icicle length vs time for saline icicle growth, case #11 in Appendix D	107
8.1.12	Icicle length vs time for saline icicle growth, case #12 in Appendix D	108
8.1.13	Icicle length vs time for saline icicle growth, case #13 in Appendix D	109
8.2.1.	Icicle length growth rate vs time for pure icicle growth, case #1 in Appendix D	110

Figure Page

8.2.2. Icicle length growth rate vs time for pure icicle growth, case #2 in Appendix D 111

8.2.3. Icicle length growth rate vs time for pure icicle growth, case #3 in Appendix D 112

8.2.4. Icicle length growth rate vs time for pure icicle growth, case #4 in Appendix D 113

8.2.5. Icicle length growth rate vs time for pure icicle growth, case #5 in Appendix D 114

8.2.6. Icicle length growth rate vs time for pure icicle growth, case #6 in Appendix D 115

8.2.7. Icicle length growth rate vs time for saline icicle growth, case #7 in Appendix D 116

8.2.8. Icicle length growth rate vs time for saline icicle growth, case #8 in Appendix D 117

8.2.9. Icicle length growth rate vs time for saline icicle growth, case #9 in Appendix D 118

8.2.10. Icicle length growth rate vs time for saline icicle growth, case #10 in Appendix D 119

8.2.11. Icicle length growth rate vs time for saline icicle growth, case #11 in Appendix D 120

8.2.12. Icicle length growth rate vs time for saline icicle growth, case #12 in Appendix D 121

8.2.13. Icicle length growth rate vs time for saline icicle growth, case #13 in Appendix D 122

8.3.1. Icicle length growth rate vs drip rate for pure icicle growth, case #1 in Appendix D 123

8.3.2. Icicle length growth rate vs drip rate for pure icicle growth, case #2 in Appendix D 124

8.3.3. Icicle length growth rate vs drip rate for pure icicle growth, case #3 in Appendix D 125

8.3.4. Icicle length growth rate vs drip rate for pure icicle growth, case #4 in Appendix D 126

8.3.5. Icicle length growth rate vs drip rate for pure icicle growth, case #5 in Appendix D 127

8.3.6. Icicle length growth rate vs drip rate for pure icicle growth, case #6 in Appendix D 128

Figure Page

8.3.7. Icicle length growth rate vs drip rate for saline icicle growth, case #7 in Appendix D 129

8.3.8. Icicle length growth rate vs drip rate for saline icicle growth, case #8 in Appendix D 130

8.3.9. Icicle length growth rate vs drip rate for saline icicle growth, case #9 in Appendix D 131

8.3.10. Icicle length growth rate vs drip rate for saline icicle growth, case #10 in Appendix D 132

8.3.11. Icicle length growth rate vs drip rate for saline icicle growth, case #11 in Appendix D 133

8.3.12. Icicle length growth rate vs drip rate for saline icicle growth, case #12 in Appendix D 134

8.3.13. Icicle length growth rate vs drip rate for saline icicle growth, case #13 in Appendix D 135

8.4.1. Model mean diameter at MGTT vs experimental mean diameter at ETT for pure icicle growth 136

8.4.2. Model mean diameter vs experimental mean diameter at ETT for saline icicle growth 137

8.4.3. Model mass at MGTT vs experimental mass at ETT for pure icicle growth 138

8.4.4. Model mass vs experimental mass at ETT for saline icicle growth 139

Nomenclature

The symbols and notation found in the equations in this thesis are listed and defined. These symbols and notation are also defined in the appropriate place in the text.

a - the linear radiation constant (K^3)

A_i - the surface area of the i^{th} cylinder (m^2)

$C_{b(n+1)}$ - the specific heat capacity of the brine leaving the tip to form the pendant drop ($Jkg^{-1}K^{-1}$)

C_{bi} - the specific heat capacity of the brine entering the i^{th} cylinder ($Jkg^{-1}K^{-1}$)

C_p - the specific heat capacity of air at constant pressure ($Jkg^{-1}K^{-1}$)

C_s - the specific heat capacity of sea salt ($Jkg^{-1}K^{-1}$)

C_w - the specific heat capacity of pure water ($Jkg^{-1}K^{-1}$)

d - the diameter of the pendant drop (m)

D - the diameter of any cylindrical segment of the icicle (m)

d_f - the diameter of the dendritic shell growing at the tip of a pure water icicle (mm)

D_i - the diameter of the i^{th} cylinder (m)

$D_{i(t-\Delta t)}$ - the diameter of the i^{th} cylinder at time $t-\Delta t$ (m)

D_{mean} - the volume mean diameter of the icicle (m)

d_s - the diameter of the dendritic shell growing at the tip of a saline icicle (mm)

$\frac{dL}{dt}$ - the length growth rate of an icicle (ms^{-1})

$\frac{dR}{dt}$ - the growth rate of the equivalent radius of a pure icicle (ms^{-1})

$\frac{dR_i}{dt}$ - the radial growth rate of the i^{th} cylinder (ms^{-1})

$\frac{dM_i}{dt}$ - is the rate of spongy ice growth on the i^{th} cylinder (kgs^{-1})

$e(0°C)$ - the saturation vapor pressure over a flat water surface at 0 °C (mb)

$e(T)$ - the saturation vapor pressure over a flat water surface at T (mb)

$e_s(T)$ - the saturation water vapor pressure over a brine surface A at T (mb)

$e_s(T_{si})$ - the saturation vapor pressure over a brine surface at the surface temperature of the i^{th} cylinder, T_{si} (mb)

$e_s(T_{s(n+1)})$ - the saturation vapor pressure over a brine surface at the surface temperature of the pendant drop, $T_{s(n+1)}$ (mb)

F - the drip rate of the pendant drops (s^{-1})

F_r - the accretion fraction (dimensionless)

g - gravitational acceleration (ms^{-2})

G_{rt} - the Grashof number for the tip (dimensionless)

G_{rw} - the Grashof number for the wall (dimensionless)

h_t - the heat transfer coefficient for the pendant drop of a pure icicle ($Wm^{-2}K^{-1}$)

$h_{t(n+1)}$ - the heat transfer coefficient for the pendant drop of a saline icicle ($Wm^{-2}K^{-1}$)

h_w - the heat transfer coefficient for the equivalent cylinder ($Wm^{-2}K^{-1}$)

h_{wi} - the heat transfer coefficient for the i^{th} cylinder ($Wm^{-2}K^{-1}$)

I - the spongy ice growth rate (kgs^{-1})

k - the thermal conductivity of air ($Wm^{-1}K^{-1}$)

K - the effective distribution coefficient (dimensionless)

K^* - the interfacial distribution coefficient (dimensionless)

L - the length of icicle (m)

L_e - the latent heat of evaporation (Jkg^{-1})

L_f - the latent heat of fusion for pure water at T (Jkg^{-1})

L_{fs} - the latent heat of fusion of the spongy accretion at T (Jkg^{-1})

Loss - the rate at which water is lost at the icicle wall due to freezing and evaporation (kgs^{-1})

$Loss_i$ - the rate at which water is lost at the i^{th} cylinder due to freezing and evaporation (kgs^{-1})

m_i - the mass of pure ice in the ice matrix (kg)

m_s - the mass of salt in the ice matrix (kg)

M_{tip} - the mass of the newly formed cylinder at the tip during a given time step (kg)

M_t - the total mass at time t (kg)

$M_{t+\Delta t}$ - the total mass at time $t + \Delta t$ (kg)

m_w - the mass of pure water in the ice matrix (kg)

M_{wall} - the total increment of mass on the surface of each cylinder during time step Δt (kg)

M_y - the dynamic viscosity of air ($kgm^{-1}s^{-1}$)

N_{ut} - the Nusselt number for the tip (dimensionless)

N_{uw} - the Nusselt number for a cylinder (dimensionless)

N_y - the kinematic viscosity of air (m^2s^{-1})

P_a - air pressure (mb)

q_{chi} - the heat flux change between the $(i-1)^{th}$ cylinder and the i^{th} cylinder (Wm^{-2})

q_{conv} - the convective heat transfer (Wm^{-2})

q_{convi} - the convective heat transfer of the i^{th} cylinder (Wm^{-2})

$q_{conv(n+1)}$ - the convective heat transfer of the pendant drop (Wm^{-2})

q_{drip} - the heat flux of the pendant drop corresponding to its temperature change (Wm^{-2})

$q_{drip(n+1)}$ - the heat flux of the pendant drop corresponding to its temperature change (Wm^{-2})

q_{evap} - the latent heat of evaporation (Wm^{-2})

q_{evapi} - the latent heat of evaporation of the i^{th} cylinder (Wm^{-2})

$q_{evap(n+1)}$ - the latent heat of evaporation of the pendant drop (Wm^{-2})

q_{freeze} - the latent heat of fusion (Wm^{-2})

$q_{freezei}$ - the latent heat of fusion of the i^{th} cylinder (Wm^{-2})

$q_{freeze(n+1)}$ - the latent heat of fusion of the pendant drop (Wm^{-2})

q_{rad} - the heat flux by long wave radiation (Wm^{-2})

q_{radi} - the heat flux by long wave radiation from the i^{th} cylinder (Wm^{-2})

$q_{rad(n+1)}$ - the heat flux by long wave radiation from the pendant drop (Wm^{-2})

r - the radius of the pendant drop (m)

r - the relative humidity (%)

R_{ed} - the Reynolds number for the pendant drop (dimensionless)

R_{ew} - the Reynolds number for the cylinder (dimensionless)

r_f - the radius of the pendant drop for a pure icicle (m)

r_s - the radius of the pendant drop for a saline icicle (m)

S_b - the salinity of the brine leaving A (g/g)

S_i - the salinity of the ice accretion on A (g/g)

S_w - the salinity of the brine entering A (g/g)

T - temperature (°C)

T_a - the air temperature (°C)

T_i - the supercooling of the run-off water entering the tip (°C)

T_m - the supercooling of the pendant drop just before it leaves the tip (°C)

T_s - the surface equilibrium temperature of A (°C)

T_{si} - the surface equilibrium temperature of the i^{th} cylinder (°C)

$T_{s(n+1)}$ - the surface equilibrium temperature of the pendant drop (°C)

T_{sp} - the supercooling close to the ice/water interface (°C)

v - the wind speed (ms^{-1})

V - the total volume of the accretion (m^3)

V_b - the volume of the brine (m^3)

v_i - the ice-growth rate (ms^{-1})

V_i - the volume of the pure ice (m^3)

W_o - the initial water supply rate from the root (kgs^{-1})

W_t - the water flux to the tip (kgs^{-1})

W_t - the brine flux to cylinder A (kgs^{-1})

W_t' - the brine flux leaving cylinder A (kgs^{-1})

W_{ti} - the brine flux to the i^{th} cylinder (kgs^{-1})

$W_{t(n+1)}$ - the brine flux leaving the tip to form the pendant drop (kgs^{-1})

x - the mass of brine (kg)

δ - the wall thickness of the ice tube formed at the tip (m)

σ - the Stefan-Boltzman constant ($Wm^{-2}K^{-4}$)

σ - the surface tension of the liquid (Nm^{-1})

σ_f - the surface tension of pure water (Nm^{-1})

σ_s - the surface tension of brine (Nm^{-1})

ψ - the Harkins factor (dimensionless)

ρ_a - the density of the ice accretion on the wall of the icicle (kgm^{-3})

ρ_{air} - the density of air (kgm^{-3})

ρ_{ai} - the density of the ice accretion on the wall of the i^{th} cylinder (kgm^{-3})

$\rho_{a(n+1)}$ - the density of the newly formed cylinder at the tip (kgm^{-3})

ρ_b - the density of the brine (kgm^{-3})

ρ_f - the density of pure water (kgm^{-3})

ρ_i - the density of pure ice (kgm^{-3})

ρ_s - the density of brine (kgm^{-3})

ρ_w - the density of pure water (kgm^{-3})

λ - the liquid fraction (g/g)

π - A mathematical constant (dimensionless)

ΔL_i - length of the i^{th} cylinder (m)

Δt - a time step (s)

ΔT - the temperature change of the pendant drop from the wall temperature to the temperature at which it leaves the tip (°C)

ΔT_{fd} - the difference in equilibrium temperature between the pendant drop and the n^{th} cylinder (°C)

ΔT_{sd} - the supercooling of the pendant drop (°C)

1. Introduction

In cold seas, icing events are a frequent occurence for fishing trawlers, supply vessels, and drilling platforms under environmental conditions of low air temperature (below the freezing point of seawater) and high wind. Icing is especially hazardous to small ships because of their low freeboard and large surface area to displacement ratio. Icing loads on such vessels can affect their stability and cause them to capsize. Every year, losses of crews and ships due to sea icing are reported. In 1979, ten vessels capsized during an icing storm in the North Pacific Ocean(Shellard,1974; Aksyutin,1979).

There has been evidence that icing on sea structures is considerably augmented by icicles (Makkonen, 1988). Of course, these icicles on sea structures do not consist of pure water, but brine. The objective of this thesis is to develop a mathematical model to predict the growth rate of saline icicles. This model can also be applied to predict the growth rate of pure water icicles. Laboratory simulated saline and pure water icicles have been produced in the coldroom in the Division of Meteorology at the University of Alberta in order to test the model's predictions.

Considerable literature on marine icing has been published. Gates, Lozowski, and Makkonen (1986) have discussed marine icing and spongy ice. Zakrzewski, Blackmore, and Lozowski (1988) have developed a mathematical model for icing on a ship's superstructure. The effects of the salinity of the moving water film and of the ice sponginess are taken into account. Zakrzewski (1986) has discussed icing on fishing vessels. Makkonen (1987) has discussed sea spray icing, giving an equation to calculate the accretion fraction. With this equation, the salinities of the accretion and of the brine film on the accretion can be calculated. The effect of salinity on some thermodynamic properties was also included. Much more has been written discussing marine icing from various aspects which will not be reviewed here.

Although the growth mechanisms of saline icicles have not yet been studied, much has been published about pure water icicles, including their formation, growth mechanisms, shapes, special features such as horizontal bumps and spikes, and crystalline structure.

Knight (1980) has discussed the crystallization phenomena of icicles. The growth conditions, sponginess, crystal size and orientation, icicle shapes, and the air bubbles in icicles were examined. Laudise and Barns (1979) collected about 60 icicles and examined their crystaline properties. A growth mechanism was proposed, but it is not as detailed as the one proposed by Makkonen(1988). Some unusual icicles were also observed and discussed. Burt (1982) has observed and described horizontal icicles. Maeno and Takahashi (1984b) gave a detailed account of bent icicles, horizontal bumps (or ridges), and spikes on icicles. Growth mechanisms of icicles have been proposed by Walker (1988), Makkonen (1988), and Maeno and Takahashi (1984a). The growth mechanisms proposed by these four people are basically the same. Maeno and Takahashi (1984a) also performed some experiments to study the growth of fresh water icicles. Makkonen (1988), has developed a mathematical model to predict the growth rate of fresh water icicles. A Russian paper was also published (Apytynnyen et al. 1988) in which the tension and deformation of an icicle were estimated, so that the moment of collapsing/splitting of an icicle from its foundation could be predicted.

Although the growth mechanisms of saline icicles have not yet been studied, it is believed, and it is supported by experiments and observations, that the growth mechanism of saline icicles will be similar to that of pure water icicles, except that in the case of saline icicles, the effect of salinity on the thermodynamic properties must be considered. Like a pure water icicle (hereafter, pure icicle), a saline icicle has a circular or elliptical conical shape with a brine film enclosing its body. This brine film flows downward towards the tip to form a pendant drop as long as there is a continuous supply of brine to the tip. A liquid tube, which extends a few centimeters upward from the tip, is also found in the interior of a saline icicle. In contrast to a pure icicle, numerous brine pockets are entrapped inside the body of a saline icicle. The formation of these brine pockets will be discussed in Chapter 3. In addition to the brine pockets, air bubbles are also contained inside the body of a saline icicle. These air bubbles can be observed during the experiments. The growth of a saline icicle, like that of a pure icicle, is the result of two process. The first processes is the growth in diameter, which takes place on the body of a saline icicle through the freezing of the brine film on the surface.

The second process is the growth in length, which takes place at the tip through the freezing of part of the dripping pendant drops.

The saline icicles found on various sea structures are formed by the impact of sea spray on overhanging structures under an environmental condition that favors their growth. The icicles (both pure and saline) simulated in the coldroom are formed by dripping pure water or brine onto an overhanging rod. The model's simulations are also based on the condition of continuous liquid supply from the root. Figure 1.1 gives a simple sketch of a saline icicle and Figure 1.2 shows a picture of a laboratory simulated saline icicle.

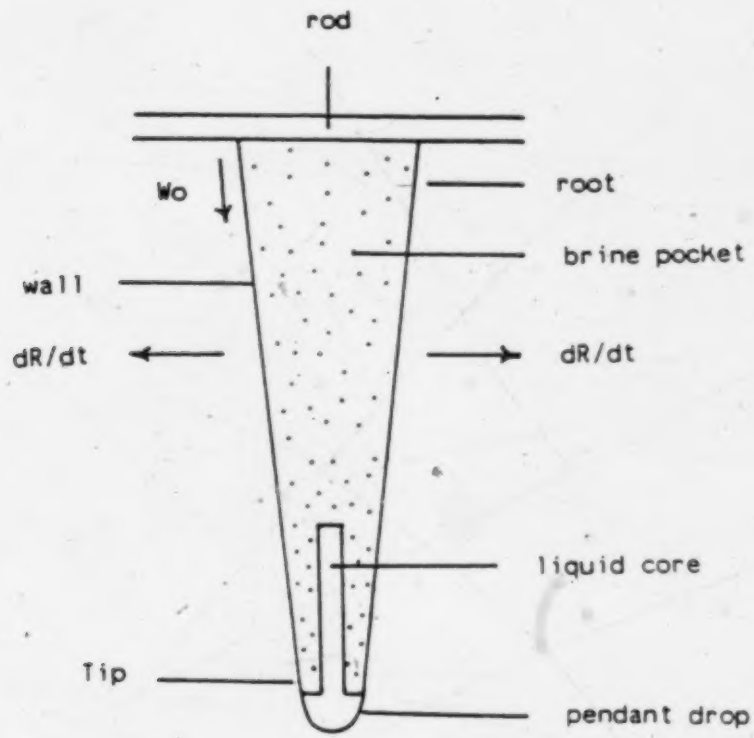

Figure 1.1 A simple sketch of a saline icicle.
(Modified from MaKKonen, 1988)

Figure 1.2 Laboratory simulated saline icicles.
Air conditions (from left to right):
1) not recorded, 2) Case #9, Ta = -10.3 C,
Wo = 19.8 mg/s, 3) Case #8, Ta = -14.6 C,
Wo = 30.5 mg/s.

2. A review of pure icicle growth

Makkonen (1987) gave a detailed discussion of the growth of a pure icicle. A growth mechanism was proposed, and two governing equations controlling the growth rates in length and width were formulated. These equations form the basis of a computer program which simulates the growth process. In this chapter, Makkonen's theory of the growth of a pure icicle will be reviewed. This theory will then be modified and applied in the next chapter to the growth mechanism of a saline icicle.

2.1 Growth mechanism of a pure icicle

A pure icicle has a narrow conical shape with a liquid film enclosing its body, if there is a continuous supply of dripping water. The thickness of this liquid film during growth is approximately 40 - 100 μm (Maeno and Takashi, 1984a). If the water supply is sufficient, a pendant drop will be formed at the tip. Since the shape of this pendant drop changes during its growth, its mean shape may be approximated by a hemisphere with a diameter of approximately 5.0 mm, regardless of the growth conditions (Maeno and Takahashi, 1984a). The method for estimating the pendant drop size will be discussed in Chapter 5.

An icicle grows in two directions. The first is the growth in diameter, which takes place on the wall through the freezing of the liquid film. The second is the growth in length, which takes place at the tip through the freezing of a portion of the pendant drop. From the shape of the icicle, it can be deduced that the growth rate in length at the tip must be typically 20 to 60 times faster than the radial growth rate. However, the heat transfer flux from the wall is of the same order of magnitude as that from the tip. One plausible explanation for this paradox is that the vertical growth rate of an icicle is faster than the radial growth rate for geometrical reasons. In other words, not all the liquid under the tip freezes. Rather, only a thin cylindrical ice shell consisting of dendrites, which enclose a liquid water core, freezes and grows vertically. As a result, a liquid tube is trapped inside the ice shell. This proposed tip growth mechanism is consistent with that proposed by Maeno and Takahashi (1984a), and by Johnson (1988). From observations of growing icicles in nature

and in the laboratory, it is found that this liquid tube extends a few centimeters up into the interior of a growing icicle.

The water film enclosing the surface of an icicle is supercooled by less than 0.02 °C (Hillig and Turnbull,1956). This small amount of supercooling does not give a significant contribution to the heat balance equation. However, the supercooling of the pendant drop may be significant, considering the rate of growth in length of an icicle. This can be deduced from the fact that, according to Hillig and Turnbull (1956), the degree of supercooling of a water surface is proportional to the ice growth rate. Since the ice growth rate at the tip is much faster (20 to 60 times) than that taking place on the wall, the degree of supercooling of the pendant drop could be more significant than that of the water film (Makkonen, 1988). Therefore, the supercooling of the pendant drop should be considered in the heat balance equation.

Since the water film enclosing the wall of the icicle is supercooled, though only by a small amount, the ice formed under this water film will be dendritic (Makkonen, 1988). This results in the growth of spongy ice. In other words, liquid water is entrapped in the ice matrix. It should also be noted that the liquid tube in the interior of the icicle, and the water entrapped in the ice matrix, will finally be frozen by heat conduction through the fully frozen root. This is the only way for heat to escape, there are virtually no temperature gradients in the horizontal and downward directions, since the wall and the tip of the icicle are enclosed by liquid water at the freezing point (actually slightly less than 0°C because of supercooling). Figure 2.1 shows a schematic cross section of a growing pure icicle.

Before discussing the mathematical model of the growth of a pure icicle, there are several assumptions that should be mentioned:

1. The icicle has a conical shape with a circular cross-section.
2. The pendant drop has a hemispherical shape and a homogeneous temperature distribution.
3. The water on the wall of the icicle has a homogeneous temperature distribution (assumed 0°C), and the thickness of the water film is also homogeneous around the

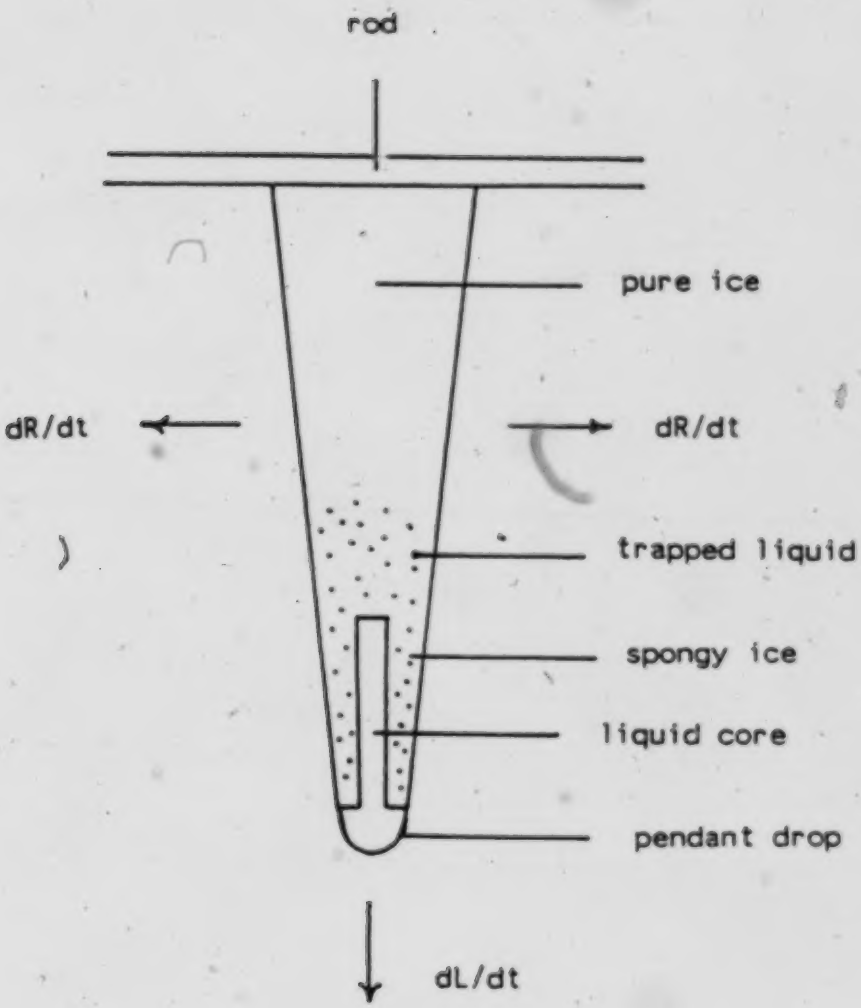

Figure 2.1 A schematic diagram of a pure icicle
(Modified from Makkonen, 1988)

circumference.

4. The emissivities of the surface of the icicle and of the environment are both unity.

5. Thermodynamical equilibrium is assumed so that a heat balance equation may be written.

2.2 Growth in length

The heat balance equation for the surface of the hemispherical tip of the icicle may be written:

$$q_{conv} + q_{evap} + q_{rad} = q_{drip} + q_{freeze} \tag{2.2.1}$$

All of these terms are heat fluxes and have units of Wm^{-2}.

q_{conv} is the convective heat flux density, which is calculated from:

$$q_{conv} = h_t(0°C - T_a) \tag{2.2.2}$$

where

h_t is the convective heat transfer coefficient for the pendant drop.

T_a is the air temperature in °C.

It should be noted that the pendant drop is actually supercooled. But, for simplicity, it is assumed to have a surface temperature of 0 °C. Furthermore, the air temperature in the cold room is much lower than the surface temperature of the pendant drop. Therefore, this assumption should not cause a significant error.

q_{evap} is the latent heat of evaporation. It is calculated from:

$$q_{evap} = h_t \frac{0.622L_e}{C_p P_a}\left(e(0°C) - \frac{r}{100}e(T_a)\right) \tag{2.2.3}$$

where

L_e is the latent heat of evaporation = 2.5×10^6 Jkg^{-1}.

C_p is the specific heat capacity of air at constant pressure.

P_a is the air pressure in mb, which can be converted to Pa by multiplying by a factor of 100.

e(0°C) is the saturation vapor pressure over a flat water surface at 0°C.

$e(T_a)$ is the saturation vapor pressure over a flat water surface at T_a.

r is the relative humidity expressed in %.

The specific heat capacity of air C_p may be calculated by:

$$C_p = 1004 + 0.046T_a. \qquad (2.2.4)$$

The saturation vapor pressure e(T) can be calculated from the integrated Clausius - Clapeyron equation:

$$e(T) = \exp\left(\frac{-6763.6}{T} - 4.9283\ln(T) + 54.23\right) \qquad (2.2.5)$$

where e(T) has units of mb and T is in K.

q_{rad} is the net heat flux by long wave radiation from the pendant drop. It may be calculated by:

$$q_{rad} = \sigma a(0°C - T_a) \qquad (2.2.6)$$

where

σ is the Stefan - Boltzman constant = 5.67×10^{-8} $Wm^{-2}K^{-4}$

a is a linear radiation constant = 8.1×10^7 K^3

The linear radiation constant, a, is deduced as follow:

$$q_{rad} = \sigma(T_s^4 - T_a^4)$$

which can be rewritten as:

$$q_{rad} = \sigma(T_s - T_a)(T_s + T_a)(T_s^2 + T_a^2)$$

where

T_s is the equilibrium surface temperature in K.

Now, let

$$a = (T_s + T_a)(T_s^2 + T_a^2).$$

Using $T_s = T_a = 273$ K, it gives $a = 8.1 \times 10^7$ K^3.

The fourth term, q_{drip}, results from the fact that the pendant drop is initially formed at the wall temperature but leaves the tip at a slightly lower temperature. The heat flux of this hemispherical pendant drop corresponding to this temperature change is given by:

$$q_{drip} = \frac{2C_w W_t \Delta T}{\pi d^2} \qquad (2.2.7)$$

where

C_w is the specific heat capacity of water at 0°C = 4218 Jkg^{-1}K^{-1}.

W_t is the mass of water flux to the tip in kgs^{-1}.

ΔT is the temperature change of the pendant drop from the wall temperature to the temperature at which it leaves the tip.

d is the diameter of the pendant drop.

The water flux to the tip may be calculated by:

$$W_t = W_o - \text{Loss} \tag{2.2.8}$$

where

W_o is the initial water supply rate from the root.

Loss is the rate at which water is lost at the icicle wall due to freezing and evaporation.

To calculate Loss, in Makkonen's model, the icicle is assumed to have a constant diameter D, which is equal to the diameter of an "equivalent" cylinder that has the same total radial heat transfer as the surface of the icicle. This is called the equivalent diameter. Then, Loss may be calculated by:

$$\text{Loss} = \pi LD[\rho_a \frac{dR}{dt} + h_w \frac{0.622}{C_p P_a}(e(0°C) - \frac{r}{100}e(T_a))] \tag{2.2.9}$$

where

L is the length of the icicle.

D is the equivalent diameter of the icicle, described above. It is assumed by Makkonen (1988) to be the mean diameter of the icicle for modelling purposes.

$\frac{dR}{dt}$ is the growth rate of the equivalent radius.

h_w is the convective heat transfer coefficient for the equivalent cylinder.

ρ_a is the density of the ice accretion (consisting of ice and water) on the wall of the icicle.

It should be noted that to assume the equivalent diameter to be the mean diameter is incorrect, because they are actually different from each other. The equivalent diameter is the diameter of a cylinder that has the same total radial heat transfer as the surface of the icicle, whereas the mean diameter is the average diameter of the icicle. Therefore, using the mean diameter as the equivalent diameter to calculate the mass accretion on the wall of the icicle

will result in error. However, if this mean diameter is used to calculate the heat transfer, its relationship to h_w must be known. It is known from Appendix A that for forced convection:

$$h_w = \frac{kNu_w}{D}.$$

The experiments were performed in the coldroom over a temperature range of -7 °C to -15 °C, and with a wind speed of ~ 0.6m/s. Under these conditions, Nu_w is related to Re_w by the following relation (Makkonen, 1988):

$$Nu_w \propto Re_w^{0.466}.$$

But,

$$Re_w \propto D$$

Therefore,

$$h_w = \frac{kNu_w}{D} \propto \frac{k}{D} Re_w^{0.466} \propto \frac{k}{D} D^{0.466} \propto D^{-0.534}.$$

Therefore, the mean value of $D^{-0.534}$ should be used in calculating h_w, not the mean diameter D.

On the right hand side of Equation (2.2.9), the first term is the rate of water loss due to freezing of water on the wall, and the second term is the rate of water loss due to the evaporation of water from the wall. ρ_a may be calculated by:

$$\rho_a = (1 - \lambda)\rho_i + \lambda\rho_w \qquad (2.2.10)$$

where

λ is the liquid fraction of the spongy ice on the wall of the icicle.

ρ_i is the density of pure ice = 917 kgm^{-3}.

ρ_w is the density of pure water = 1000 kgm^{-3}.

The ΔT in equation (2.2.7) may be written:

$$\Delta T = T_i - T_m \tag{2.2.11}$$

where

T_i is the supercooling of the run-off water entering the tip.

T_m is the supercooling of the pendant drop just before it leaves the tip.

According to Hillig and Turnbull (1956), the degree of supercooling close to the ice/water interface is related to the ice growth rate on the ice suface by the following relation:

$$v_i = 1.6\text{x}10^{-3}(T_{sp})^{1.7} \tag{2.2.12}$$

where

v_i is the ice-growth rate in m/s.

T_{sp} is the supercooling close to the ice/water interface.

Thus, T_i and T_m may be calculated by:

$$T_i = -44.05(\frac{dR}{dt})^{0.588} \tag{2.2.13}$$

$$T_m = -44.05(\frac{dL}{dt})^{0.588} \tag{2.2.14}$$

where

$\frac{dR}{dt}$ is the growth rate (in m/s) in equivalent radius.

$\frac{dL}{dt}$ is the growth rate (in m/s) in length.

Using equations (2.2.11), (2.2.13), and (2.2.14), ΔT becomes:

$$\Delta T = 44.05\left(\frac{dL}{dt} \cdot \frac{dR}{dt}\right)^{0.588} \tag{2.2.15}$$

This approximation due to Makkonen (1988) is used in the model for consistency with his equations. Test of the model in which the correct formulation for ΔT is used, show differences in final length, mean diameter, and mass of the order of 1 %. Now, q_{drip} can simply be calculated by the following equation:

$$q_{drip} = \frac{28.04}{d^2} C_w W_t \left(\frac{dL}{dt} \cdot \frac{dR}{dt}\right)^{0.588} \tag{2.2.16}$$

where W_t is calculated using Equations (2.2.8) and (2.2.9).

The last term of equation (2.2.1), q_{freeze}, is the latent heat of fusion, which may be calculated by:

$$q_{freeze} = 2L_f \rho_i \delta \frac{(d - \delta)}{d^2} \frac{dL}{dt} \tag{2.2.17}$$

where

L_f is the latent heat of fusion at 0°C = 3.334×10^5 Jkg^{-1}.

δ is the wall thickness of the ice tube formed at the tip.

To estimate δ, suppose there are several dendrites growing downward under the tip. Then, the outer one would be in contact with the flux of supercooled water running down from the wall into the pendant drop. The rate at which latent heat is transfered to the air from this outer dendrite would be faster than the others. As a result, this dendrite would grow faster than the others. Therefore, it can be concluded that the ice tube growing vertically at the tip has the thickness of single dendrite (Makkonen 1988). In view of this, according to Harrison and Tiller (1963), the thickness of a dendrite growing under supercooled water is in the range of

50 to 100 μm. Hence, a thickness of 75 μm is assumed by Makkonen (1988) for δ.

Using Equations (2.2.2), (2.2.3), (2.2.6), (2.2.16), and (2.2.17), Equation (2.2.1) becomes:

$$h_t(0°C - T_a) + h_t\frac{0.622L_e}{C_p P_a}(e(0°C) - \frac{r}{100}e(T_a)) + \sigma a(0°C - T_a) =$$

$$\frac{28.04}{d^2}C_w W_t(\frac{dL}{dt} - \frac{dR}{dt})^{0.588} + 2L_f\rho_i\delta\frac{(d - \delta)}{d^2}\frac{dL}{dt}. \qquad (2.2.18)$$

The way in which Equation (2.2.18) is solved will be discussed in Chapter 4.

2.3 Growth in diameter

The heat balance equation for the wall of the icicle is:

$$q_{conv} + q_{evap} + q_{rad} = q_{freeze}. \qquad (2.3.1)$$

The q_{drip} term has been neglected since the degree of supercooling is assumed to be only small and the same everywhere on the wall. Consequently, the effect of this supercooling is neglected in the heat balance equation.

The three terms on the left hand side of Equation (2.3.1) can be calculated by the same parameterizations as for the growth in length. Thus:

$$q_{conv} = h_w(0°C - T_a). \qquad (2.3.2)$$

$$q_{evap} = h_w\frac{0.622L_e}{C_p P_a}(e(0°C) - \frac{R}{100}e(T_a)). \qquad (2.3.3)$$

$$q_{rad} = \sigma a(0°C - Ta). \qquad (2.3.4)$$

It should be mentioned here again, that the ice growing on the wall of the icicle is under a

supercooled liquid film. Hence, the growing ice is dendritic and unfrozen water is entrapped inside the ice matrix. Therefore, in calculating the heat of fusion, q_{freeze}, for the wall, only the ice portion is considered. Thus:

$$q_{freeze} = \rho_a L_f (1 - \lambda) \frac{dR}{dt} \tag{2.3.5}$$

where λ is the liquid fraction of the spongy ice on the surface of the wall.

Substituting Equations (2.3.2), (2.3.3), (2.3.4), and (2.3.5) into Equation (2.3.1), the heat balance equation for the wall becomes:

$$h_w(0°C - T_a) + h_w \frac{0.622 L_e}{C_p P_a}(e(0°C) - \frac{r}{100} e(T_a)) + \sigma a(0°C - T_a) =$$

$$\rho_a L_f (1 - \lambda) \frac{dR}{dt}. \tag{2.3.6}$$

The growth mechanism and the theory of pure icicle growth that has been proposed by Makkonen (1988) and described in this chapter is, in fact, consistent with the one proposed by Maeno and Takahashi (1984a). This growth mechanism is also further verified through observations of how icicles grow in nature and in the laboratory. In the next two chapters, Makkonen's theory for the growth of pure icicles is applied and extended to consider the growth of saline icicles and to formulate a model of their growth.

3. A qualitative description of the growth of a saline icicle

As mentioned in Chapter 1, saline icicles and pure icicles have many similarities, including their general growth mechanisms (e.g the growth in length and in diameter), shapes (e.g circular or elliptical conical shape), and features (e.g bumps, liquid core, and sponginess). All of this has been verified through observations of the growth of saline icicles in the laboratory. The major difference between a saline icicle and a pure icicle is that the former is formed by the freezing of brine, while the latter is formed by the freezing of pure water. Since brine has a lower equilibrium temperature with ice than pure water, it is apparent that a saline icicle should grow more slowly than a pure icicle. The sponginess found in a saline icicle is also different from the sponginess found in a pure icicle. The former consists of pure ice and brine while the latter consists of pure ice and pure water (Makkonen, 1987). The unfrozen brine entrapped in the ice matrix of a saline icicle is called a brine pocket.

3.1 Brine pockets

The body of a growing saline icicle is enclosed by a brine film. Under a temperature which is low enough for the saline icicle to grow, the ice formed on the solid/liquid interface will be dendritic due to constitutional supercooling (Knight (1967), Weeks and Ackley (1982)). These dendrites consist of pure ice and have a tree-like shape. As these dendrites grow, salt is rejected from the accretion surface causing the salinity of the brine film to increase (Knight (1967), Makkonen (1987)). As the dendrites grow larger, branches of adjacent dendrites start to merge and trap the brine inside to form so-called brine pockets (Makkonen, 1987). It is assumed in the model that there is thorough horizontal mixing between the cavities formed among the dendrites, and the brine film flowing beside them. Hence, when the brine pockets are newly formed, their salinity will be the same as that of the adjacent brine film. Figure 3.1.1 illustrates this situation. The salinity of the brine pockets changes later because pure ice continues to deposit on the inner solid/liquid interface of the brine pockets. However, it is assumed that the latent heat released in these brine pockets does not affect the heat balance on the surface of the saline icicle. This questionable assumption is

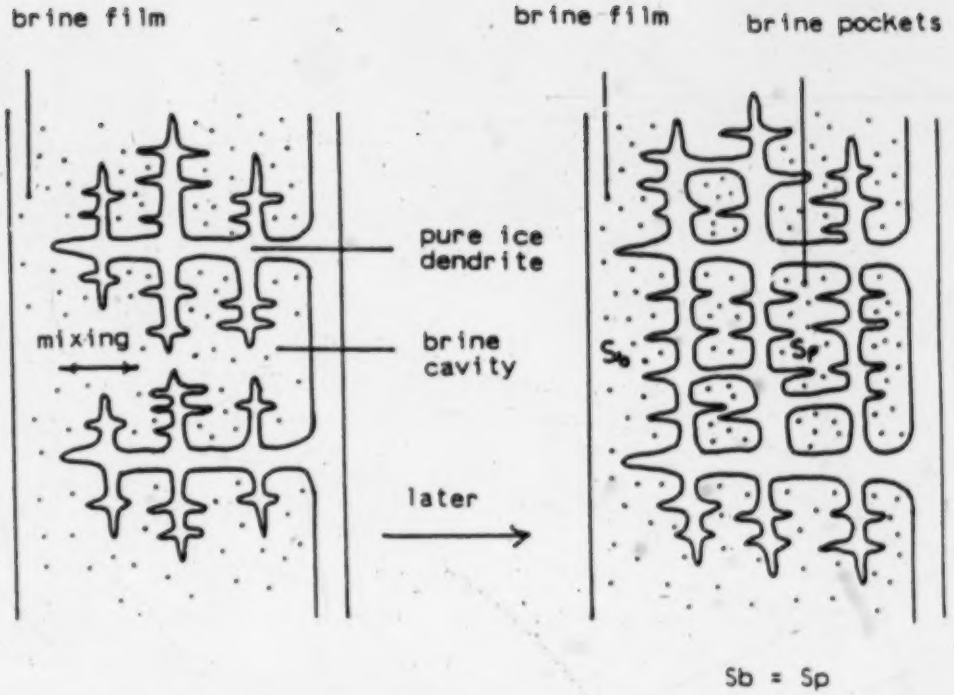

Sb is the salinity of the brine pockets

Sp is the salinity of the brine film.

Figure 3.1.1 A schematic illustration of the formation of brine pockets.

made for simplicity. It should be re-examined in future versions of the model. As the brine pockets become smaller due to ice growth, the salinity of the entrapped brine increases. This higher salinity brine can only be in equilibrium if the temperature drops. Since the icicle temperature cannot drop below the air temperature, this limits the freezing process in the brine pockets.

3.2 Growth rate of a saline icicle

Consider a small volume of brine, which flows downward from the root to the tip of a growing saline icicle to form the pendant drop. As this brine flows downward, pure ice continues to deposit on the accretion surface and salt is continuously rejected to this brine. As a result, the brine mass decreases due to the formation of pure ice and brine pockets. At the same time, its salt concentration increases. Therefore, the salinity of this brine will increase until it gets to the tip and forms the pendant drop. Since the equilibrium temperature of the brine is inversely related to its salinity, the equilibrium temperature of this brine will decrease as it moves from the root to the tip. Now, if we consider a case with a continuous brine film moving downward, we may expect a profile with salinity increasing and equilibrium temperature decreasing downward. The equilibrium temperature difference between the root and the tip will mainly depend on the length of the saline icicle. The longer the icicle, the greater the difference will be.

From the above considerations, it can be expected that when the saline icicle grows to a certain size, the growth rate in length should start to decrease until the equilibrium temperature of the pendant drop equals the air temperature. Then the growth in length will stop. This qualitative prediction will be tested by model simulation and experiment in Chapters 6 and 7. It can also be expected that the maximum width to length ratio of a saline icicle should be greater than that of a pure icicle, due to the fact that the liquid film of a saline icicle has an equilibrium temperature profile which is decreasing downward. This will cause faster radial growth at the root than at the tip. The liquid film of a pure icicle has a homogeneous temperature distribution. Hence, the relative growth rates at the root and the tip

are determined largerly by differences in the heat transfer coefficient. Since the heat transfer coefficient varies approximately inversely as the square root of diameter, the radial growth rate at the tip for a dripping pure icicle will exceed that at the root. This will tend to make pure icicles very slender. Figure 3.2.1 shows two pictures. The upper one shows pure icicles. The lower one shows saline icicles. All these icicles were grown in the coldroom at the University of Alberta. From these pictures, it can be seen that the saline icicles do indeed have greater width to length ratio than the pure icicles. Because all these icicles were grown under different environmental conditions, they provide only a crude comparison.

The growth mechanisms of a pure icicle and the characteristics of the growth of a saline icicle have been discussed in Chapters 2 and 3, respectively. In chapter 4, the heat balance equations that govern the growth of a saline icicle will be formulated. These equations form the basis of a computer model which is created to simulate the growth of a saline icicle.

Air conditions (from top to bottom) : 1) Ta = -11.0 C, Wo = 22.6 mg/s, 2) not recorded, 3) Ta = -8.0 C, Wo = 24.2 mg/s.

Air conditions (from top to bottom) : 1) not recorded, 2) Ta = -10.3 C, Wo = 19.8 mg/s, 3) Ta = -14.6 C, Wo = 30.5 mg/s.

2 cm

Figure 3.2.1

4. A mathematical investigation of the growth of a saline icicle

4.1 Introduction to the finite element time step method

Like a pure icicle, a saline icicle has two growth directions. The first is growth in diameter, which takes place on the wall through the freezing of the brine film. The second is growth in length, which takes place at the tip through the partial freezing of the pendant drop. Because the equilibrium temperature of the brine film decreases downward, Makkonen's method, which assumes a homogeneous wall temperature and considers only the growth in mean diameter, is not appropriate for modelling the growth in width of a saline icicle. In order to deal with this problem, a time dependent finite element method is used. The saline icicle is divided into cylindrical segments (disks) according to the number of time steps; that is, the number of disks equals the number of time steps. Each of these cylinders has a different diameter and length (see figure 1.3). What this time step method does is to divide the saline icicle into cylindrical segments, such that each segment has a unique equilibrium temperature for the surface brine. The radial growth rate of these cylinders, then, depends on their individual surface equilibrium temperature and diameter. For example, after n time steps of length Δt, the saline icicle will have $n+1$ cylinders, including the one corresponding to the zeroth time step. The last, $(n+1)^{th}$, segment represents the newly formed cylinder resulting from the freezing of part of the pendant drop during the time period Δt. At the end of one more time step, at $t = (n+1)\Delta t$, each of the $n+1$ cylinders has grown radially at a different rate according to its individual surface equilibrium temperature and diameter. Right at the new tip, a new cylindrical segment, the $(n+2)^{th}$, has grown. The time step chosen for the present model will be $\Delta t = 2$ minutes (Makkonen, 1988). The reason for choosing 2 minutes as the time step is that under the air condition at which the experiments are performed in the coldroom, the model simulation shows that the maximum length growth for either pure or saline icicle for 2 minutes is less than 2 cm. This length resolution is good enough for the present modelling purpose. With this time step of 2 minutes being used, the length (ΔL) of the cylinder formed at the tip can be calculated by $\Delta L = (dL/dt)\Delta t$. Figure 4.1.1 gives a

schematic illustration of this time step method.

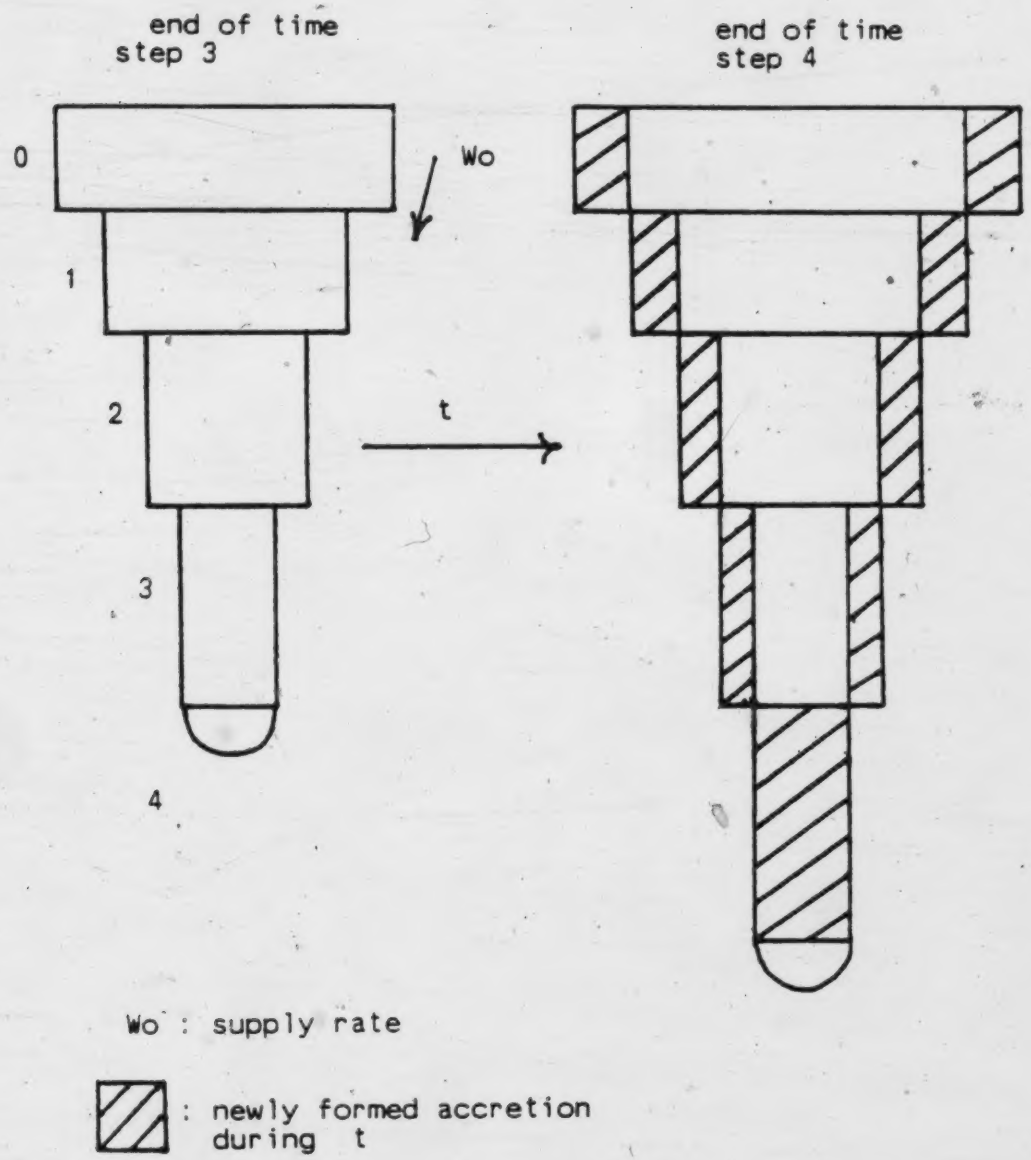

Figure 4.1.1 A schematic illustration of the time step method.

Two heat balance equations will be formulated in Sections 4.3 and 4.4. The first is used to calculate the radial growth rate for each of the individual cylinders. The second is used to calculate the length growth rate at the tip. The radial growth rate is calculated first, and then the length growth rate. This completes the calculations for one time step. For the next time step, the same calculation procedure is repeated. Since the growth of a saline icicle is strongly influenced by the effect of salinity, it is worthwhile to spend some time to discuss how salinity affects the thermodynamic properties, which in turn affect the growth rate.

4.2 The effect of salinity on the thermodynamic properties

Consider a cylindrical section (shaded) of a saline icicle (Figure 4.2.1).

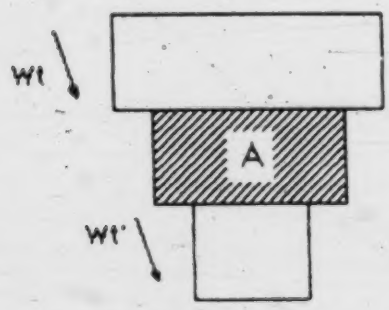

Figure 4.2.1

W_t is the brine flux to cylinder A and W_t' is the brine flux leaving cylinder A. The salt balance equation for A is (Makkonen, 1987):

$$W_t S_w = I S_i + (W_t - I) S_b \qquad (4.2.1)$$

where

I is the spongy ice growth rate on A.

S_w is the salinity of the brine entering A.

S_i is the salinity of the ice accretion on A.

S_b is the salinity of the brine leaving A.

The salinity is defined as the mass fraction of salt in the brine. It should be noted that accretion here means the spongy deposit on A. This accretion consists of ice, water, and salt. Dividing Equation (4.2.1) by $W_t S_b$, yields:

$$\frac{S_w}{S_b} = \frac{I}{W_t}\frac{S_i}{S_b} + (1 - \frac{I}{W_t}). \tag{4.2.2}$$

$\frac{I}{W_t}$ is the accretion fraction (the fraction of the incoming brine that remains on A) and is designated as F_r. Multiplying the left hand side of Equation (4.2.2) by S_i/S_i and using $F_r = \frac{I}{W_t}$, Equation (4.2.2) becomes:

$$\frac{S_i}{S_b}\frac{S_w}{S_i} = \frac{S_i}{S_b}F_r + (1 - F_r). \tag{4.2.3}$$

Letting $K = \frac{S_i}{S_w}$ and $K^* = \frac{S_i}{S_b}$, Equation (4.2.3) becomes:

$$K = \frac{K^*}{1 - (1 - K^*)F_r} \tag{4.2.4}$$

where K is called the effective distribution coefficient and K^* is called the interfacial distribution coefficient (Makkonen, 1987). According to Makkonen (1987), it can be shown that K^* is equal to the liquid fraction λ of the accretion. This can be shown as follows:

$$K^* = \frac{S_i}{S_b} = \frac{m_s/(m_i + m_s + m_w)}{m_s/(m_s + m_w)} = \frac{m_s + m_w}{m_i + m_s + m_w} = \lambda \tag{4.2.5}$$

where

m_s is the mass of salt in the ice matrix.

m_i is the mass of pure ice in the ice matrix.

m_w is the mass of pure water in the ice matrix.

It should be noted that $m_s/(m_s + m_w)$ is the salinity of the draining brine leaving A, which is assumed to be the same as the salinity of the entrapped brine pockets (see Figure 3.1.1). The liquid fraction λ of the accretion on the surface of a saline icicle has not yet been investigated. A value of $\lambda = 0.26$ is used for the present (Makkonen, 1987). In order to determine how good this assumption is, further experimental work is needed. By using $\lambda = 0.26$, Equation (4.2.4) may be written:

$$K = \frac{0.26}{1 - 0.74F_r}. \tag{4.2.6}$$

Since $K = \frac{S_i}{S_w}$ and $K^* = \frac{S_i'}{S_b}$, two expressions for S_i and S_b can be obtained:

$$S_i = \frac{0.26}{1 - 0.74F_r}S_w \tag{4.2.7}$$

$$S_b = \frac{1}{1 - 0.74F_r}S_w. \tag{4.2.8}$$

S_i and S_b are therefore related by:

$$S_i = 0.26S_b. \tag{4.2.9}$$

Equations (4.2.6) and (4.2.7) show that both S_i and S_b can be expressed as a function of the accretion fraction (F_r) on A, and the salinity of the brine influx to A. We will now consider other thermodynamical properties related to the surface of A.

1) The surface equilibrium temperature of A may be approximated by (Makkonen, 1987):

$$T_s = -54.0S_b - 600S_b^3 \qquad (4.2.10)$$

where S_b is expressed as a dimensionless fraction (g/g).

2) The equilibrium water vapor pressure over the surface of A at surface temperature T may be expressed as (Makkonen 1987):

$$e_s = (1 - 0.537S_b)e(T) \qquad (4.2.11)$$

where

e(T) is the equilibrium water vapor pressure over a pure water surface at temperature T.

3) The latent heat of fusion of the spongy accretion on A is (Makkonen, 1987):

$$L_{fs} = (1 - \frac{S_i}{S_b})L_f \qquad (4.2.12)$$

where

L_f is the latent heat of fusion for pure water at temperature T.

By using $S_i = 0.26S_b$, Equation (4.2.12) may be rewritten as:

$$L_{fs} = 0.74L_f. \qquad (4.2.13)$$

Because the equilibrium surface temperature could be well below 0°C, the effect of temperature on L_f has to be considered. Since the experiments were performed in the coldroom over a temperature range -5°C to -15°C, L_f is calculated as a function of temperature within that range. In this range, L_f is linearly related to T by the relation:

$$L_f = 2.24x10^3T + 3.334x10^5$$

where T is in °C and L_f is in Jkg^{-1}.

4) The specific heat capacity of the brine leaving A.

Consider x kg of brine with salinity S_b. Then, the amount of heat required to raise the temperature of the solution by ΔT is:

$$C_b x\Delta T = C_s m_s \Delta T + C_w m_w \Delta T. \qquad (4.2.14)$$

Dividing Equation (4.2.14) by $x\Delta T$, it becomes:

$$C_b = \frac{m_s}{x}C_s + \frac{m_w}{x}C_w. \qquad (4.2.15)$$

Since $\frac{m_s}{x} = S_b$ and $\frac{m_w}{x} = 1 - S_b$, then:

$$C_b = S_b C_s + (1 - S_b)C_w \qquad (4.2.16)$$

where C_w and C_s are the specific heat capacities of pure water and sea salt, respectively. m_s and m_w are the mass of sea salt and pure water, respectively. According to the literature on the heat capacity of seawater solutions published by Millers, Perron, and Desnoyers (1973), the specific heat capacity of brine (4 % salinity) at 0°C is smaller than that of pure water at 0°C by approximately 6%. This implies that the specific heat capacity of sea salt must be very much smaller than that of pure water. In addition, S_b is, most of the time, very much smaller than $(1 - S_b)$. Therefore, the first term of Equation (4.2.16) can be neglected. Thus, Equation (4.2.16) becomes:

$$C_b \simeq (1 - S_b)C_w. \qquad (4.2.17)$$

Since C_w is not strongly dependent on temperature, the value, 4218 $JKg^{-1}K^{-1}$, for 0°C is used.

5) The density of the brine leaving A.

By definition:

$$\rho_b = \frac{m_w + m_s}{V_b} \tag{4.2.18}$$

where V_b is the volume of brine leaving A.

But,

$$S_b = \frac{m_s}{m_s + m_w}. \tag{4.2.19}$$

Therefore,

$$m_s = \frac{S_b}{1 - S_b} m_w. \tag{4.2.20}$$

Substituting Equation (4.2.20) into Equation (4.2.18), using the fact that the density of pure water is simply $\frac{m_w}{V_b}$, and assuming that the dissolved salt does not affect the liquid volume, then the density of the brine leaving A can be calculated by:

$$\rho_b = (1 + \frac{S_b}{1 - S_b})\rho_w \tag{4.2.21}$$

where

ρ_w is the density of pure water.

6) The density of the accretion on A.

The overall density of the accretion, ρ_a, is defined to be:

$$\rho_a = \frac{m_w + m_s + m_i}{V} \tag{4.2.22}$$

where V is the total volume of the accretion. Let $m_b = m_w + m_s$ be the mass of the brine entrapped in the ice matrix, and rewrite V as $V_i + V_b$, the sum of the volume of pure ice and brine. Equation (4.2.22) can then be rewritten as:

$$\rho_a = \frac{m_b + m_i}{V_i + V_b}. \tag{4.2.23}$$

It has been shown in (4.2.5) that the liquid fraction of the accretion λ can be expressed as:

$$\lambda = \frac{m_s + m_w}{m_i + m_s + m_w} = \frac{m_b}{m_i + m_b} = K^*. \tag{4.2.24}$$

Rearranging this equation, yields:

$$m_b = \frac{\lambda}{1 - \lambda} m_i \tag{4.2.25}$$

Also, by definition:

$$V_i = \frac{m_i}{\rho_i} \text{ and } V_b = \frac{m_b}{\rho_b} \tag{4.2.26}$$

where ρ_i and ρ_b are respectively the densities of the pure ice and brine entrapped in the ice matrix. Substituting Equations (4.2.25) and (4.2.26) into Equation (4.2.23), yields:

$$\rho_a = \frac{\rho_i \rho_b}{(1 - \lambda)\rho_b + \lambda \rho_i}. \tag{4.2.27}$$

In the next two sections, the heat balance equations for the growth in diameter and in length will be formulated. Most of the formulations are similar to those in Chapter 2, except that the effect of salinity on the thermodynamic properties is included.

4.3 Growth rate in diameter

Consider the i^{th} cylinder of a saline icicle (see Figure 4.1.1). The surface temperature T_{si} is assumed to be the equilibrium freezing temperature. Supercooling is neglected since its effect on the heat balance is likely to be insignificant, as discussed in Chapter 2. The heat balance equation for the surface of the i^{th} cylinder may therefore be written:

$$q_{convi} + q_{evapi} + q_{radi} = q_{chi} + q_{freezei} \tag{4.3.1}$$

This equation is similar to equation (2.3.1) except that a new term q_{chi} has been added. This term results from the fact that the surface temperatures of the cylinders are different from one another. When the brine flows from the $(i-1)^{th}$ cylinder to the i^{th} cylinder, its temperature has to fall from $T_{s(i-1)}$ to T_{si} before freezing takes place. Thus this term is a source of heat on the i^{th} cylinder. The three terms on the left hand side of Equation (4.3.1) have the same meaning as those in Equation (2.3.1). These terms can be parameterized as follows:

$$q_{convi} = h_{wi}(T_{si} - T_a) \tag{4.3.2}$$

$$q_{evapi} = h_{wi}\frac{0.622L_e}{C_p P_a}(e_s(T_{si}) - \frac{r}{100}e(T_a)) \tag{4.3.3}$$

$$q_{radi} = \sigma a(T_{si} - T_a) \tag{4.3.4}$$

where

h_{wi} is the heat transfer coefficient for the i^{th} cylinder (see Appendix A).

$e_s(T_{si})$ is the saturation vapor pressure over a brine surface at the surface temperature of the i^{th} cylinder, T_{si}.

$e(T_a)$ is the saturation vapor pressure over a pure water surface at temperature T_a.

$e_s(T_{si})$ and $e(T_a)$ can be calculated using Equations (2.2.5) and (4.2.10). The calculation of h_{wi} is described in Appendix A.

The fourth term, q_{chi}, may be calculated by:

$$q_{chi} = \frac{W_{ti}C_{bi}}{D_i \pi \Delta L_i}(T_{s(i-1)} - T_{si}) \tag{4.3.5}$$

where

W_{ti} is the brine flux to the i^{th} cylinder.

C_{bi} is the specific heat capacity of the brine entering the i_{th} cylinder.

D_i is the diameter of the i^{th} cylinder.

ΔL_i is the length of the i^{th} cylinder.

It should be noted that ΔL_i is different for different i, because the length growth rate is different for different i. W_{ti} may be calculated by subtracting the amount of brine lost due to freezing, brine trapping, and evaporation, on each of the i-1 cylinders lying above i, from the initial supply rate. Thus:

$$W_{ti} = W_o - \Sigma Loss_j. \tag{4.3.5a}$$

The summation here is from j = 1 to j = i - 1. Referring to Equation (2.2.9), $\Sigma Loss_j$ can be calculated by replacing the mean diameter and total length of the entire icicle by the diameter and length of the j^{th} cylinder alone Thus:

$$W_{ti} = W_o - \Sigma \Delta L_j \pi D_j [\rho_{aj} \frac{dR_j}{dt} + h_{wj} \frac{0.622}{C_p P_a}(e_s(T_{sj}) - \frac{f}{100} e(T_a))]. \tag{4.3.5b}$$

It should be noted again that the summation is from j = 1 to j = i - 1.

The fifth term, $q_{freezei}$, is calculated according to:

$$q_{freezei} = \frac{L_{fs}\, dM_i}{A_i\ dt} \tag{4.3.6}$$

where

A_i is the surface area of the i^{th} cylinder.

$\frac{dM_i}{dt}$ is the rate of spongy ice growth on the i^{th} cylinder.

$\frac{dM_i}{dt}$ is calculated from:

$$\frac{dM_i}{dt} = A_i \frac{dR_i}{dt} \rho_{ai} \tag{4.3.7}$$

where

$\frac{dR_i}{dt}$ is the radial growth rate.

ρ_{ai} is the density of the accretion on the i^{th}cylinder.

By substituting Equation (4.3.7) into Equation (4.3.6), $q_{freezei}$ becomes:

$$q_{freezei} = \rho_{ai} L_{fs} \frac{dR_i}{dt}. \tag{4.3.8}$$

Now using Equations (4.3.2),(4.3.3),(4.3.4),(4.3.5), and (4.3.8), Equation (4.3.1) can be expressed in the following form:

$$h_{wi}(T_{si} - T_a) + h_{wi}\frac{0.622L_e}{C_p P_a}(e_s(T_{si}) - \frac{r}{100}e(Ta)) + \sigma a(T_{si} - T_a) =$$

$$\frac{W_{ti} C_{bi}}{D_i \pi \Delta L_i}(T_{s(i-1)} - T_{si}) + \rho_{ai} L_{fs} \frac{dR_i}{dt}. \tag{4.3.9}$$

Equation (4.3.9) can be solved directly to determine $\frac{dR_i}{dt}$. This equation is applied to each of the cylinders in turn in order to calculate their individual radial growth rates. A flowchart is

given in appendix C to show how Equation (4.3.9) is solved.

4.4 Growth rate in length

The heat balance equation for the hemispherical pendant drop is given by:

$$q_{conv(n+1)} + q_{evap(n+1)} + q_{rad(n+1)} = q_{drip(n+1)} + q_{freeze(n+1)}. \quad (4.4.1)$$

The subscripts n+1 represents the pendant drop, where a cylindrical segment with the same diameter as the pendant drop is going to form. The length of this cylindrical segment is determined by the rate of heat transfer between the pendant drop and the air. The heat transfer terms on the left hand side of Equation (4.4.1) can be formulated as:

$$q_{conv(n+1)} = h_{t(n+1)}(T_{s(n+1)} - T_a) \quad (4.4.2)$$

$$q_{evap(n+1)} = h_{t(n+1)} \frac{0.622L_e}{C_p P_a}(e_s(T_{s(n+1)}) - \frac{r}{100}e(T_a)) \quad (4.4.3)$$

$$q_{rad(n+1)} = \sigma a(T_{s(n+1)} - T_a) \quad (4.4.4)$$

where

$h_{t(n+1)}$ is the heat transfer coefficient for the pendant drop (see Appendix B).

$e_s(T_{s(n+1)})$ is the saturation vapor pressure over a brine surface at the surface temperature of the pendant drop.

$e(T_a)$ is the saturation vapor pressure over a pure water surface at temperature T_a.

$e_s(T_{s(n+1)})$ and $e(T_a)$ are calculated using Equations (2.2.5) and (4.2.11). The calculation of $h_{t(n+1)}$ is shown in Appendix B.

The fourth term, $q_{drip(n+1)}$, as mentioned in Chapter 2, results from the fact that the pendant drop is initially formed at the wall temperature but leaves the tip at a slightly lower

temperature. In the case of a saline icicle, the equilibrium temperature difference between the last (n^{th}) cylinder and the pendant drop also has to be taken into account. Thus,

$$q_{drip(n+1)} = \frac{2W_{t(n+1)}C_{b(n+1)}}{\pi d^2}(\Delta T_{sd} + \Delta T_{fd}) \qquad (4.4.5)$$

where

$W_{t(n+1)}$ is the brine flux leaving the tip to form the pendant drop.

d is the diameter of the pendant drop.

$C_{b(n+1)}$ is the specific heat capacity of the brine leaving the tip to form the pendant drop.

ΔT_{sd} is the supercooling of the pendant drop.

ΔT_{fd} is the difference in equilibrium temperature between the pendant drop and the n^{th} cylinder.

The calculation of $W_{t(n+1)}$ is similar to that shown in Chapter 2 for the case of a pure icicle. However, with the use of the time step method for the present case, Equation (2.2.9) is used to calculate the brine lost on each cylinder. Hence, the mean diameter and the total length in Equation (2.2.9) has to be replaced by the diameter and the length of the i^{th} cylinder. Then, the brine lost on all the cylinders is summed up, and the total brine loss calculated. Finally, $W_{t(n+1)}$ is simply calculated from $W_o - \Sigma Loss_i$, where the summation over i is from 1 to n. Thus:

$$W_{t(n+1)} = W_o - \Sigma\Delta L_i \pi D_i[\rho_{ai}\frac{dR_i}{dt} + h_{wi}\frac{0.622}{C_p P_a}(e_s(T_{si}) - \frac{r}{100}e(T_a))]. \qquad (4.4.6)$$

To calculate ΔT_{sd}, Eqution (2.2.14) will be used, since the crystalization velocity under supercooled brine is not known at present. Further investigation of this topic is necessary in order to get more accurate results in the simulation model. Thus:

$$\Delta T_{sd} = 44.05(\frac{dL}{dt} - \frac{dR_n}{dt})^{0.588} \qquad (4.4.7)$$

ΔT_{fd} can simply be calculated by:

$$\Delta T_{fd} = T_{sn} - T_{s(n+1)} \tag{4.4.8}$$

By substituting Equations (4.4.6), (4.4.7) and (4.4.8) into Equation (4.4.5), $q_{drip(n+1)}$ can then be calculated.

The last term $q_{freeze(n+1)}$ has the same form as Equation (2.2.16), because we assume the same mechanism for dendritic ice formation in the saline pendant drop. Hence:

$$q_{freeze(n+1)} = 2L_f\rho_i\delta\frac{d-\delta}{d^2}\frac{dL}{dt} \tag{4.4.9}$$

It is not known whether the thickness of the ice shell formed in the saline pendant drop will be the same as that formed in the pure water pendant drop. However, they are assumed to be the same. Since $d >> \delta$, Equation (4.4.9) can be written as:

$$q_{freeze(n+1)} \approx 2L_f\rho_i\frac{\delta}{d}\frac{dL}{dt}. \tag{4.4.10}$$

With the use of Equations (4.4.2), (4.4.3), (4.4.4), (4.4.5), and (4.4.10), Equation (4.4.1) becomes:

$$h_{t(n+1)}(T_{s(n+1)} - T_a) + h_{t(n+1)}\frac{0.622L_e}{C_p P_a}(e_s(T_{s(n+1)}) - \frac{r}{100}e(T_a)) +$$

$$\sigma a(T_{s(n+1)} - T_a) =$$

$$\frac{2W_{t(n+1)}C_{b(n+1)}}{\pi d^2}(\Delta T_{sd} + \Delta T_{fd}) + 2L_f\rho_i\frac{\delta}{d}\frac{dL}{dt}. \tag{4.4.11}$$

Equation (4.4.11) is a non-linear equation and cannot be solved analytically. The bisection

method (see Appendix C) has been adopted to solve it. By solving Equations (4.3.9) and (4.4.11) together, the growth rates in diameter and in length can be completely described. To calculate the new diameter for each cylinder after time Δt, the following equation can be used:

$$D_i = D_{i(t-\Delta t)} + 2\frac{dR_i}{dt}\Delta t. \tag{4.4.12}$$

Then the volume mean diameter, is given by:

$$D_{mean} = \frac{\Sigma \Delta L_i D_i}{\Sigma \Delta L_i}. \tag{4.4.13}$$

The calculation of the total length after Δt is quite simple:

$$L = \frac{dL}{dt}\Delta t + \Sigma \Delta L_i \tag{4.4.14}.$$

where $\frac{dL}{dt}$ is calculated from (4.4.11).

It should be noted that the summations in Equations (4.4.13.) and (4.4.14) are from i = 1 to i = n.

4.5 Growth in mass

The mass of a saline icicle can be calculated by summing up the total mass of ice growth in each cylinder during Δt, and the mass of the newly formed cylinder at the tip, then adding this total mass increment to the mass of the saline icicle at the end of the previous time step. In equation form, this can be written as:

$$M_{wall} = \Sigma \Delta L_i \pi D_i \rho_{ai} \frac{dR_i}{dt}\Delta t \tag{4.5.1}$$

$$M_{tip} = \frac{\pi}{4} d^2 \rho_{a(n+1)} \frac{dL}{dt}\Delta t \tag{4.5.2}$$

$$M_{t+\Delta t} = M_t + M_{wall} + M_{tip} \qquad (4.5.3)$$

where

M_{wall} is the total increment of mass on the surface of each cylinder during time step Δt.

M_{tip} is the mass of the newly formed cylinder at the tip during a given time step.

M_t is the total mass at time t.

$M_{t+\Delta t}$ is the total mass at time $t + \Delta t$

The brine inside the ice shell formed under the tip will eventually freeze and become spongy ice. Hence, in calculating M_{tip}, it is assumed that the liquid core in the newly formed cylinder at the tip is frozen. Then, using Equation (4.2.27), the accretion density ($\rho_{a(n+1)}$) of this newly formed cylinder can be calculated. In other words, in calculating M_{tip} the unfrozen brine in the core is also included.

4.6 Drip rate

The drip rate of the pendant drops can be calculated by:

$$F = \frac{\text{mass flux leaving the tip}}{\text{mass of one pendant drop}}$$

Hence:

$$F = \frac{6W_{t(n+1)}}{\pi d^3 \rho_{b(n+1)}} \qquad (4.6.1)$$

where

F is the drip rate.

ρ_{bn+1} is the density of the pendant drop.

4.7 Discussion of assumptions

There are several assumptions that have been made in order to solve the heat balance equations to yield the growth in diameter and in length. In the following section, these assumptions, and their effects on the growth of the saline icicle, will be discussed.

4.7.1 Homogeneous liquid film thickness

It has been assumed that for each of the cylinders of the saline icicle, the brine film is uniformly distributed about the circular circumference of the icicle. However, from observations of growing saline icicles in the coldroom, it has been discovered that after the saline icicles have grown to certain sizes, the brine film is unevenly distributed, and a preferred flowing path develops. Because of this preferred flowing path, ice growth can only form on the side with the brine. As a result, the entire surface of each cylinder may not be at its equilibrium freezing temperature (Johnson, 1987). This may lead to a temperature gradient across the cylinder and internal heat conduction may occur. However, since a saline icicle is spongy and contains numerous brine pockets inside the ice matrix, it is unlikely that the surface of the cylinder could cool significantly below the equilibrium freezing temperature (Johnson, 1987). Thus, the effect of radial heat conduction within the cylinder is neglected.

4.7.2 Circular cross section

Another effect of the preferred flowing path is that the saline icicle does not retain a circular cross section. Since ice can only grow on the side where the brine is flowing, a cross section with an elliptical shape will develop. Incorporating this changing shape with time into the present model would be a very complicated task and is beyond the scope of this thesis. Therefore, a circular cross section is assumed. However, when comparing model and experimental results, the model diameters will be compared with the geometrical mean diameters of the experimental icicles.

4.7.3 Vertical heat conduction

Because the saline icicle is divided into different cylindrical sections and each cylinder has a different surface temperature (decreasing downward), there could be a downward heat conduction through the cylinder. If this is the case, a vertical heat conduction term has to be incorporated into the heat balance equation. Nonetheless, as mentioned in Section 4.7.1, the conductivity of spongy ice is low. Thus, any vertical heat conduction flux through the cylinders should be small and is neglected in the heat balance equation.

5. Model implementation

All the equations involved in calculating the growth of a saline icicle have been programmed into a computer in Fortran VS 77 language. The program is listed in Appendix C.

A cylinder corresponding to the zeroth time step is assumed to be the initial condition. This cylinder is assumed to have the diameter and length of a pendant drop (see Figure 5.1). The length of this cylinder is simply the radius of the pendant drop. Clearly, the volume of this cylinder is different from that of the pendant drop. However, this is a small error in the initial conditions which does not amplify with time. The growth in radius and in length of this cylinder can be calculated by the heat balance equations formulated in Chapter 4. In the model, a time step of 2 minutes is used. The reasons for using 2 minutes as the time step has been discussed in Section 4.1. However, a time step of 1 minute has also been tried and the difference in the prediction of final length and mass is only a few percent. Figure 5.1 illustrates how the simulation proceeds.

Several parameters need to be mentioned here. The values of some of these parameters are different for the pure and saline cases. These parameters are i) the liquid fraction, ii) the diameter of the pendant drop, and iii) the thickness and diameter of the dendritic shell growing at the tip.

i) The liquid fraction

For the pure water case, the liquid fraction is assumed to be zero, which means the icicle is essentially solid. This is different from Makkonen's (1988) model assumption where $\lambda = 0.26$. The reason for using the zero liquid fraction assumption is that it gives better agreement with the experiment than $\lambda = 0.26$ for the present model. For the saline water case, a value of 0.26 is used for the liquid fraction, as suggested by Makkonen(1987) for sea spray icing.

ii) The diameter of the pendant drop

The size of the pendant drop of a pure icicle is slightly different from that of a saline icicle, because pure water and saline water have different densities and surface tensions. An

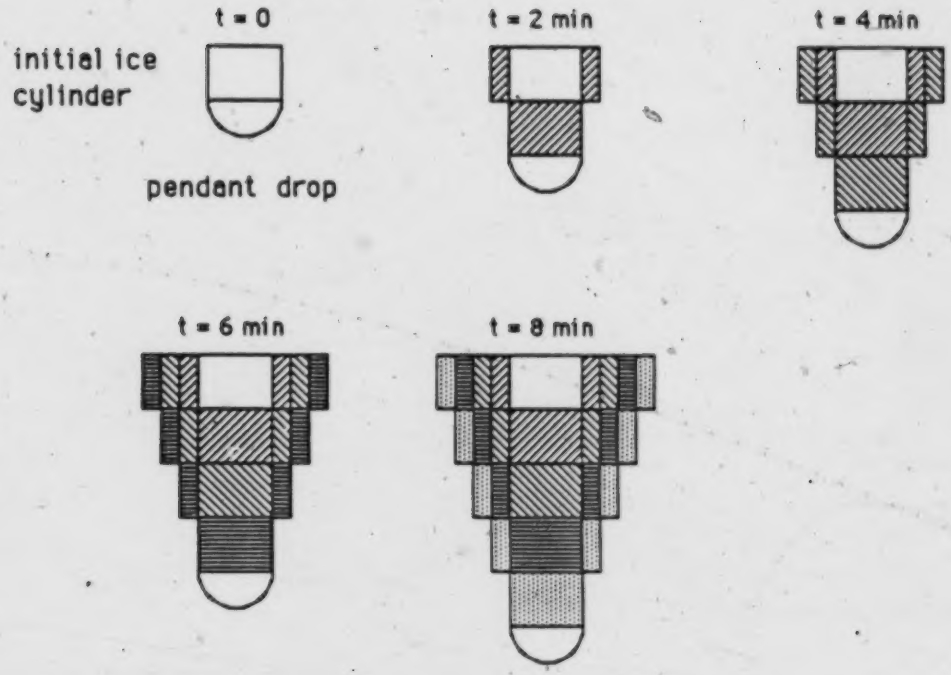

Figure 5.1 Schematic illustration of how the simulation proceeds.

Table 5.1

Pendant drop size for a pure icicle grown in an independent experiment

Trials #	Number of drops collected	Total mass of the collected drops (g)
1	50	3.50 g
2	50	3.48 g
3	50	3.27 g
4	50	3.49 g
5	50	3.12 g
Total	250	16.86 g

Average pendant drop mass = 0.06744 g

Average pendant drop diameter = 5.05 mm

average diameter of the pendant drops for a pure icicle grown in the cold room has been determined to be 5.05 mm (see Table 5.1). It is assumed that the pendant drop size is independent of the environmental conditions. Hence, the value 5.05 mm is used as the diameter of the pendant drops of pure icicles for all cases. This value obtained in Table 5.1 is a little greater than the values suggested by Makkonen (1988) (4.88 mm) and Johnson (1987) (5.0 mm).

Since the salinity of the pendant drop on a saline icicle increases with time, a direct measurement of the size of the pendant drop by collecting and weighing a large number of them is inappropriate. However, the diameter of the pendant drop for a saline icicle can be estimated by making use of the diameter of the pendant drop for a pure icicle. Suppose a hemispherical pendant drop for a certain liquid hanging at the tip of the icicle is under mechanical equilibrium (Figure 5.2a). If liquid is supplied to the pendant drop, it will grow bigger and its weight will increase while the vertical component of surface tension goes down, so the pendant drop falls (Figure 5.2b). Before calculating the radius of the pendant drop, one assumption must be made. This is that the diameter of the tip of the icicle = the diameter of the pendant drop at equilibrium = the diameter of the falling drop. Then, the radius of the pendant drop can be calculated as follows (Clift et al. 1978):

$$2\pi r\sigma = \frac{1}{\psi}\left(\frac{4}{3}\pi r^3 \rho g\right) \tag{5.1}$$

where

σ is the surface tension of the liquid.

ρ is the density of the liquid.

g is the gravitational constant = 9.8 ms^{-2}.

ψ is the Harkins factor which results from the fact that a residual drop remains at the tip when the pendant drop falls, causing the volume of the pendant drop to be less than the volume at which the net gravity force exactly balances the surface tension forces (Clift, et al. 1978).

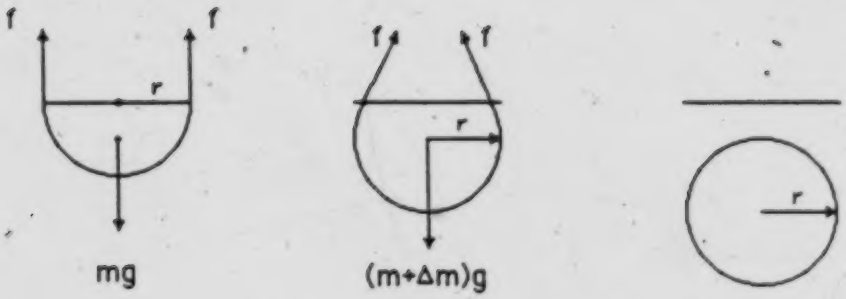

a) Equilibrium b) Non-equilibrium

f = Surface tension force

Figure 5.2 Schematic description of how a pendant drop falls. It has been assumed that the diameter of the pendant drop in a) is the same as that of the falling drop in b).

Solving equation (5.1) for r, yields:

$$r = (\psi \frac{3\sigma}{2\rho g})^{1/2} \tag{5.2}$$

This result can be applied to both pure water and brine. Then, two equations for r_f and r_s are obtained:

$$r_f = (\psi \frac{3\sigma_f}{2\rho_f g})^{1/2} \tag{5.3}$$

$$r_s = (\psi \frac{3\sigma_s}{2\rho_s g})^{1/2} \tag{5.4}$$

where

r_f is the radius of the pendant drop for a pure icicle.

r_s is the radius of the pendant drop for a saline icicle.

σ_f is the surface tension of pure water.

σ_s is the surface tension of brine.

ρ_f is the density of pure water.

ρ_s is the density of brine.

It should noted that, for lack of information, the Harkins factor for pure water and brine are assumed to be the same. Dividing Equation (5.3) by (5.2), r_s can be expressed in terms of r_f:

$$r_s = (\frac{\rho_f}{\rho_s} \frac{\sigma_s}{\sigma_f})^{1/2} r_f. \tag{5.5}$$

The average salinity of the pendant drops for six experiments on growing saline icicles was measured by using a Fisher Hand salinometer (Catalog Number 11-800-0). Since this salinometer is not very accurate and there was no other salinometer available, a calibration of the salinometer was performed. By comparing the measured salinometer reading for fifteen

prepared brine solutions with their known salinities, a calibration table was constructed. The calibration is given in Appendix E. Then, the ice/brine mixture in the beaker, which was a collection of the pendant drops throughout the entire experiment, was melted and its salinity measured. An average salinity of 5.4 % for the pendant drops was obtained (see Table 5.2). According to a report on the thermal properties of salt solutions published by Walta(1966), σ_s is greater than σ_f by approximately 1% for a salinity (NaCl solution) of 5.4%. It should be noted that "salinity" means the mass fraction of salt in the solution. The brine used in the experiment is made of Rila Marine Mix (Obreiter, 1987). NaCl is the major component of this sea salt. Lacking a knowledge of the thermodynamic properties of the other salt components, NaCl solution with a salinity of 5.4 % was used in the model as an approximation to the brine pendant drop with an average salinity of 5.4 %. Thus, it can be concluded that $\sigma_s \simeq 1.01\sigma_f$ in the present case. Therefore, equation (5.4) becomes:

$$r_s = \left(\frac{1.01\rho_f}{\rho_s}\right)^{1/2} r_f. \qquad (5.6)$$

Using $\rho_f = 1000\ \text{kgm}^{-3}$, $\rho_s = 1057\ \text{kgm}^{-3}$ for a salinity of 5.4 %, and $r_f = 2.525$ mm, a value of 2.468 mm is obtained for r_s. It can be seen that r_s is less than r_f by only 3 %. Therefore, we can conclude that salinities up to 5.4 % do not cause a significant effect on the diameter of the pendant drop.

iii) The thickness and diameter of the dendritic shell growing at the tip

The thickness of the dendritic shell for pure icicles has been estimated to be 75μm (Makkonen 1988). This value will also be used for saline icicles since no other data are available. The validity of this assumption should be checked in future experiments. In both cases, the diameter of the dendritic shell is assumed to be the same as the diameter of the pendant drop. Thus:

$$d_f = 5.05 \text{ mm}$$

Table 5.2

The salinities of the pendant drops
for various air conditions
(Salinity of the feed brine = 3.3 %)

Experiment Case #	Average salinity of the pendant drops (%)
7	6.0 %
8	5.0 %
9	5.6 %
10	5.1 %
11	5.6 %
12	5.2 %

The average salinity of the pendant drops for all cases = 5.4 %.

The environmental conditions for the above experiments are given in Appendix D.

$d_s = 4.94$ mm

where d_f is the diameter of the dendritic shell growing at the tip of a pure water icicle.

d_s is the diameter of the dendritic shell growing at the tip of a saline icicle.

6. Model predictions

The present mathematical model can simulate the growth of both saline and pure icicles. By using the model, not only the growth in length, diameter, and mass can be calculated as a function of time, but also the equilibrium surface temperatures and surface and pendant drop salinities for saline icicles. In the following sections, the sensitivity of the model and some simulated results for both saline and pure icicles will be presented and discussed. Since seawater has a salinity of about 3 %, a feedwater salinity of 3 % is used in this chapter for all the simulations of the growth of saline icicles.

6.1 Sensitivity of the model

It happens in both pure and saline icicle growth that the length growth rates reach a maximum sometime after the initiation of growth. In pure icicle growth, the length growth rate reaches a maximum just before the water stops dripping at the tip. But, in saline icicle growth, the length growth rate reaches a maximum at the time (well before the growth in length stops) when the rate of heat transfer from the pendant drop to the environment is a maximum. Figures 6.1.1 to 6.1.5 show how this maximum length growth rate $(dL/dt)_{max}$ is affected by the air temperature (Ta), relative humidity (R), air pressure (Pa), wind speed (V), and supply rate (Wo) for saline and pure icicle growth. The curves marked with circles represent pure icicles, and those marked with squares represent saline icicles. From these figures, it can be seen that $(dL/dt)_{max}$ is very sensitive to Ta and V for both the saline and pure icicles. Figure 6.1.1 shows that $(dL/dt)_{max}$ increases almost linearly with decreasing T_a. Equation (4.4.11) can be used to explain this. In this equation, dL/dt is related to T_a linearly in the q_{conv} and q_{rad} terms, but exponentially in the q_{evap} term. Since q_{evap} is not the dominant factor in Equation (4.4.11) (Johnson, 1987), it only slightly affects the linear relation shown in Figure 6.1.1. Figure 6.1.2 shows that $(dL/dt)_{max}$ increases approximately parabolically with increasing V. This implies that the effect of changes in V on the absolute value of $(dL/dt)_{max}$ is greater at low values of V. This can be explained by examining Equations (4) and (5) in Appendix B (Makkonen, 1988), and (4.4.11) in Chapter 4. From

Equations (4) and (5) in Appendix B, it can be seen that $N_{ut} \propto V^{1/2}$, but $h_t \propto N_{ut}$. Therefore, $h_t \propto V^{1/2}$. Then, from Equation (4.4.11), dL/dt is linearly related to h_t. Hence, dL/dt is also related to $V^{1/2}$. Because of this relation, for $V < 1$ m/s, dL/dt can vary by a factor of ~ 2 with an uncertainity of $\pm$ 0.5 m/s in the wind speed. In all cases, $(dL/dt)_{max}$ is greater for pure icicles than for saline icicles, becuse pure icicles always grow faster than saline icicles. The curves for the pure icicles are less smooth than the curves for the saline icicles. This is a problem of time resolution. Since saline icicles grow at a much slower rate than fresh water icicles, the saline curve is less sensitive to the time resolution of the model, and hence, is smoother than the fresh water curve. By decreasing the time step to 1 min, the curves for the pure icicle become smoother. The relative humidity (R) and air pressure (Pa) have only a slight effect on $(dL/dt)_{max}$ for both the saline and pure icicles, as shown in Figures 6.1.3 and 6.1.4. Figure 6.1.5 shows how $(dL/dt)_{max}$ is affected by the supply rates, Wo, for pure and saline icicles growth. It can be seen that $(dL/dt)_{max}$ is insensitive to Wo for pure icicle growth but decreases slowly with increasing supply rates for saline icicle growth. The reason is that for the case of pure icicle, (dL/dt) mainly depends on the water flux flowing to the tip. Therefore, under indentical environmental conditions, $(dL/dt)_{max}$ does not vary much with supply rates. For the case of saline icicle, however, dL/dt not only depends on the brine flux flowing to the tip, but also the salinity of the pendant drop, because it can affect the equilibrium surface temperature of the pendant drop. $(dL/dt)_{max}$ for pure icicles is higher than the $(dL/dt)_{max}$ for saline icicle by approximately a factor of two for all conditions, with regard to the above five parameters, and for the range of cases considered here.

The sensitivity tests of the present model show that Ta and V are both important factors affecting the growth of icicles. Therefore, these two parameters should be carefully measured during experiments on growing both saline and pure icicles. In addition, Wo is also an important factor affecting the growth of saline icicle. The sensitivity of the model presented here is qualitatively consistent with the results of Johnson (1987) and Makkonen (1988) on pure icicles.

In the following sections, standard environmental conditions of air temperature Ta = -15°C, relative humidity R = 80%, air pressure Pa = 1000 mb, supply rate Wo = 50 mg/s, and wind speed V = 2.0 m/s are chosen for the model simulation of the growth of both pure and saline icicles. A total duration of 120 minutes and a time step of 2 minutes are also used.

6.2 Model prediction of icicle length and growth rate

It is shown in Figure 6.2.1 that the pure icicle grows faster than the saline icicle. For this case, the saline icicle stops growing in length 42 minutes after the pure icicle does. The faster growth rate outweighs the effect of a shorter growth time, however, so that the final predicted length of the pure icicle is longer than that of the saline icicle by about 6 cm. The length growth rate of the pure icicle increases with time, and then it suddenly stops growing at 54 minutes. This occurs because the water supply freezes entirely on the wall and, hence, there is no water left to form the pendant drop and the growth in length stops.

The length growth rate of the saline icicle also increases with time, but at a much slower rate, over the first 42 minutes. After this, the growth rate starts to decrease and the growth stops at 96 minutes. This initially increasing and then decreasing growth rate of saline icicles has been discussed in Section 3.2. It occurs because the equilibrium temperature of the pendant drop decreases with time in response to its increasing salinity. The rate of heat transfer associated with the pendant drop increases with decreasing drip rate, and decreases with decreasing equilibrium temperature of the pendant drop (see Equations 4.4.11 and 4.2.10). During the early growth of a saline icicle, the effect of drip rate on the rate of heat transfer of the pendant drop is dominant. Since the drip rate decreases with time (see figure 6.2.3), the growth rate increases with time. However, later, the effect of the declining equilibrium temperature on the rate of heat transfer of the pendant drop is dominant. Consequently, the growth rate decreases with time. Eventually, the equilibrium temperature of the pendant drop equals the air temperature, the rate of heat transfer from the pendant drop to the air is essentially zero, and the growth stops (see Figures 6.2.1 and 6.2.2). The simulations show that, unlike the pure icicle, when the growth in length stops, the drip rate of

the saline icicle is not zero (see Figure 6.2.4). Rather it decreases slowly with time (see Figure 6.2.3). This can be explained by the fact that as the pendant drops form around the tip without freezing, they continue to fall. However, for the case of the pure icicle, the equilibrium temperature of the pendant drop is essentially constant (0 °C). Therefore, dL/dt always increases with decreasing drip rate. When there is no more water entering the tip to form the pendant drop (drip rate = 0), the growth in length stops (see Figure 6.2.4). Thus, the model predicts, somewhat paradoxically, that the growth of pure icicles stops precisely at the time the growth rate is a maximum.

Figure 6.2.2 shows the growth rate (dL/dt) as a function of time, for both saline and pure icicles. This figure is actually a reflection of Figure 6.2.1. For the pure icicle, dL/dt increases rapidly with time until 54 minutes, then it drops to zero. This implies a sudden cut-off in the growth due to the reasons explained in Section 6.2. For the saline icicle, dL/dt increases slowly and almost linearly with time for about 42 minutes. Subsquently, dL/dt starts to decrease to zero at 96 minutes. The reasons for this behaviour have also been discussed above.

6.3 Model prediction of diameter variation with length

Figures 6.3.1 and 6.3.2 show the profile of the icicle diameter as a function of length at the time when they stop growing in length and at 120 minutes. In the first figure, the pure icicle has a mean diameter of 1.53 cm, while the saline icicle has a mean diameter of 2.36 cm. In the second figure, the pure icicle has a mean diameter of 2.80 cm, while the saline icicle has a mean diameter of 2.74 cm. For this case, at the end of the growth in length, the saline icicle therefore has a bigger mean diameter than the pure icicle. This occurs because the saline icicle stops growing in length at 96 minutes, while the pure icicle stops growing in length at 54 minutes. This gives the saline icicle 42 minutes more to grow radially. Consequently, when comparing their mean diameters at the same time, as in Figure 6.3.2, the pure icicle has a bigger mean diameter because of the higher rate of heat transfer in the pure water case. This result seems to be true for other conditions as well. Another noteworthy feature of Figure

6.3.1, is that the saline icicle, at the end of its growth in length, has a higher maximum diameter/length ratio than the pure icicle. The reasons for this were discussed in Chapter 3.

6.4 Predicted growth in mass

The predicted growth in mass as a function of time for pure and saline icicles, grown under otherwise identical conditions, is shown in Figure 6.4.1. For this case, the mass of the pure icicle is always larger than that of the saline icicle because of the higher rate of heat transfer for the pure water case. Figure 6.4.1 also shows that the mass growth rate of the pure and saline icicles initially increases with time. Then, at 54 minutes for the pure water case (the time when the pure icicle stops growing in length) and at 96 minutes for the saline case (the time when the saline icicle stops growing in length), the mass growth rates become constant. Another noteworthy feature of Figure 6.4.1 is that the mass growth is apparently quadratic up to the point where the growth in length stops. This can be explained as follows: The mass growth rate of an icicle is given by the: mass flux from the root less the mass flux of water dripping from the tip. Because the drip rate decreases with time and the supply rate is constant, the mass growth rate increases with time.

In concluding this section, it should be mentioned that Sections 6.2 to 6.5 describe the model's predictions for length, diameter, and mass for only one environmental condition. In fact, there are numerous ways to analyze the model's predictions by using different air conditions, salinities, and supply rates. A complete sensitivity study of the model is beyond the scope of this thesis. Instead, the emphasis will be on intercomparisons with experiments. In Chapter 8, the model's predictions will be compared with the experimental results for both pure and saline icicles.

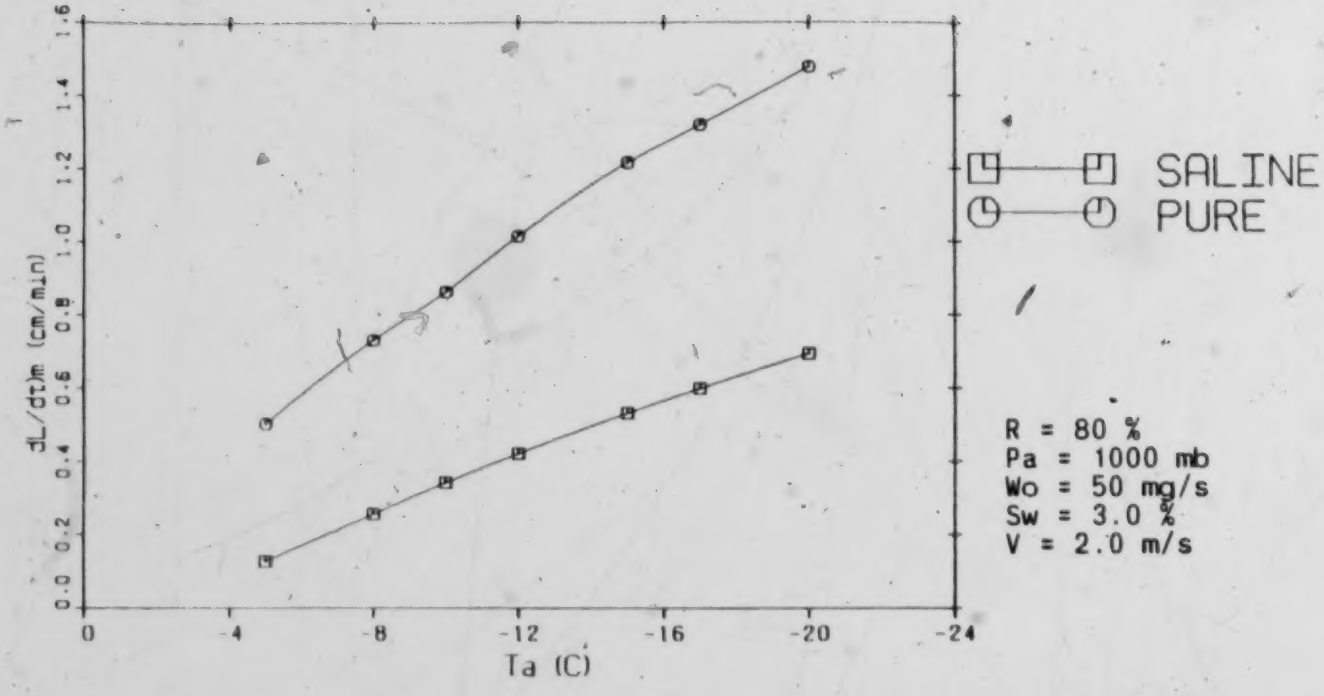

Figure 6.1.1 The maximum length growth rate dL/dt)m (cm/min) vs air temperature (C) for both pure and saline icicle growth.

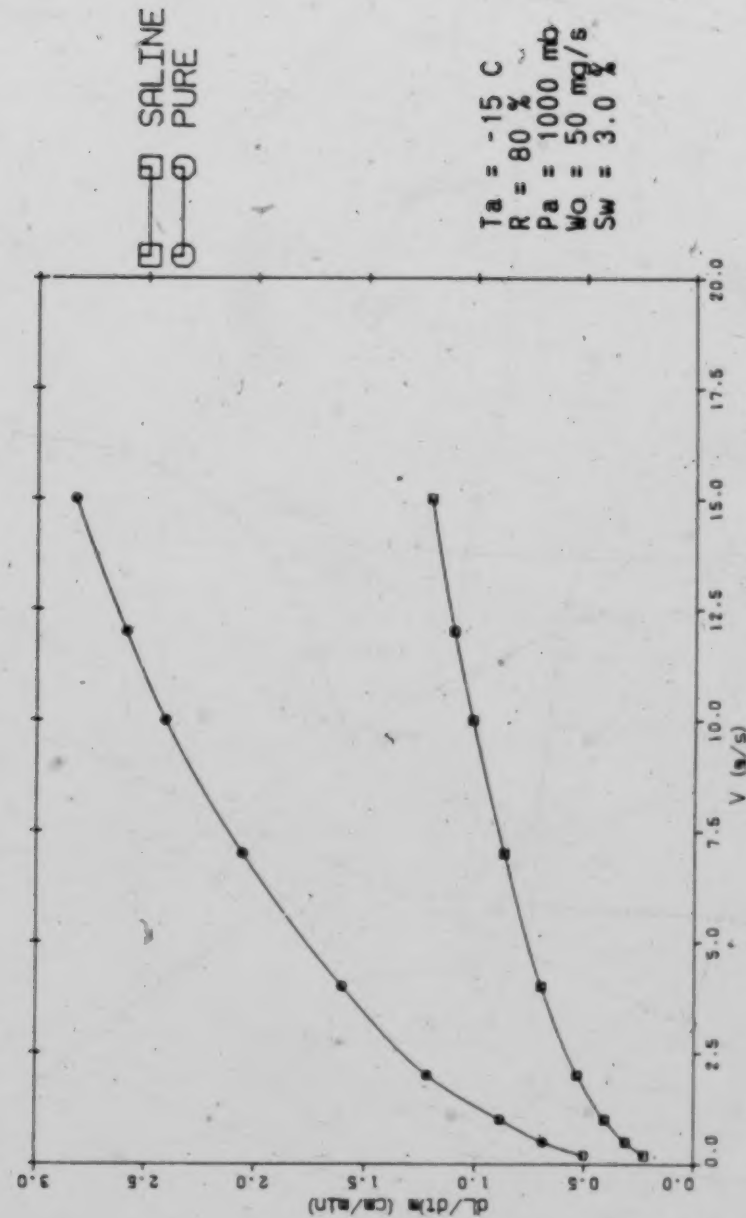

Figure 6.1.2 The maximum length growth rate dL/dt)m (cm/min) vs wind speed V (m/s) for both pure and saline icicle growth. Natural convection occurs at V = 0.02 m/s.

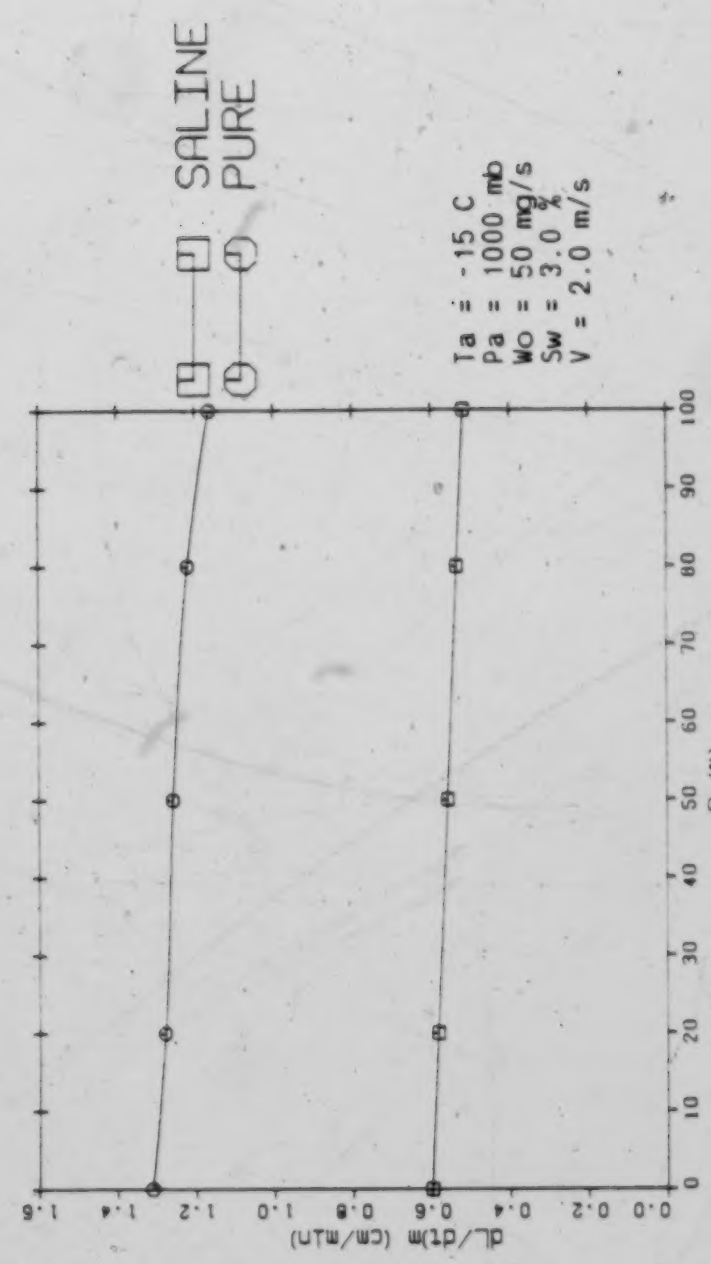

Figure 6.1.3 The maximum length growth rate dL/dt)m (cm/min) vs relative humidity (%) for both pure and saline icicle growth.

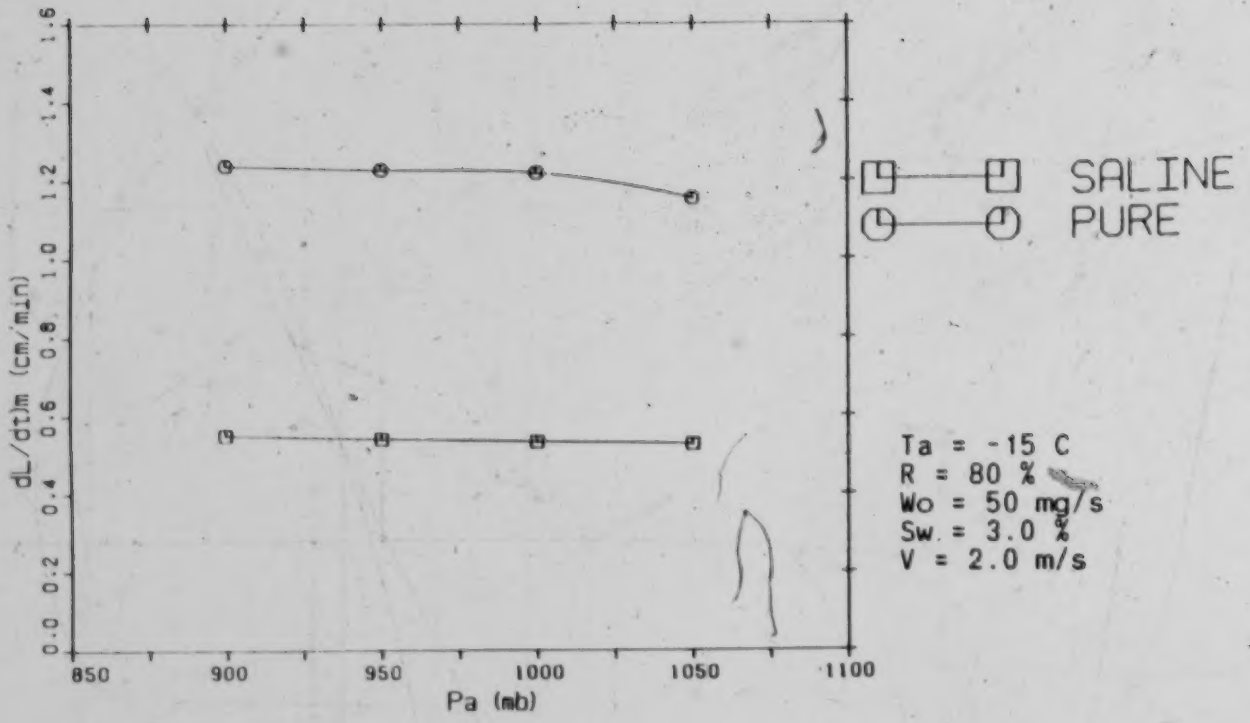

Figure 6.1.4 The maximum length growth rate dL/dt)m (cm/min) vs air pressure (mb) for both pure and saline icicle growth.

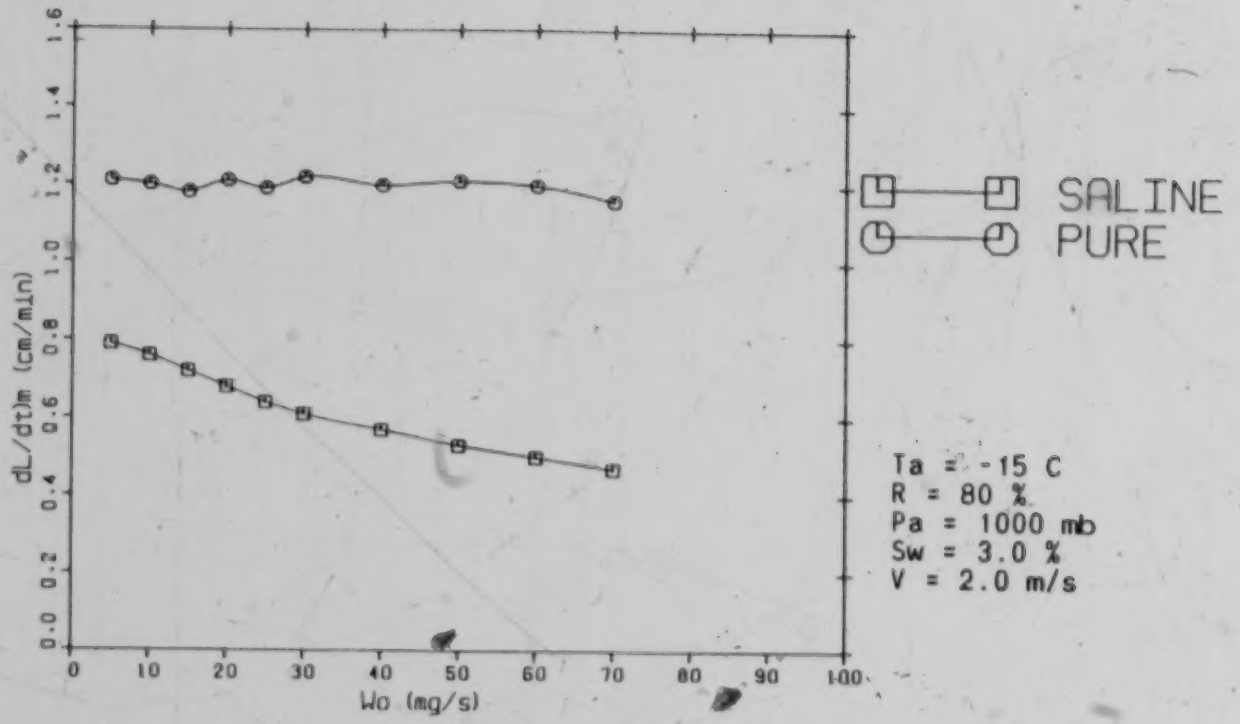

Figure 6.1.5 The maximum length growth rate dL/dt)m (cm/min) vs supply rate Wo (mg/s) for both pure and saline icicle growth.

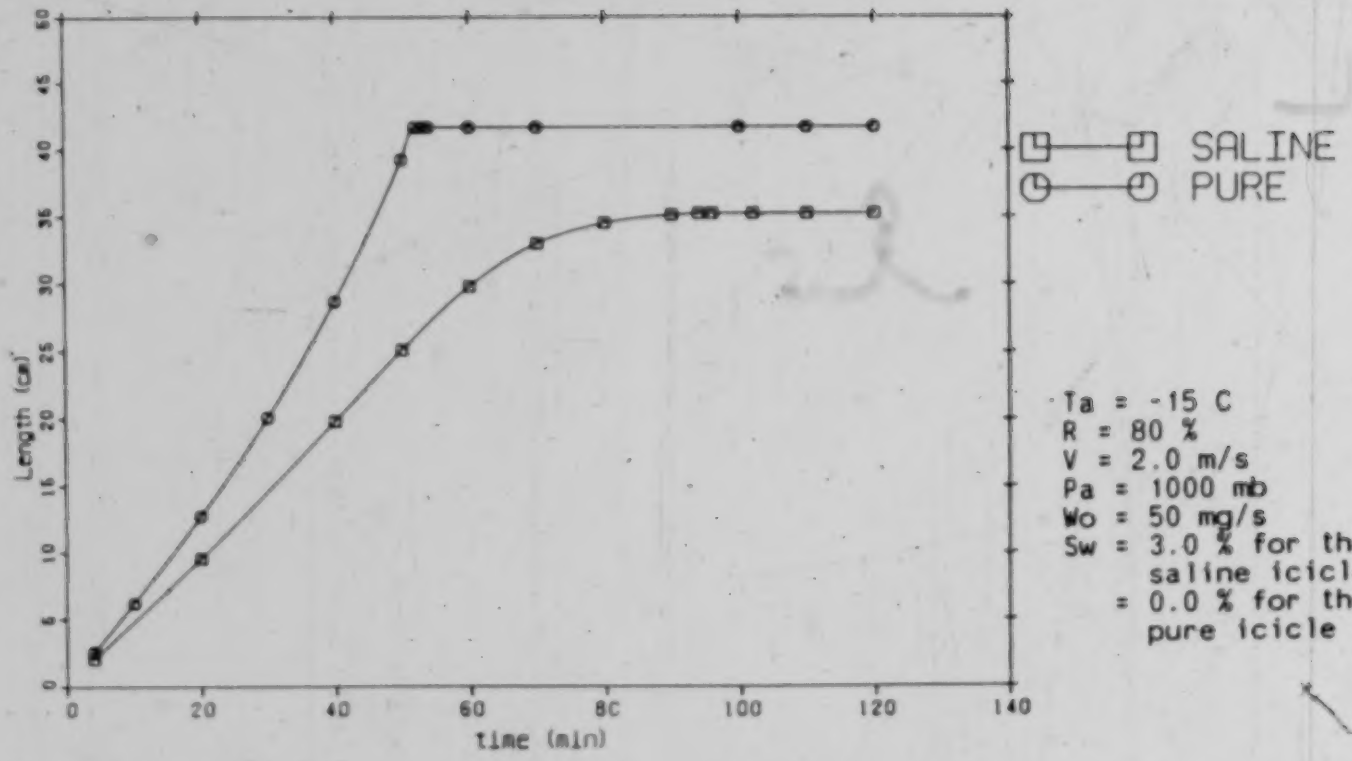

Figure 6.2.1 The length L (cm) vs time (min) for a pure and saline icicle.

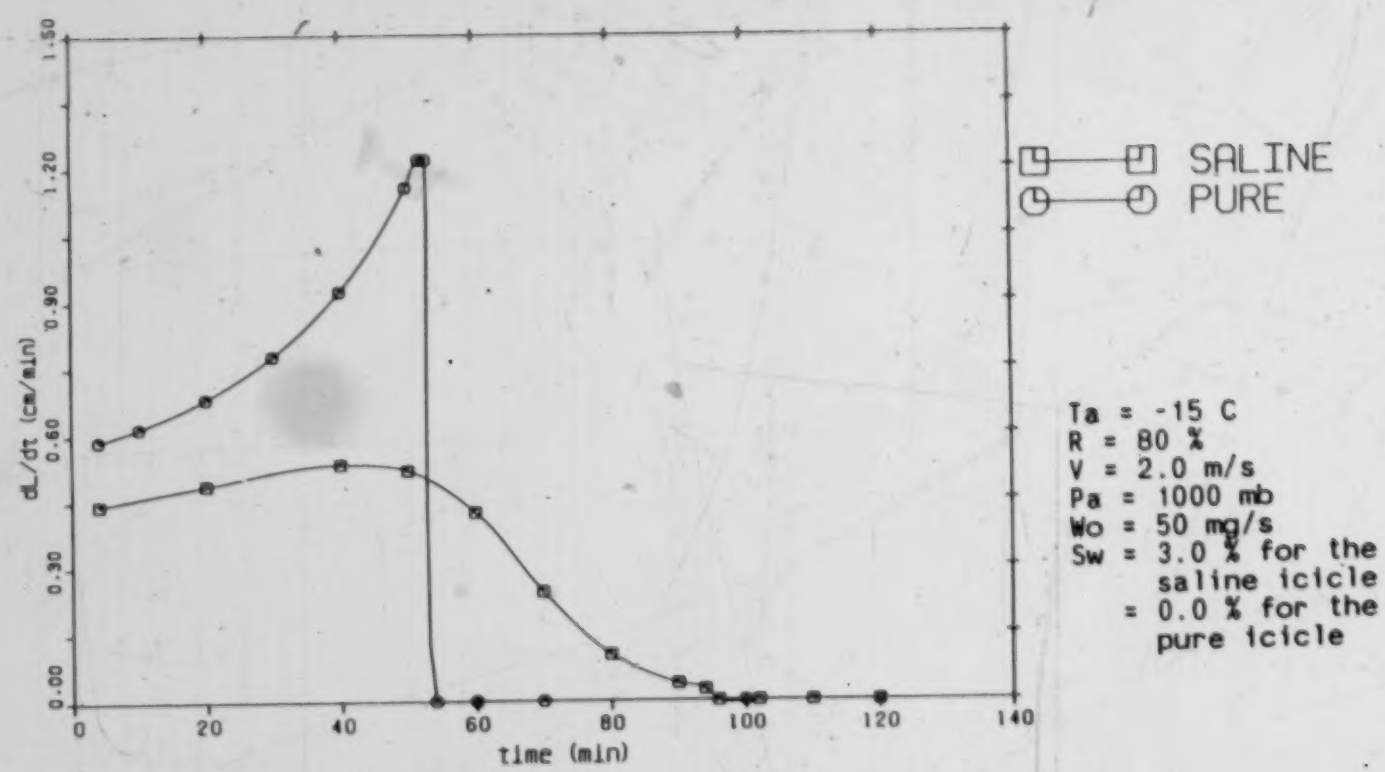

Figure 6.2.2 The length growth rate dL/dt (cm/min) vs time (min) for a pure and saline icicle.

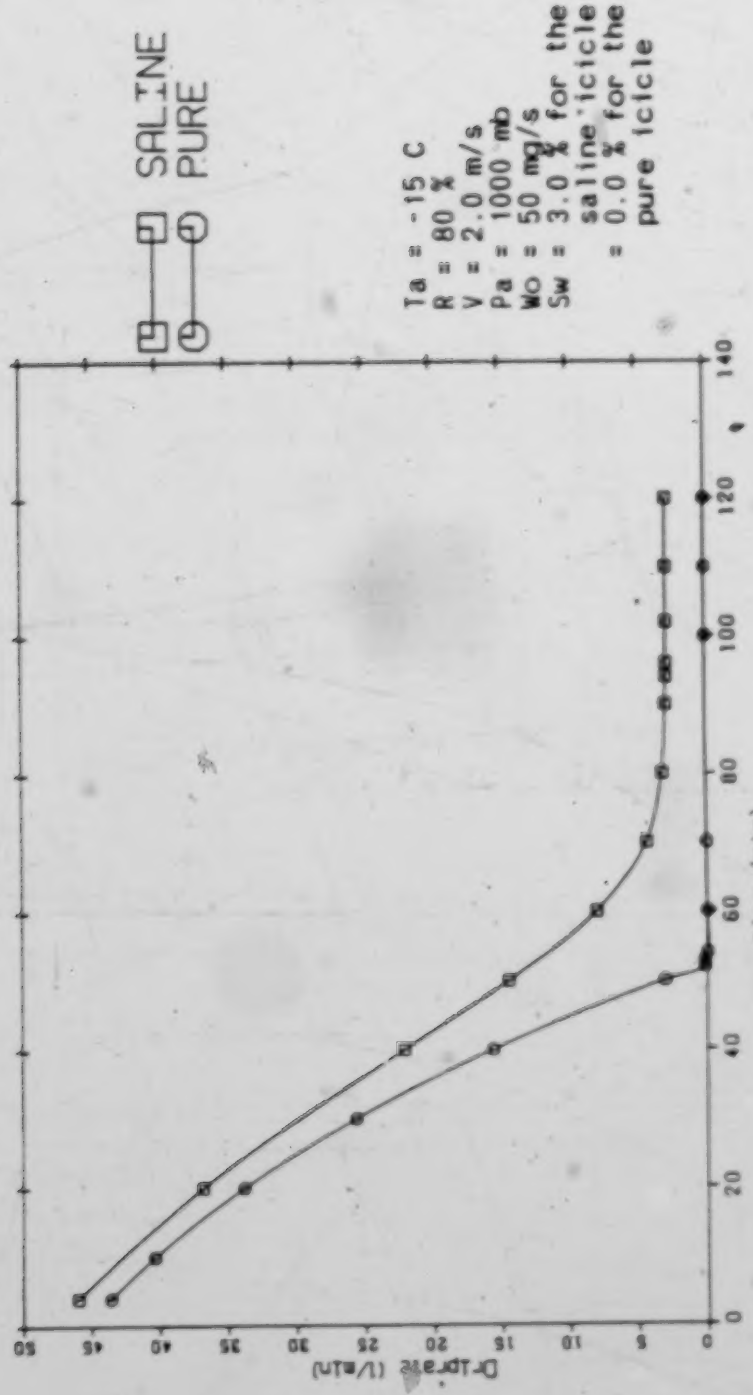

Figure 6.2.3 The Drip rate (l/min) vs time (min) for a pure and saline icicle.

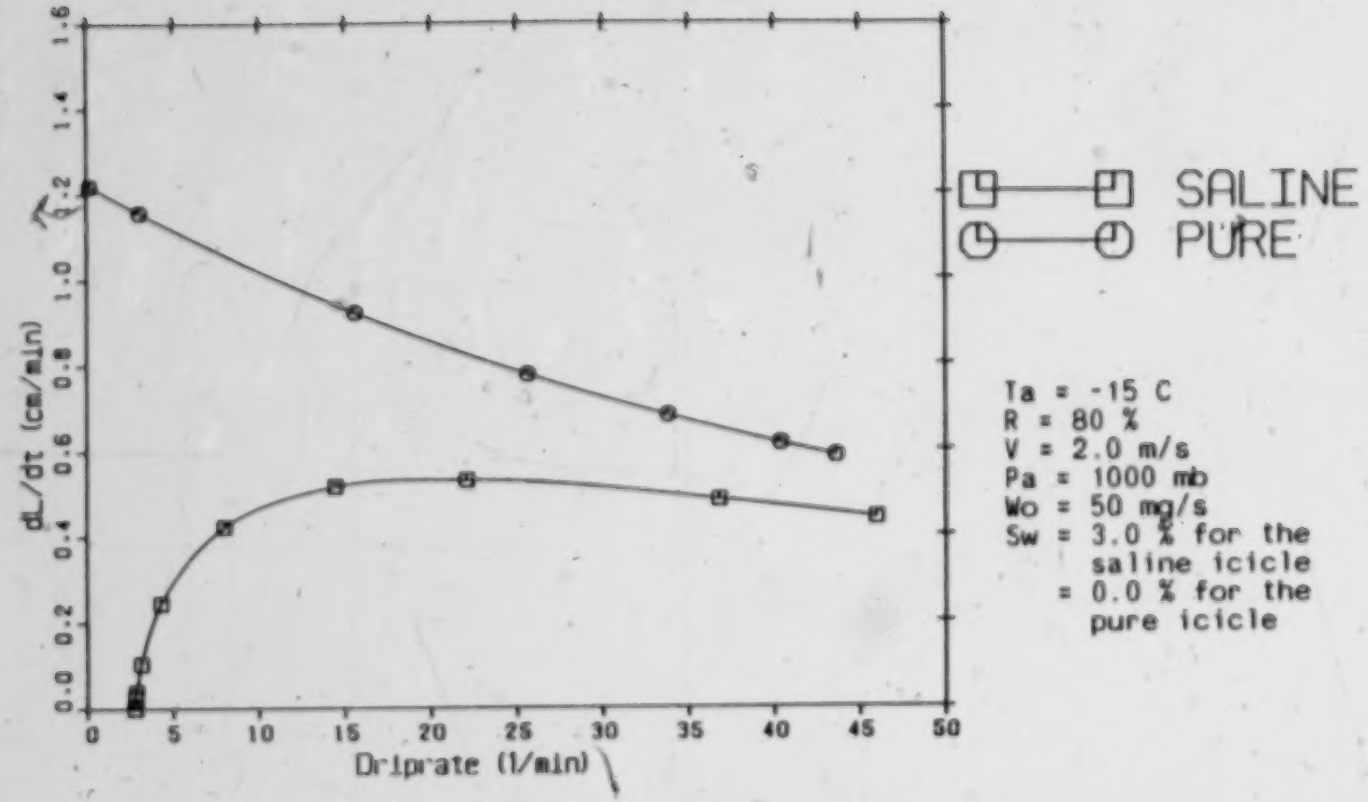

Figure 6.2.4 The length growth rate dL/dt (cm/min) vs Drip rate (1/min) for a pure and saline icicle.

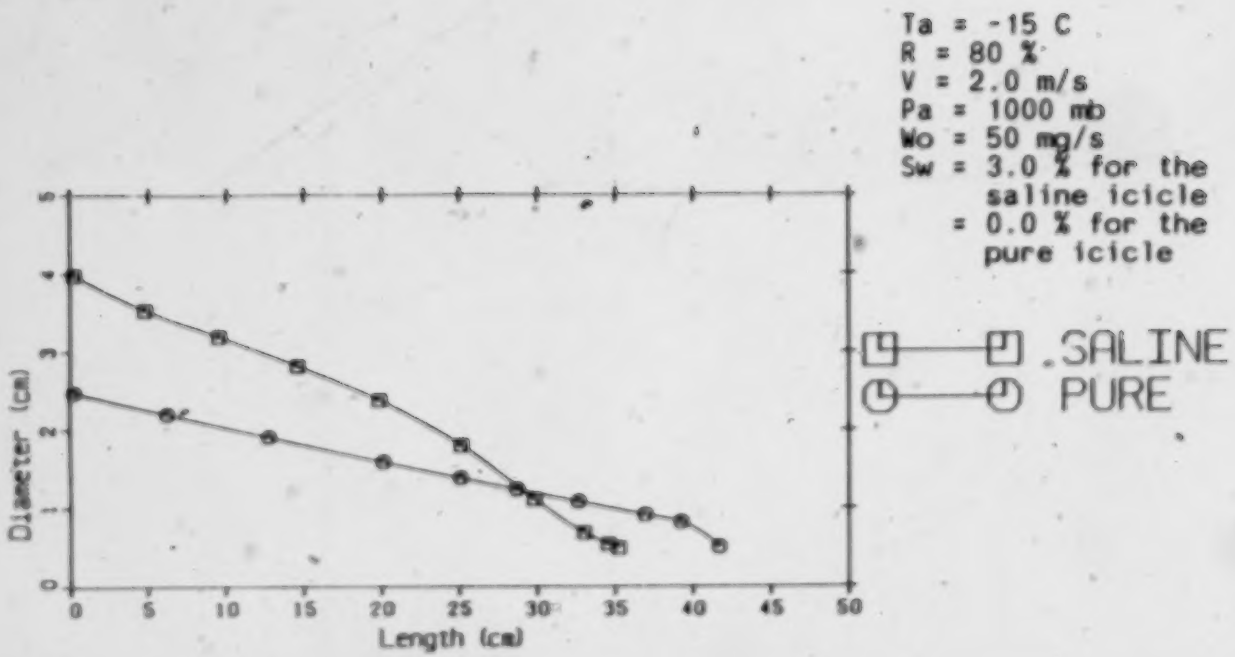

Figure 6.3.1 The profiles of the diameters (cm) of the pure and saline icicles as a function of distance (cm) from the root at the time when the growth in length stops.
The pure icicle stops growing in length at t = 54 min.
The saline icicle stops growing in length at t = 96 min.

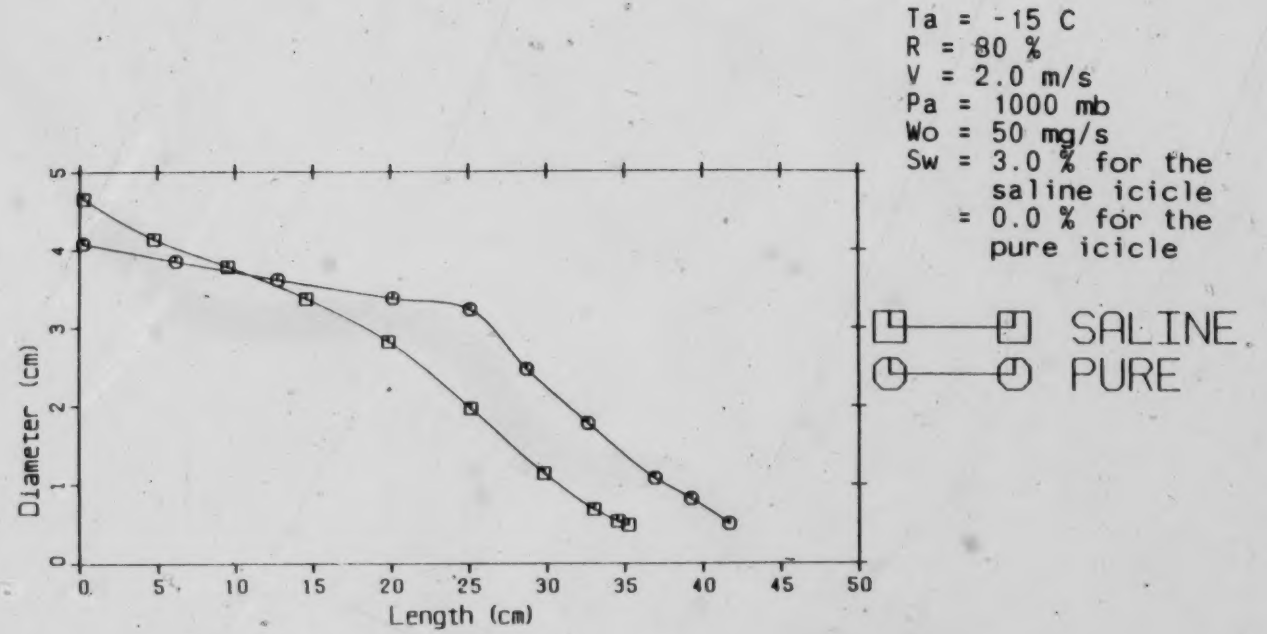

Figure 6.3.2 The profiles of the diameters (cm) of the pure and saline icicles as a function of distance (cm) from the root at time t = 120 min.

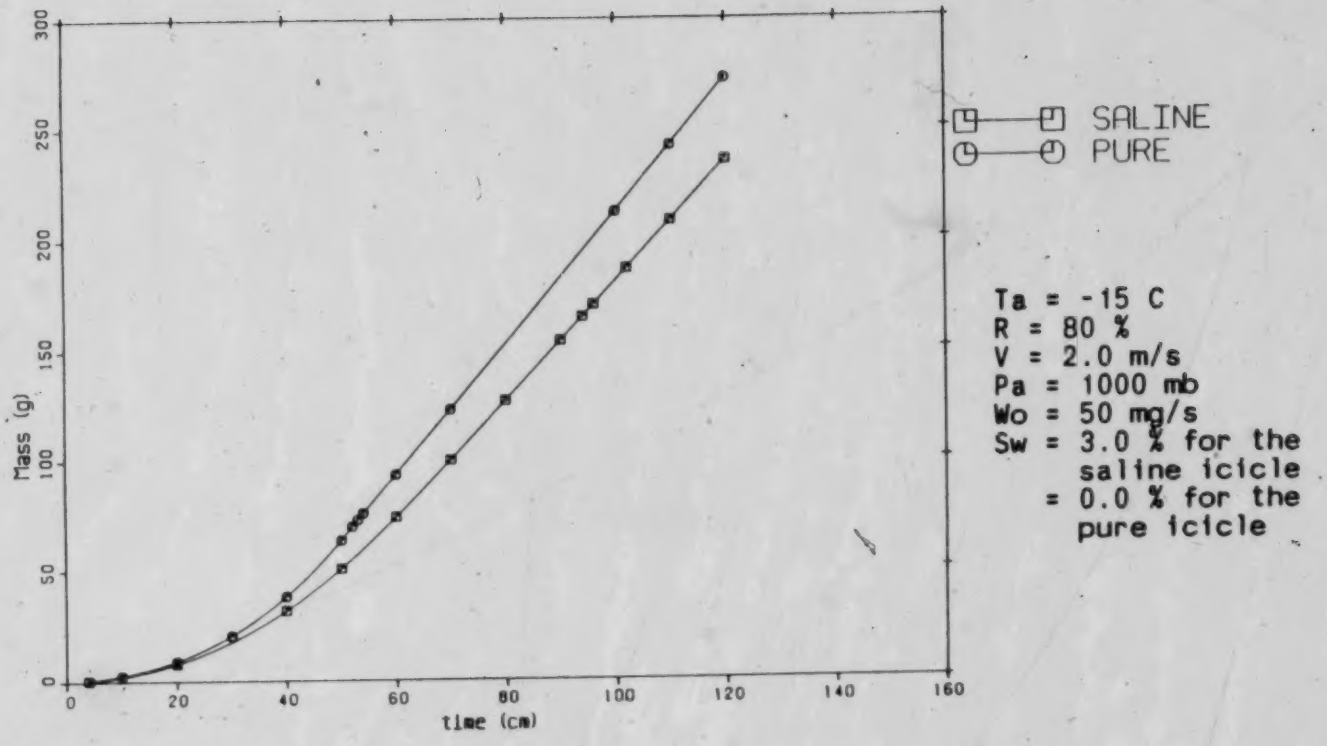

Figure 6.4.1 The masses (g) of pure and saline icicles as a function of time (min).

7. Icicle growth experiments

In order to produce icicles in the laboratory, a supply of liquid with a temperature slightly above the freezing point by 0.5 °C to 1 °C is allowed to drip onto a collection point which is exposed to a cold environment. This is a very tedious task. If the supply liquid's temperature is too low, the liquid will freeze before dripping onto the collection point. If it is too high, no icicle forms. Consequently, it is very important to adjust the temperature of the supply liquid to be close to the freezing point, if realistic icicles are to be produced. But, what happens in nature is that ice is melted by the heat of the Sun. This melted water flows onto a collection point such as a roof which is exposed to a cold environment. Then, as it runs off, this melted water (~0 °C) is frozen again and icicles form. Over northern seas, however, icicles are formed through the spraying of supercooled brine droplets onto the superstructures of ships.

In addition to the feedwater temperature, the flow rates, air temperature, and wind speed also have to be controlled in the experiments. Two sets of experiments were performed in the cold room of the Division of Meteorology. In the first six experiments, pure icicles were produced under various air conditions and flow rates. In the next seven experiments, saline icicles were produced by using simulated seawater of 33 o/oo salinity under various air conditions and flow rates. The simulated seawater was prepared by dissolving Rila Marine Mix (Obreiter, 1987) in tap water. The thirteen experiments were performed in the cold room over the temperature range -7 °C to -15 °C. The reason of using this range is that if the temperature in the cold room is is too high (>7 °C), it takes too long to complete one experiment, especially for the case of saline icicle (see appendix D for the duration of the experiments). On the other hand, if the temperature is <15 °C, pure icicles rarely form in nature. Saline icicles can still form under this temperature, but in open sea areas, the air temperature is very unlikely to be below -15 °C. Therefore, the limited set of experiments in the cold room cover the relevant temperature range. However, the experiments did not cover a wide range of wind speed because of the limitions of the cold room. The results of these two sets of experiments will be compared with the model's predictions in Chapter 8.

7.1 Pure icicle growth experiments

To grow pure icicles in the cold room, tap water, with a temperature slightly above freezing, was allowed to drip onto a fixed glass rod (7 mm in diameter) so that an icicle would grow below the rod. The apparatus used to achieve this is shown in Figure 7.1.1.

7.1.1 Temperature and flowrate of the water supply

It was mentioned above that the temperature of the water supply has to be controlled in order to produce realistic icicles. To do this, an insulated bath of ice water (1.5 liters) was used as the water source. A 2 mm (inside diameter) burette was connected to the container so that the water could flow through it. By adjusting the valve of the burette, a desired flow rate could be obtained. Since the burette was exposed to the cold air (<0°C), the water flowing out of it was very likely supercooled. After a short while, water froze inside the burette. To avoid this problem, a heating wire was wrapped around the burette. This heating wire was connected to a variable power supply. By adjusting the power supply, the amount of heat generated could be roughly controlled. The heating wire and the burette were wrapped with a piece of foil-backed fibreglass insulation to reduce heat loss to the air. With this design, freezing of water inside the burette was prevented. It has been mentioned that the water dripping out from the burette should be close to 0°C. In order to achieve this criterion, attention was paid to the ice dome that grew on the upper side of the rod. If the dome was melting, the temperature of the supply water was considered to be too high. The power supply was then turned down. On the other hand, if the ice dome was growing rapidly, the temperature of the water supply was considered to be too low, and the water inside the burette could freeze. In this case, the power supply was turned up. In other words, as long as the ice dome was neither melting nor growing very fast, the temperature of the solid/liquid interface on the dome was very likely close to 0 °C. Consequently, the water flowing from the ice dome to the root of the icicle should also have been close to 0 °C. This was very tedious work and required careful observation and attention. An automatic system for controlling the supply temperature would have been preferable.

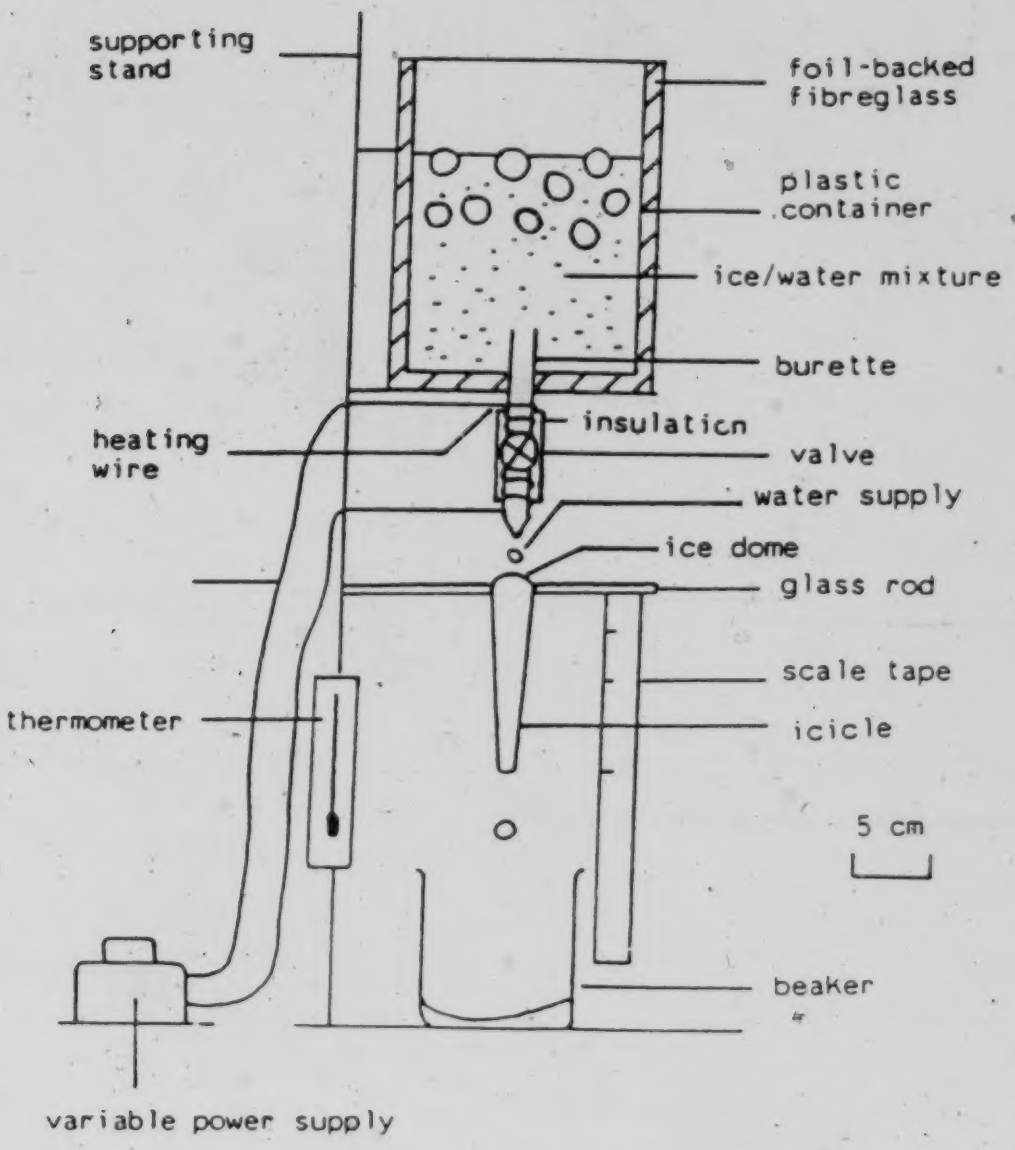

Figure 7.1.1 The apparatus used in the coldroom to grow pure icicles.

The flowrate from the burette, which was determined by counting the drops falling onto the rod, was found to vary with time, even if the valve was fixed. Consequently, the valve had to be adjusted repeatedly in order to minimize the variation in the flowrate. The reason for the varying flowrate is not known, but it may have to do with ice in the burette. Because of these problems with the temperature of the supply water and the constancy of the flowrate, a good quantitative result was not easy to obtain. Further improvements to the apparatus are highly recommended.

7.1.2 Air temperature, wind speed, relative humidity, and air pressure

During the experiments, the air temperature in the cold room was constant to within ± 1 °C. An average temperature was computed after observing the temperature every 15 minutes during the course of an experiment. The temperature was measured with an alcohol in glass thermometer mounted on the stand (Figure 7.1.1).

The airspeed at the location where the icicles were grown varied with time and height. This turbulent wind was generated by the two cooling system fans located near the roof of the cold room. The wind speed, averaged over 30 minutes, was measured by using a wind run anemometer, oriented into the wind direction at 6 different heights, ranging from the table top to a little above the glass rod, at the location where the icicle was grown. The response time of the wind run anemometer is approximately a few seconds. The 30 minute average wind speeds (ranging from 0.47 m/s to 0.77 m/s) at different heights were then averaged again to obtain an overall mean (weighted average) wind speed (see Table 7.1.2 and Figure 7.1.2). These measurements were performed before the experiments. However, it was found that the wind direction and the wind speed at different heights did not vary with time very much regardless of the air temperature and the days of operation. An overall mean wind speed of 0.7 m/s was obtained at the spot where the pure icicles were grown.

The relative humidity in the cold room was measured after every experiment by using an Assman psychrometer. Since relative humidity is not a primary factor controlling the growth of icicles (see Section 5.1), accurate measurements were not necessary. These

Table 7.1.2

The measured mean wind speed at different heights ranging from the table top to a little above the rod at the locations where pure icicles and saline icicles were grown

Saline icicle

Height locations	Mean wind speed
16 cm	0.89 m/s
31 cm	0.92 m/s
48 cm	0.50 m/s
58 cm	0.36 m/s
63 cm	0.34 m/s
67 cm	0.24 m/s

The weighted average wind speed = 0.6 m/s

Pure icicle

Height locations	Mean wind speed
16 cm	0.74 m/s
31 cm	0.47 m/s
48 cm	0.73 m/s
58 cm	0.76 m/s
63 cm	0.77 m/s
67 cm	0.55 m/s

The weighted average wind speed = 0.7 m/s.

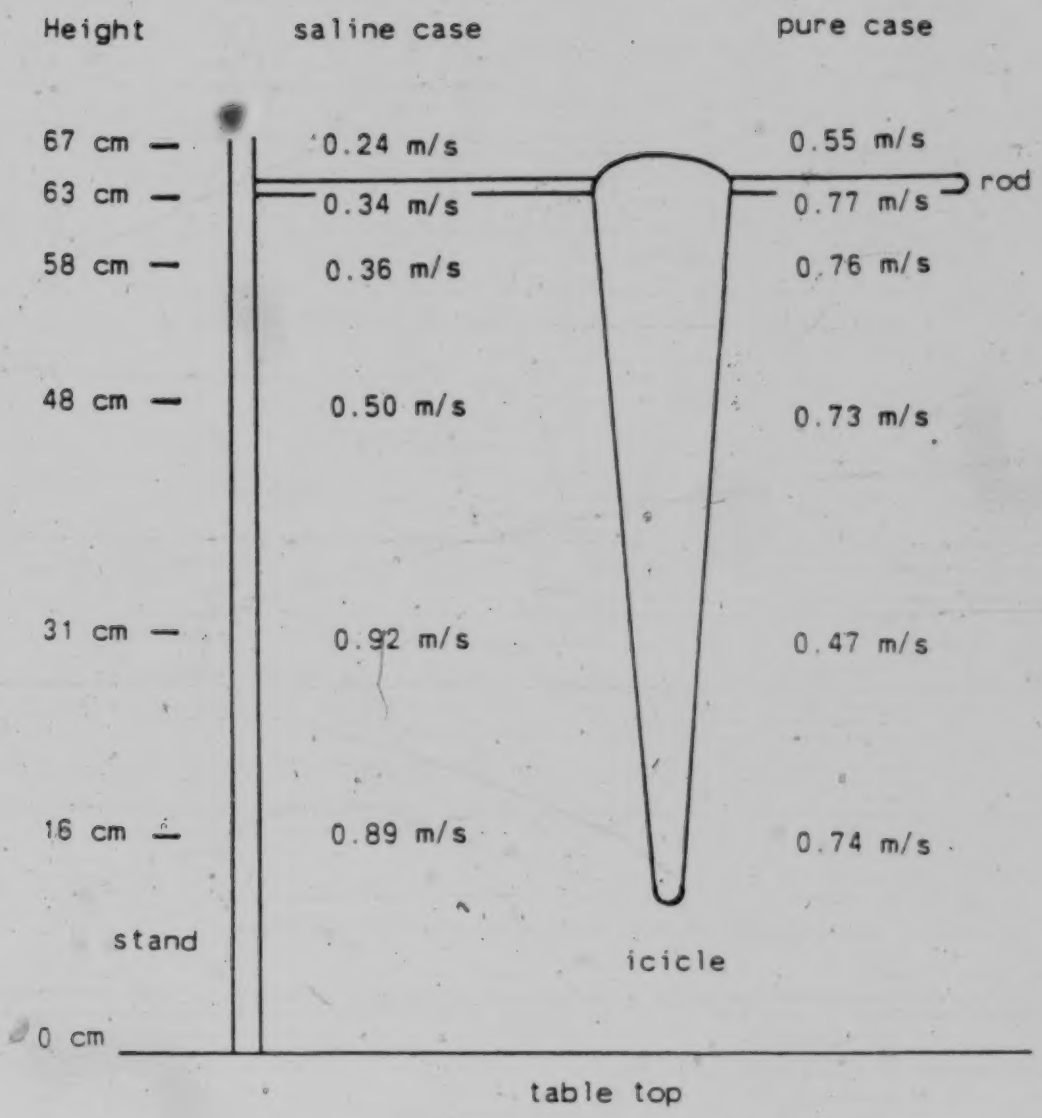

Figure 7.1.2 A schematic illustration of how the wind speed varies with height at the locations where the pure icicles and saline icicles were grown.

measurements are considered to have an error of no more than ± 5 %.

The air pressure in the cold room was assumed to be the same as that outside. The barometer located in the adjoining technician's room was used to measure the air pressure after every experiment. Again, accurate measurements were not necessary because the growth rates are insensitive to air pressure (see Section 5.1). The pressure measurements nevertheless had an accurancy to within ± 1 mb.

7.1.3 Length of the pure icicle

The length of the icicle at different times was measured using a paper tape, acting as a scale, hanging from the rod next to the icicle (see Figure 7.1.1). At each measurement time (see appendix D), the length of the growing icicle was marked on the paper tape. Then, after the experiment, an ordinary ruler was used to measure the marks on the paper tape. Using this technique, the length of the icicle at different times could be computed. The accurancy of this measurement was ±0.3 cm.

7.1.4 Diameter of the pure icicle

The diameter of the pure icicle as a function of distance from the root was measured every 2 cm along the length using a Vernier calliper, after the experiment had been completed. Because the icicle has a lot of ribs, the measurement was allowed to make a little more and less than 2 cm along the length and the average of the two was used. Also, since the icicle cross sections were generally not circular, the length of the major and minor axes were measured, and the geometric mean of these two values was taken as the mean diameter. After obtaining all the mean diameters as a function of distance from the root, an overall average diameter of the icicle was calculated.

7.1.5 Drip rate, mass of the pure icicle, and supply rate

The drip rate was determined simply by counting the number of drops dripping from the tip over a time interval of 1 minute. The mass of the icicle was measured after the

experiment using a Mettler triple beam balance accurate to ±0.01g. An average supply rate throughout the experiment was obtained by adding the mass of the icicle and the mass of the ice in the beaker (see Figure 7.1.1), and then dividing this value by the total duration of the experiment. Unfortunately, the instantaneous supply rate during the experiments was unknown.

7.2 Saline icicle growth experiments

The method for growing saline icicles in the cold room was very similar to that for growing pure icicles, except that brine of 33 o/oo salinity was used instead of pure water. It should be noted that the equilibrium temperature of 33 o/oo brine is around -1.8°C. Consequently, the temperature of the supply brine had to be slightly higher (0.5 °C to 1 °C) than -1.8 °C so that it would not freeze inside the burette. The brine used in the experiment was a solution of Rila Marine Mix in tap water (Oberiter, 1987). In order to keep the salinity of the supply brine constant, the brine in the container could not contain any ice, because melting or freezing of the ice would affect the salinity of the brine. Consequently, the brine in the container was prepared by dissolving the marine salt in tap water which was a few degrees above 0 °C. The insulated container was then put into a styrofoam box so that the temperature of the brine would drop only slowly in the cold room. In this way, it was certain that ice would not appear in the liquid throughout the experiment, and a constant salinity could be maintained. In addition, a thermocouple was inserted into the tip of the burette so that the temperature of the dripping brine could be measured. By adjusting the power supply, the temperature of the dripping brine was adjusted to a value between 0 °C and -1.8 °C. The apparatus used to grow saline icicles was identical to that used to grow pure icicles except for the thermocouple and the styrofoam box. The burette used was 1.2 mm in diameter (inside) instead of 2.0 mm, and a metal rod (4 mm in diameter) was used as the collector. The reason for using the narrower burette was that the flowrate could be adjusted easier. The reason for using a metal rod instead of a glass rod was that the metal rod was long enough to be fixed under the burette for the apparatus set up to grow saline icicles. This equipment is

shown in Figure 7.2.1.

The method of adjusting the flow rate, and the temperature of the brine dripping from the burrete, and the methods of measuring the air temperature, wind speed, relative humidity, and air pressure were similar to those described in Sections 7.1.1, and 7.1.2. However, since the location where the saline icicle was grown was slightly different from the location where the pure icicle was grown, the overall mean (weighted average) wind speed had to be re-measured. A value of 0.6 m/s was obtained (see Table 7.1.2.1 and Figure 7.1.2.1). The diameter and length of the saline icicles, drip rate, supply rate, and the mass of the saline icicle were obtained in a similar way to that described in Sections 7.1.3, 7.1.4, and 7.1.5. In addition, the average salinity of the pendant drops was also measured, by simply melting the ice in the beaker and measuring its salinity using a Fisher Hand salinometer (see Chapter 5). This salinometer has an accurancy of $\pm$ 0.2 %.

7.3 Qualitative observations

7.3.1 Pure icicles

The pure icicles produced in the coldroom, generally speaking, were conical. The cross-sections were not exactly circular but tended to be elliptical. This observation has been discussed in Section 4.7.2 (also in Johnson, 1987). Once the icicle had a root diameter greater than about 1.5 cm, water would tend to flow along a preferred path. As a result, ice grew faster on one side than on the other, and an elliptical shape developed with the major axis along the mean wind direction. In addition, horizontal bumps or ribs were also found on the wall (see Figure 7.3.1.1). The growth of the ribs seems to be affected by the wind, because those on the downwind side were bigger than those on the upwind side (see Figure 7.3.1.1). It could be that the wind pushed the water towards the downwind side so that the water film on that side was thicker. A liquid tube was found in the interior of the icicle, which extended about 2 to 5 cm from the tip. This observation is consistent with the theory proposed in Chapter 2. Also, near the surface of the pendant drop, dendrites are formed. Johnson (1987),

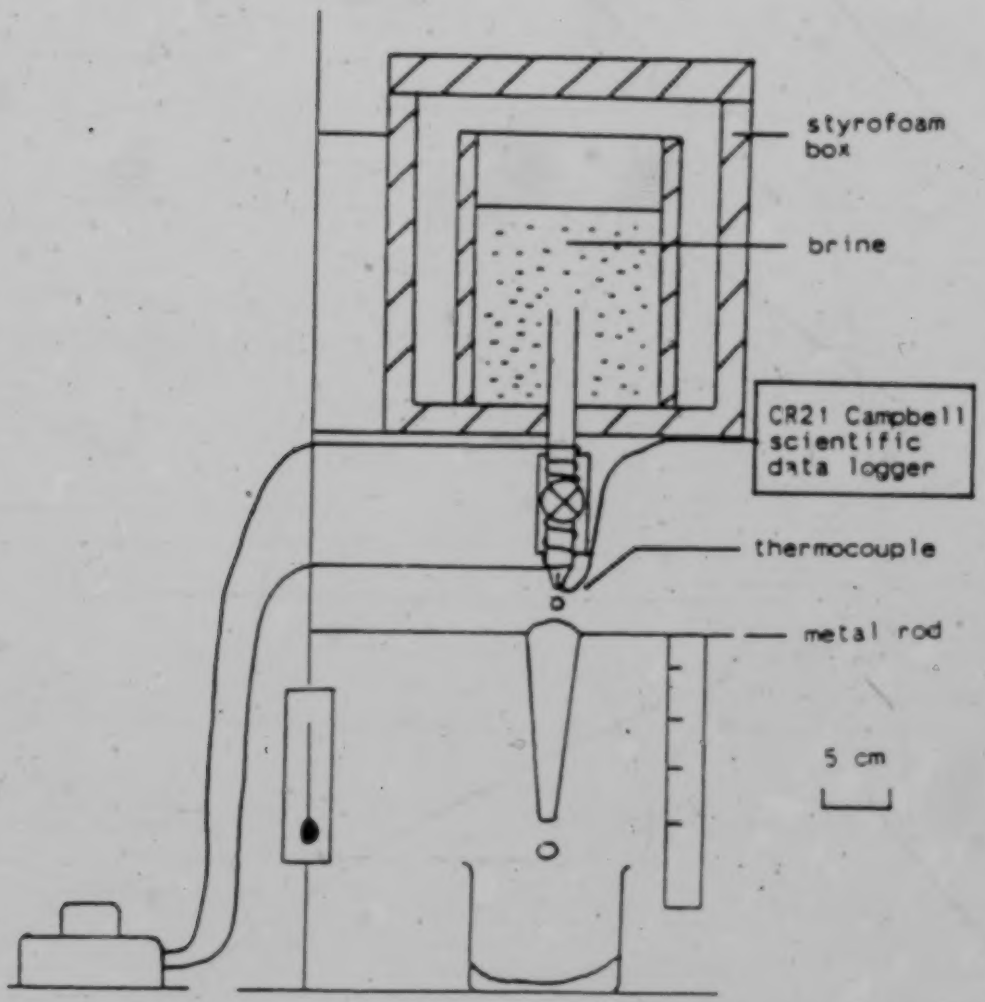

Figure 7.2.1 The apparatus used in the coldroom to grow saline icicles.

Figure 7.3.1.1 Laboratory simulated pure icicles. The sides with the more pronounced ribs are the downwind sides. For air conditions and scale, see Figure 3.2.1.

shows some macrophotographs of these dendrites. Early in the experiment (up to ~30 minutes), the wall of the icicle was quite spongy, and could be penetrated with a wire to a depth of a few millimeters. However, later in the experiment, the wall, except for the portion one third of the icicle length from the tip, became quite solid and not spongy at all. This suggests that the entrapped liquid inside the ice matrix had frozen.

7.3.2 Saline icicles

The general appearance of the saline icicles grown in the coldroom was similar to that of the pure icicles discussed in Section 7.3.1. However, several differences are worth noting. The saline icicles had more irregular cross sections than the pure icicles (see Figure 7.3.2.1). As well, the ribs on the walls of the saline icicles were bigger than those on the walls of the pure icicles. This difference can be seen clearly in Figure 7.3.2.2. The reasons why the saline icicles had more irregular cross sections and bigger ribs than the pure icicles are not obvious. One possibility could be the difference of the surface tensions between brine and pure water, although the difference is less than 1 % on the average. Figure 7.3.2.2 also shows that the saline icicles, generally, had higher maximum width to length ratios and bigger diameters than the pure icicles. This has been discussed in Sections 3.2 and 6.4, and is also consistent with the model's predictions. The saline icicles also appeared to be more spongy (by their milky appearance) than the pure icicles during their entire growth. Even at the end of their growth in length, the roots of the saline icicles were still spongy and could be penetrated with a wire. This result may be explained by the fact that the brine pockets of the saline icicles cannot freeze completely because the salinity of the brine pockets increases as freezing of pure ice proceeds on their walls. As a result, the equilibrium temperatures of the brine pockets is depressed. It was also found that when the saline icicles had grown to a certain size and length, they stopped growing even though brine was still dripping from the tip. This is also consistent with the model's prediction.

Figure 7.3.2.1: The cross-sections of a saline icicle (right) are more irregular than those of a pure icicle (left). The growth conditions for this picture were unfortunately not recorded.

For air conditions, see Figure 3.2.1.

2 cm

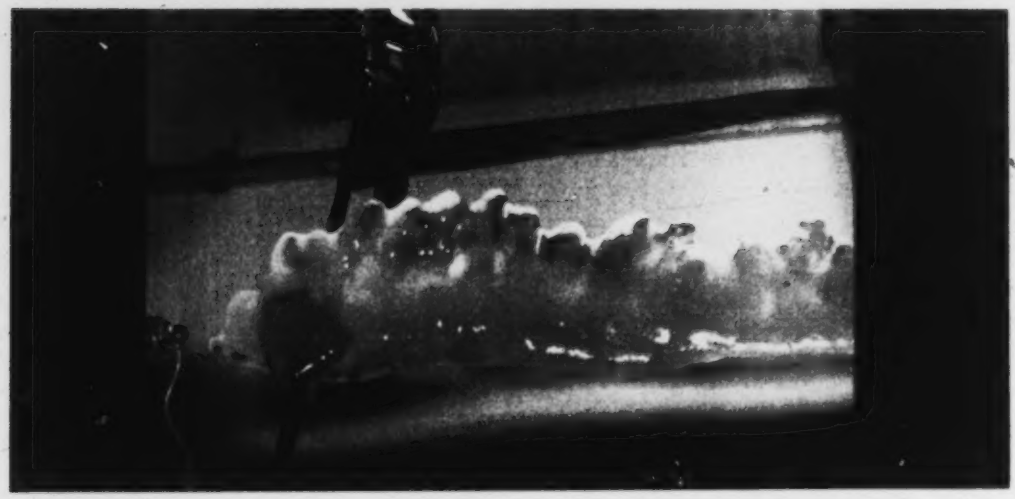

The air conditions for this picture were unfortunately not recorded.

2 cm

Figure 7.3.2.2 The ribs on the wall of the saline icicle (lower) are bigger than those on the walls of the pure icicles (upper).

8. Results and discussion

The results of the experiments on both pure and saline icicles are listed in tabular form in Appendix D. Cases #1 to #6 are the results from the pure icicle experiments and Cases #7 to #13 are the results from the saline icicle experiments. The time, driprate, length, length growth rate, and diameter as a function of distance from the root, as well as the mean diameter and total mass are all listed in the tables. The variation in supply rates throughout each experiment was also listed for reference. These results will be compared with the model results in graphical form so that the model's performance can be evaluated and discussed. All these graphs are shown at the end of this chapter. Since the experiments were not very precise due to variations in the air temperature and supply rates, and because of the irregular cross sections of the icicles, a difference between the experimental and model results is expected. In the next few sections, the discussions will be focused on comparisons between the experimental results and model predictions of i) length, ii) length growth rate, iii) length growth rate verses driprate, and iv) mean diameter and mass. To make the discussion clearer, several terms will be defined here:

1. Experiment Termination Time (ETT) - the time at which the experiment is terminated.
2. Model Termination Time (MTT) - the time at which the model simulation stops. For the present simulations, MTT is set to be equal to ETT.
3. Experiment Growth Termination Time (EGTT) - the time at which the growth in length stops ($dL/dt = 0$) during the experiment.
4. Model Growth Termination Time (MGTT) - the time at which the growth in length stops ($dL/dt = 0$) in the model simulation.

Between EGTT and ETT as well as between MGTT and MTT, the icicle continues to grow but only in diameter and mass, not in length.

8.1 Length

Figures 8.1.1 to 8.1.13 are graphical illustrations of the model predictions and experimental results for the length of the icicles as a function of time. Figures 8.1.1 to 8.1.6 are for pure icicles while Figures 8.1.7 to 8.1.13 are for saline icicles.

These 13 graphs show a common characteristic, namely that the model tends to overestimate the growth rates in length in most cases, especially for pure icicle growth. Also, the time at which the growth in length stops, as predicted by the model, is generally shorter than that found in the experiments, especially in the case of pure icicle. The exceptional case (#10) is shown in Figure 8.1.10. In this case, because the experiment was terminated before the end of the growth in length, it is impossible to determine whether the model also underestimates the time at which the growth in length stops. Table 8.1.1 shows this termination time difference. From this table, it can be seen that the model produces slightly better results for the time at which the growth in length stops (hereafter, the model growth termination time) for saline icicles than for pure icicles. Morever, the model's prediction of the growth termination time for saline icicles is better at higher temperatures and higher supply rates than at lower temperatures and lower supply rates. For the case of pure icicles, this pattern does not appear. One possible explanation for this overestimate of the length growth rate and underestimate of the growth termination time in the model, is that during the experiments the liquid film on the wall of the icicle tends to flow along preferred paths. This means the liquid film is not evenly distributed around the wall. Thus, the mass accretion on the wall of the icicle calculated for the model will be overestimated. On the other hand, with a circular cross section assumption, the heat transfer coefficients for the wall of the icicle calculated for the model may be too high. Furthermore, if the liquid flow is greater along the downwind side of the icicle, the effect of wind on the heat transfer from the liquid film may be diminished (Kreith, 1973). The circumferential variation of the Nusselt number $Nu(\Theta)$ for a circular cylinder in crossflow is shown in figure 8.1. Thus, the growth rate on the wall of the icicle will be smaller, and more liquid can flow down to the tip, thereby slowing down the length growth rate. In fact, as mentioned in Chapter 7, this is what is observed in the

Table 8.1.1

Model and experiment growth termination time difference

Pure icicle

Case #	MGTT	EGTT	% Difference
1	62 min	95 min	35 %
2	84 min	135 min	38 %
3	74 min	125 min	41 %
4	96 min	140 min	31 %
5	112 min	130 min	14 %
6	126 min	195 min	35 %

The average % difference = 32 %

Saline icicle

Case #	MGTT	EGTT	% Difference
7	104 min	135 min	23 %
8	142 min	180 min	21 %
9	162 min	190 min	15 %
10	uncertain	250 min	uncertain
11	234 min	270 min	13 %
12	296 min	350 min	15 %
13	94 min	195 min	52 %

The average % difference = 23 %

** The environmental conditions for the above cases are given in Appendix D **

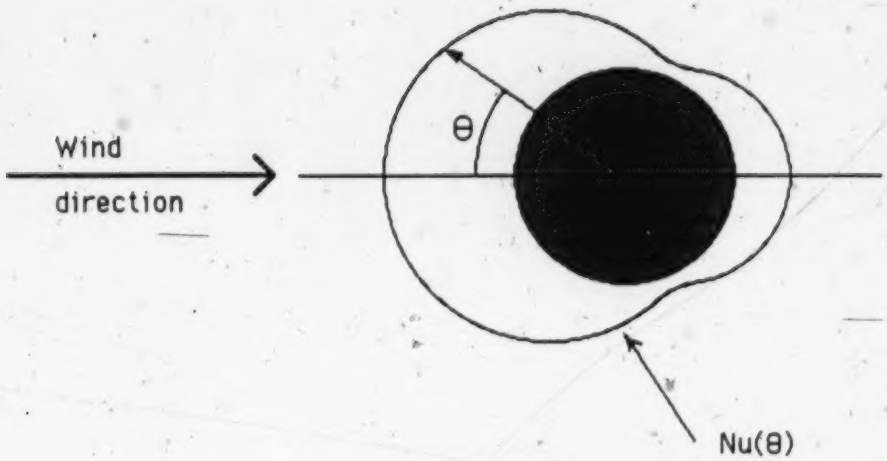

Figure 8.1 A schematic illustration of the circumferential variation of the Nusselt number for a cylinder in crossflow with the Reynolds number less than 4000.

(Modified from Kreith, 1973)

experiments. Since the model assumes an evenly distributed liquid film, it overestimates the length growth rate and underestimates the termination time for both saline and pure icicles. The reason why the model does better for the saline icicles than for the pure icicle is not obvious.

The model's prediction of the final length for both the pure and saline icicles is generally an underestimate at lower temperatures and an overestimate at higher temperatures. These data are summarized in Table 8.1.2. The only exception to this trend is in case #2 corresponding to pure icicle growth where the model overestimates the final length by 1%. The percent differences between the model's predictions and the experimental results are also shown in Table 8.1.2. It is obvious that the model does a better job of predicting the final lengths of the pure icicles. The greatest difference occurs in case #1 where the model understimates the final length by 18%. The smallest difference is for case #2 where the model overestimates the final length by only 1%. For saline icicles, the model does not do as well. In case #13, the model underestimates the final length by 26%. The best it can do is in case 8.8 where the model underestimates the final length by 4%.

Up to this point, it can be said that the model, in general, does not perform well in predicting the length of both saline and pure icicles, though it does a little better in predicting the length of the pure icicles. However, qualitatively speaking, the model does hit the mark. For all 6 cases of pure icicle growth, the experimental results show a gradual increase in length growth rates.The model's predictions are consistent with this. Likewise, for all 7 cases of saline icicles growth, the experimental results show that the growth rate is almost linear at first, and near the end of the growth, the growth rate starts to decline and growth eventually stops. The model's predictions are also consistent with this.

8.2 Length growth rate

Figures 8.2.1 to 8.2.13 give graphical illustrations of the length growth rates as a function of time for both pure and saline icicles. Figure 8.2.1 to 8.2.6 are for the pure cases while the rest are for the saline cases. These 13 graphs are reflections of Figures 8.1.1 to

Table 8.1.2

Final length of the pure icicles

Case #	Model	Experiment	% difference
1	36.0 cm	44.1 cm	-18 %
2	44.1 cm	43.7 cm	1 %
3	36.5 cm	38.2 cm	-4 %
4	45.5 cm	40.9 cm	11 %
5	40.2 cm	38.5 cm	4 %
6	47.3 cm	40.4 cm	17 %

The average absolute % difference = 9.3 %

Final length of the saline icicles

Case #	Model	Experiment	% difference
7	29.5 cm	36.2 cm	-18 %
8	37.7 cm	39.3 cm	-4 %
9	35.3 cm	39.8 cm	-11 %
10	47.2 cm	41.5 cm	14 %
11	38.5 cm	34.1 cm	13 %
12	46.4 cm	37.8 cm	23 %
13	27.5 cm	37.3 cm	-26 %

The average absolute % difference = 15.6 %

** The environmental conditions for the above cases are given in Appendix D **

8.1.13 because dL/dt is the slope of the growth curves. The experimental data shown in these 13 figures exhibit a great deal of scatter. The reason is that small errors in the measurement of L can give rise to large errors in dL/dt. Although the experimental data are very scattered, a general pattern can still be traced which is similar to the pattern of the model's prediction. In the pure icicle cases, the experimental data tend to follow a pattern where dL/dt increases with time until the end of the growth. In the saline icicle cases, the experimental data tend to follow a different pattern where dL/dt initially increases slowly with time, and then subsequently decreases rapidly until growth stops. Therefore, qualitatively speaking, the model agrees with the experiments for the growth of both saline and pure icicles. Table 8.2.1. shows the average growth rates from the model and the experiments.

From this table, it can be seen that the model's prediction of the length growth rate for both saline and pure icicles overestimates the experimental results by as much as 58% for the saline cases and 81% for the pure cases. As mentioned earlier, the liquid tends to stream along preferred paths down the walls of the icicles. Therefore, incorporation of a heat transfer coefficient which accounts for such preferred flowing paths should give a better prediction of the length growth rates.

8.3 Length growth rate versus drip rate

It is also interesting to explore the relation between dL/dt and drip rate in the model and in the experiments. Figures 8.3.1 to 8.3.6 show this relation for the pure icicles, while Figures 8.3.7 to 8.3.13 show the relation for the saline icicles. Again, the experimental data are very scattered. One cause of the scatter is the variation in supply rates. If the supply rates could be controlled properly, better results could be obtained. In the case of the saline icicles (Figures 8.3.7 to 8.3.13), the model's results show that dL/dt at first increases slowly with decreasing drip rate. Then, after dL/dt reaches a maximum, it decrease rapidly with decreasing drip rate. Finally, dL/dt goes to zero with a non-zero drip rate. The explanation of this relationship has been discussed in Section 6.2. Although the data are scattered, they do follow a pattern that is similar to the model's prediction. In the case of the pure icicles

Table 8.2.1

Average length growth rates

Pure icicles

Case #	Model	Experiment	% difference
1	0.59 cm/min	0.46 cm/miin	28 %
2	0.54 cm/min	0.32 cm/min	69 %
3	0.51 cm/min	0.32 cm/min	59 %
4	0.48 cm/min	0.28 cm/min	71 %
5	0.37 cm/min	0.31 cm/min	19 %
6	0.38 cm/min	0.21 cm/min	81 %

The average % difference = 54.5 %

Salines icicles

	Model	Experiment	% difference
7	0.29 cm/min	0.27 cm/min	7 %
8	0.27 cm/min	0.22 cm/min	23 %
9	0.22 cm/min	0.21 cm/min	5 %
10	0.19 cm/min	0.17 cm/min	12 %
11	0.17 cm/min	0.13 cm/min	31 %
12	0.16 cm/min	0.11 cm/min	45 %
13	0.30 cm/min	0.19 cm/min	58 %

The average % difference = 25.9 %

** The environmental conditions for the above cases are given in Appendix D **

(Figures 8.3.1 to 8.3.6), the experimental data are also very scattered. However, they also follow a pattern which is similar to that of the model. That is, dL/dt increases with decreasing drip rate. It should be noted that the relation between dL/dt and drip rate (for pure icicles) obtained in the model is not linear. The curves are slightly concave upward. This concave upward pattern cannot be seen from the experimental data because they are too scattered.

8.4 Mean diameter and mass

Since the model underestimates the growth termination time, to compare the mean diameter and mass for the model and experiments at the ETT may not be appropriate. This is especially true for the pure icicles, where the masses predicted by the model at the ETT are very much greater than those of the experiments. This can be seen in table 8.4.3B. For the saline icicles, the masses predicted by the model at the ETT are not very much greater than those of the experiments (see Table 8.4.4B). This suggests that the mass growth rate of pure icicles predicted by the model is very much faster than that obtained in the experiments, while for the growth of saline icicles, the difference is much less. Consequently, to give a more meaningful comparison, for the saline icicles, the mean diameters and masses will be compared at the ETT, whereas, for the pure icicles, the mean diameters and masses at the MGTT will be compared with the experimental mean diameters and masses at the ETT. However, for most of the experiments, the ETT is not right at the time at which the growth in length stops (i.e ETT $\geq$ EGTT), but rather a short period of time after. Therefore, a little adjustment should be made to the MGTT. For example, in the first experiment for pure icicle growth, the growth in length stops at 95 minutes (EGTT = 95 minutes) but the experiment stops 5 minutes later (ETT = 100 minutes), so 5 minutes are added to the MGTT in the model in order to compare with the experimental results.

Tables 8.4.1. to 8.4.4. show the mean diameters and masses predicted by the model at the adjusted MGTT (A) and at the ETT (B). The experimental results are also shown in these tables. Tables 8.4.1B, 8.4.2A, 8.4.3B, and 8.4.4A are included for reference only and

Table 8.4.1

Pure icicle mean diameter

A

Case #	Model (at MGTT)	Experiment (at ETT)
1	1.39 cm	1.42 cm
2	1.58 cm	1.68 cm
3	1.27 cm	1.55 cm
4	1.46 cm	1.62 cm
5	1.22 cm	1.29 cm
6	1.46 cm	1.57 cm

B

Case #	Model (at ETT)	Experiment (at ETT)
1	1.92 cm	1.42 cm
2	2.33 cm	1.68 cm
3	2.01 cm	1.55 cm
4	2.16 cm	1.62 cm
5	1.47 cm	1.29 cm
6	2.18 cm	1.57 cm

** The environmental conditions for the above cases are given in Appendix D **

Table 8.4.2

Saline icicle mean diameter

A

Case #	Model (at MGTT)	Experiment (at ETT)
7	1.98 cm	2.13 cm
8	2.39 cm	2.79 cm
9	1.97 cm	1.98 cm
10	2.40 cm	2.68 cm
11	1.95 cm	2.31 cm
12	2.12 cm	2.52 cm
13	2.45 cm	3.01 cm

B

Case #	Model (at ETT)	Experiment (at ETT)
7	2.31 cm	2.13 cm
8	2.71 cm	2.79 cm
9	2.20 cm	1.98 cm
10	2.40 cm	2.68 cm
11	2.18 cm	2.31 cm
12	2.42 cm	2.52 cm
13	3.11 cm	3.01 cm

** The environmental conditions for the above cases are given in Appendix D **

Table 8.4.3

Pure icicles mass

A

Case #	Model (at MGTT)	Experiment (at ETT)
1	52.06 g	67.74 g
2	85.36 g	98.48 g
3	45.54 g	70.0 g
4	77.14 g	86.45 g
5	43.45 g	52.27 9
6	79.74 g	82.34 g

B

Case #	Model (at ETT)	Experiment (at ETT)
1	102.18 g	67.74 g
2	188.94 g	98.48 g
3	114.03 g	70.0 g
4	167.40 g	86.45 g
5	67.25 g	52.27 g
6	177.04 g	82.34 g

** The environmental conditions for the above cases are given in Appendix D **

Table 8.4.4

Saline icicle mass

A

Case #	Model (at MGTT)	Experiment (at ETT)
7	101.68 g	130.02 g
8	192.68 g	227.99 g
9	118.87 g	125.16 g
10	240.87 g	208.62 g
11	127.65 g	127.68 g
12	182.95 g	181.30 g
13	148.19 g	229.84 g

B

Case #	Model (at ETT)	Experiment (at ETT)
7	139.46 g	130.02 g
8	248.10 g	227.99 g
9	149.28 g	125.16 g
10	240.87 g	208.62 g
11	157.31 g	127.68 g
12	238.50 g	181.30 g
13	258.70 g	229.84 g

** The environmental conditions for the above cases are given in Appendix D **

will not be discussed in detail. They demonstrate why a different time is chosen for comparison in the case of the pure icicles while the same time is chosen for comparison in the case of the saline icicles.

It can be seen from Table 8.4.1A that the model underestimates the mean diameters of the pure icicles by 2-18% compared to the experimental results. The results are plotted in Figure 8.4.1.

Table 8.4.2B shows the model and experimental results for mean diameters of the saline icicles. The largest difference between the model and the experimental results occurs in case #3 in which the model overestimates the mean diameter by 11%. The rest of the results show a difference of less than 10 %. The results are plotted in Figure 8.4.2.

In table 8.4.3A, the masses of the pure icicles obtained in the model are all less than those obtained in the experiments, by 3 to 35%. The results are plotted in Figure 8.4.3. In table 8.4.4B, it can be seen that the model overestimates the experimental masses by 7 to 24%. The results are plotted in the Figure 8.4.4.

From the above discussion and analysis, it can be concluded that the model performs better in predicting the mean diameters and masses of saline icicles, at the growth termination time. For the case of pure icicles, one can conclude that the pure icicles produced in the laboratory grew much slower than the model predicts. As a result, the masses of the pure icicles obtained in the experiment are always much smaller than the model predicts when compared at the same time. One possible reason why the model overpredicts the mass growth rate for pure icicles is that the supercooling of the pure water film enclosing the body of the icicle may be greater than 0.02°, as suggested by Hillig and Turnbull (1956). Since the supercooling of the liquid film is neglected in the model for simplicity, if this is indeed greater than 0.02°, the radial growth may be overestimated. On the other hand, the air-speed in the coldroom during the experiments is less than 1 m/s. It has been shown, from the sensitivity test in Chapter 6, that model simulation is very sensivity to the wind speed, especially at low wind speeds (see Section 6.1). Therefore, a small uncertainity in windspeed can cause a large error in the model's predictions. For the case of saline icicles, the difference in mass growth

rate between the model and experimental results is much less.

A summary of the results of the final length, mean diameter, and mass is given in Table 8.4.5. It should be noted that for the case of the pure icicles, the model's result is given at the MGTT. The M and E which appear in the table stand for model and experiment, respectively. There is one comment concerning this table. In case #8, the length and mean diameter of the saline icicle predicted by the model are smaller than the values obtained in the experiment. Therefore, it is not possible for the model's mass to be greater than the experimental mass. The only explaination of this contradiction seems to be that the measurement of mass in that experiment may be erroneous.

Before ending this chapter, it should be noted that the model runs the pure icicle simulation with zero liquid fraction and the saline icicle simulation with a liquid fraction of 0.26. The former value is chosen for simulating pure icicle growth because it gives a better comparison with the final mass in the experiments, though the deviation is still large. Furthermore, it is observed in the experiments that after a short period of time, the wall of the icicle is essentially solid except near the tip. Therefore, a zero liquid fraction seems appropriate. The value of 0.26 is chosen for simulating saline icicle growth because no research has been done on the sponginess of saline icicles, and therefore the value proposed by Makkonen, 1987, has been used. Furthermore, it was observed in the experiments that the walls of the saline icicles are very spongy throughout the experiments. So, the choice of a non-zero value for the liquid fraction in the model is not unreasonable.

Table 8.4.5

A summary of the model and experimental results of pure and saline icicles growth

(A) Pure icicles

Case #	Length (M)	Length (E)	Mean Diameter (M)	Mean Diameter (E)	Mass (M)	Mass (E)
1	35.59 cm	44.1 cm	1.39 cm	1.42 cm	52.06 g	67.74 g
2	44.11 cm	43.7 cm	1.58 cm	1.68 cm	85.36 g	98.48 g
3	36.54 cm	38.2 cm	1.27 cm	1.55 cm	45.54 g	70.0 g
4	45.53 cm	40.9 cm	1.46 cm	1.62 cm	77.14 g	86.45 g
5	40.16 cm	38.5 cm	1.22 cm	1.29 cm	43.45 g	52.27 g
6	47.27 cm	40.4 cm	1.46 cm	1.57 cm	79.74 g	82.34 g

(B) Saline icicles

	Length (M)	Length (E)	Mean Diameter (M)	Mean Diameter (E)	Mass (M)	Mass (E)
7	29.53 cm	36.2 cm	2.31 cm	2.13 cm	139.46 g	130.02 g
8	37.66 cm	39.3 cm	2.71 cm	2.79 cm	248.10 g	227.99 g
9	35.32 cm	39.8 cm	2.20 cm	1.98 cm	149.28 g	125.16 g
10	47.15 cm	41.5 cm	2.40 cm	2.68 cm	240.87 g	208.62 g
11	38.49 cm	34.1 cm	2.18 cm	2.31 cm	157.31 g	127.68 g
12	46.39 cm	37.8 cm	2.42 cm	2.52 cm	238.50 g	181.30 g
13	27.53 cm	37.3 cm	3.11 cm	3.01 cm	258.70 g	229.84 g

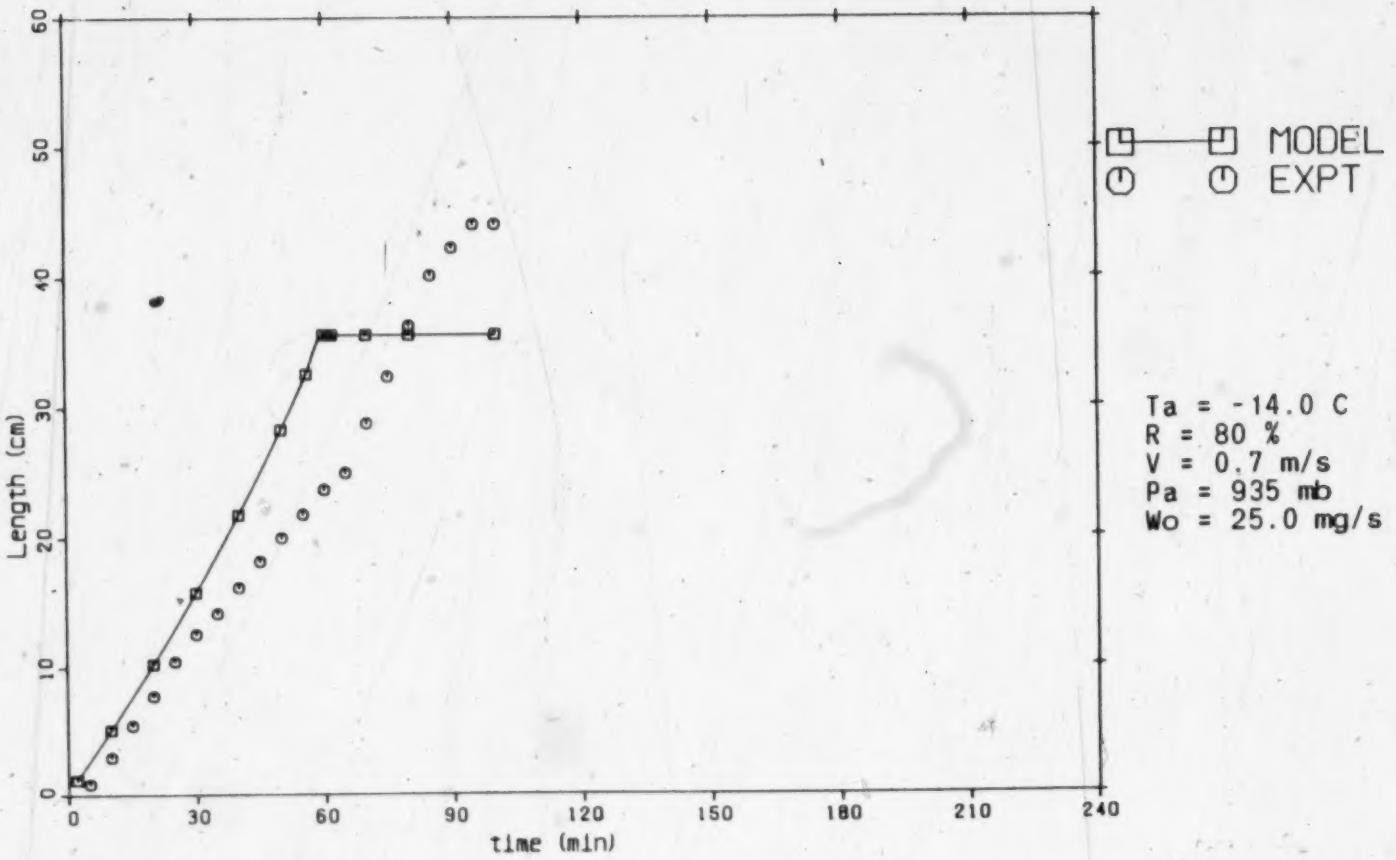

Figure 8.1.1 Icicle length (cm) vs time (min) for pure icicle growth, case #1 in Appendix D.

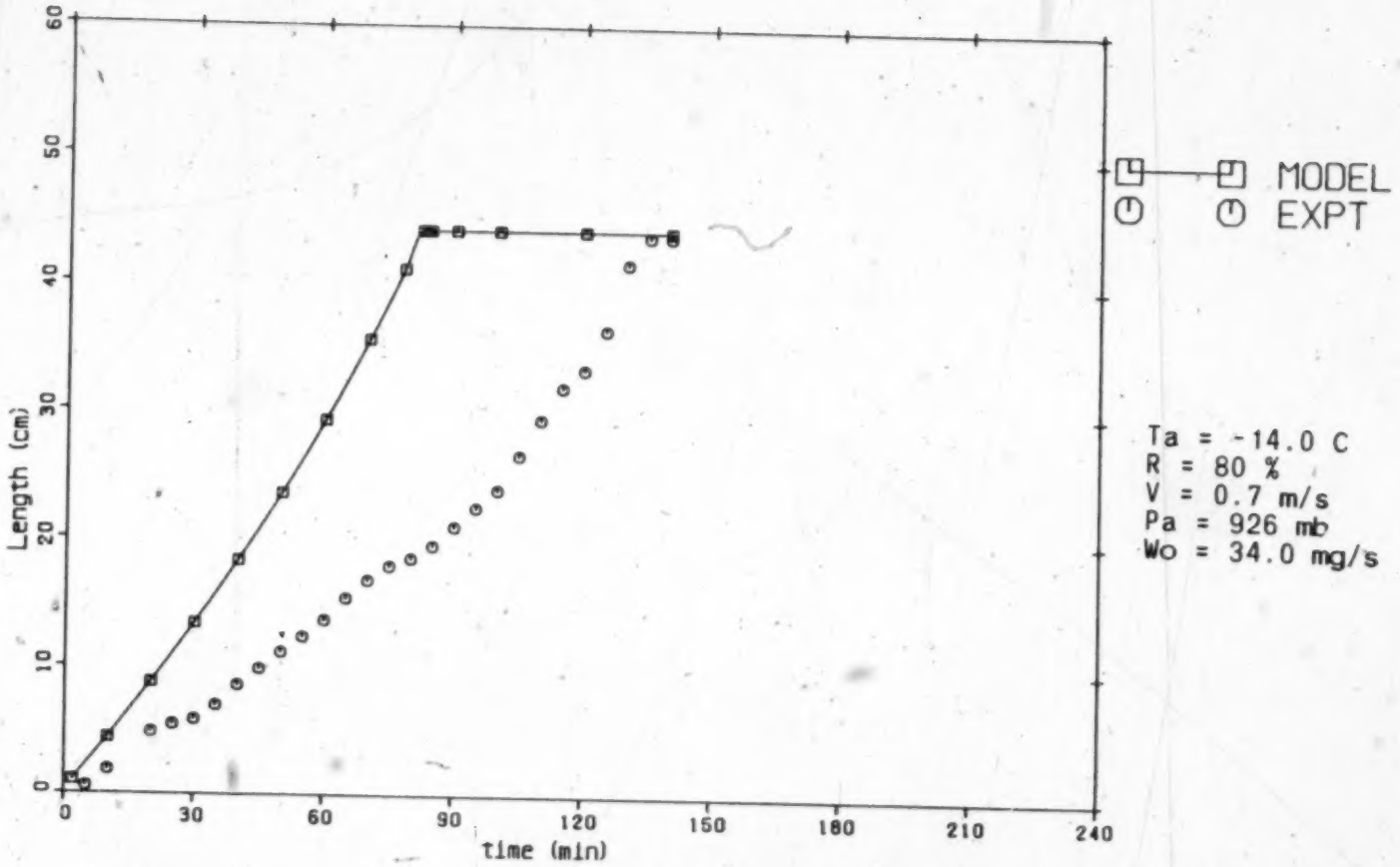

Figure 8.1.2 Icicle length (cm) vs time (min) for pure icicle growth, case #2 in Appendix D.

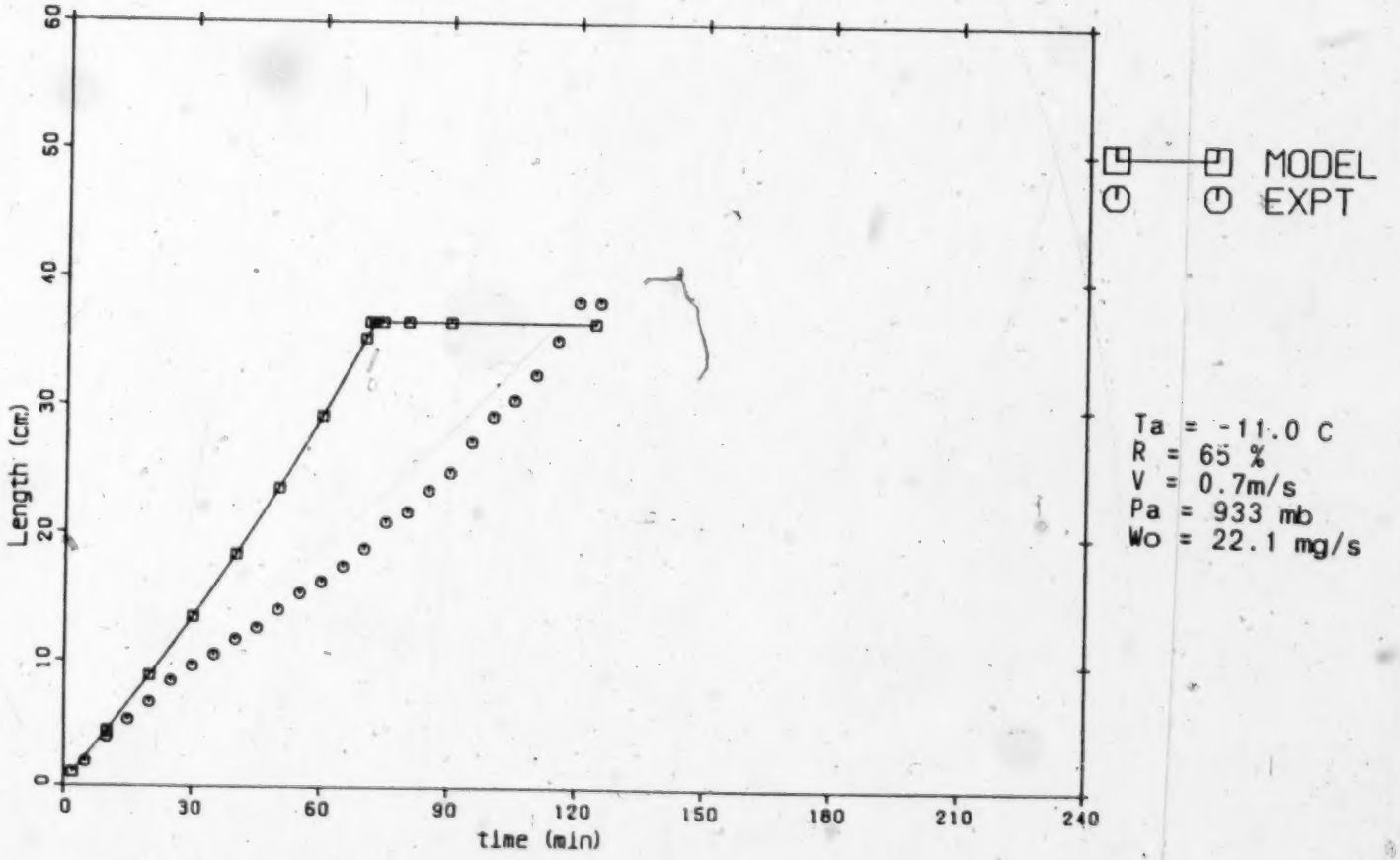

Figure 8.1.3 Icicle length (cm) vs time (min) for pure icicle growth, case #3 in Appendix D.

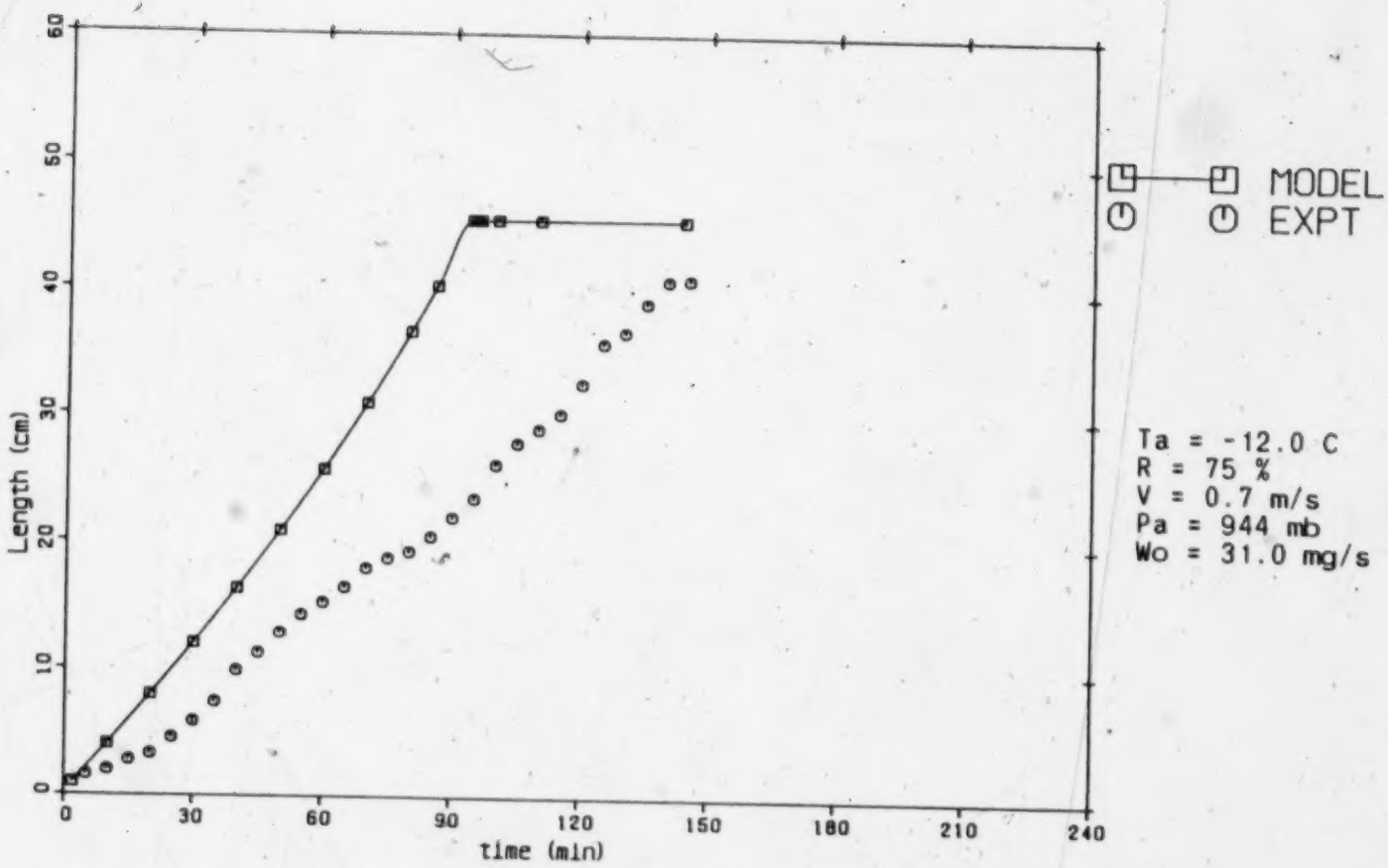

Figure 8.1.4 Icicle length (cm) vs time (min) for pure icicle growth, case #4 in Appendix D.

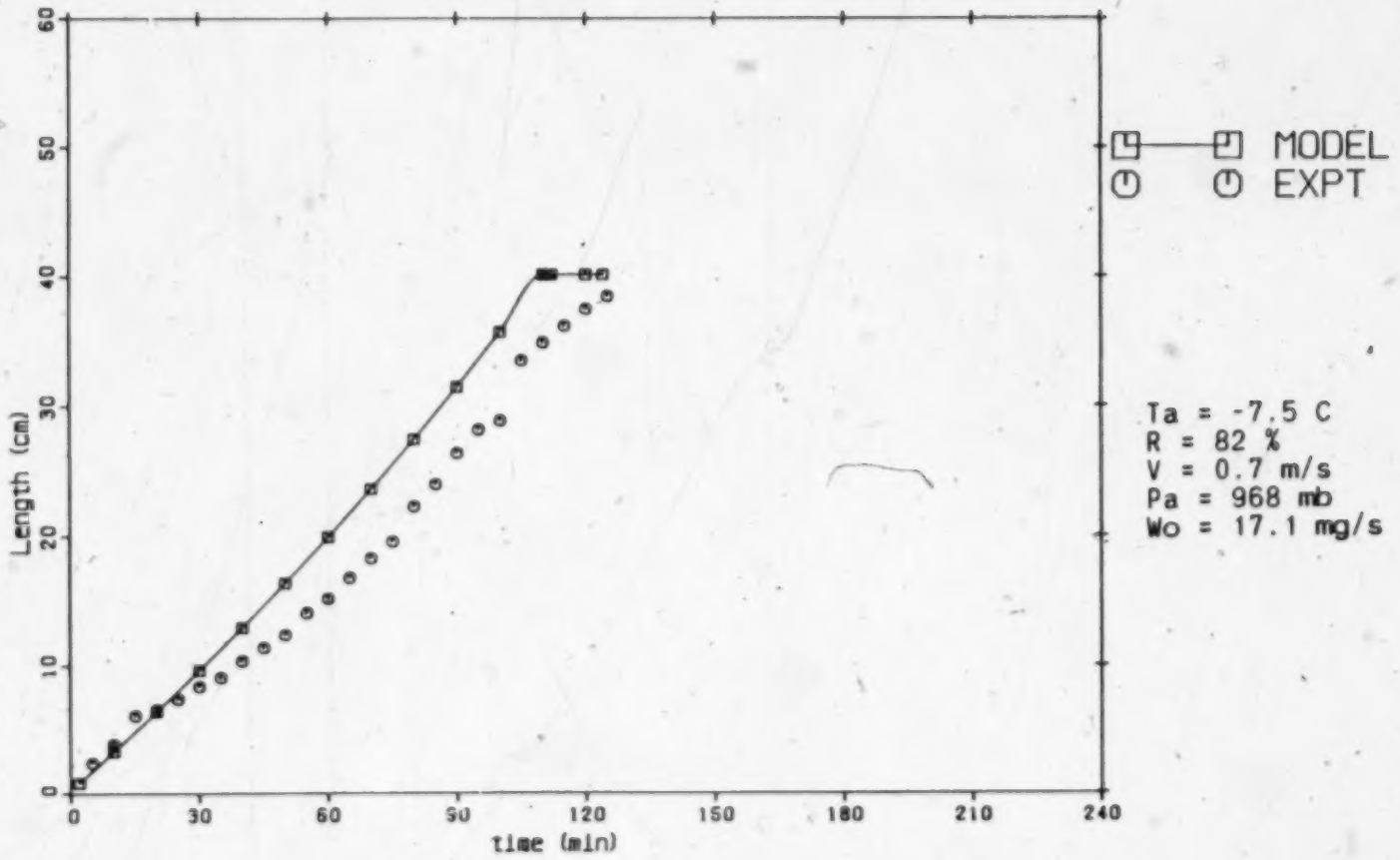

Figure 8.1.5 Icicle length (cm) vs time (min) for pure icicle growth, case #5 in Appendix D.

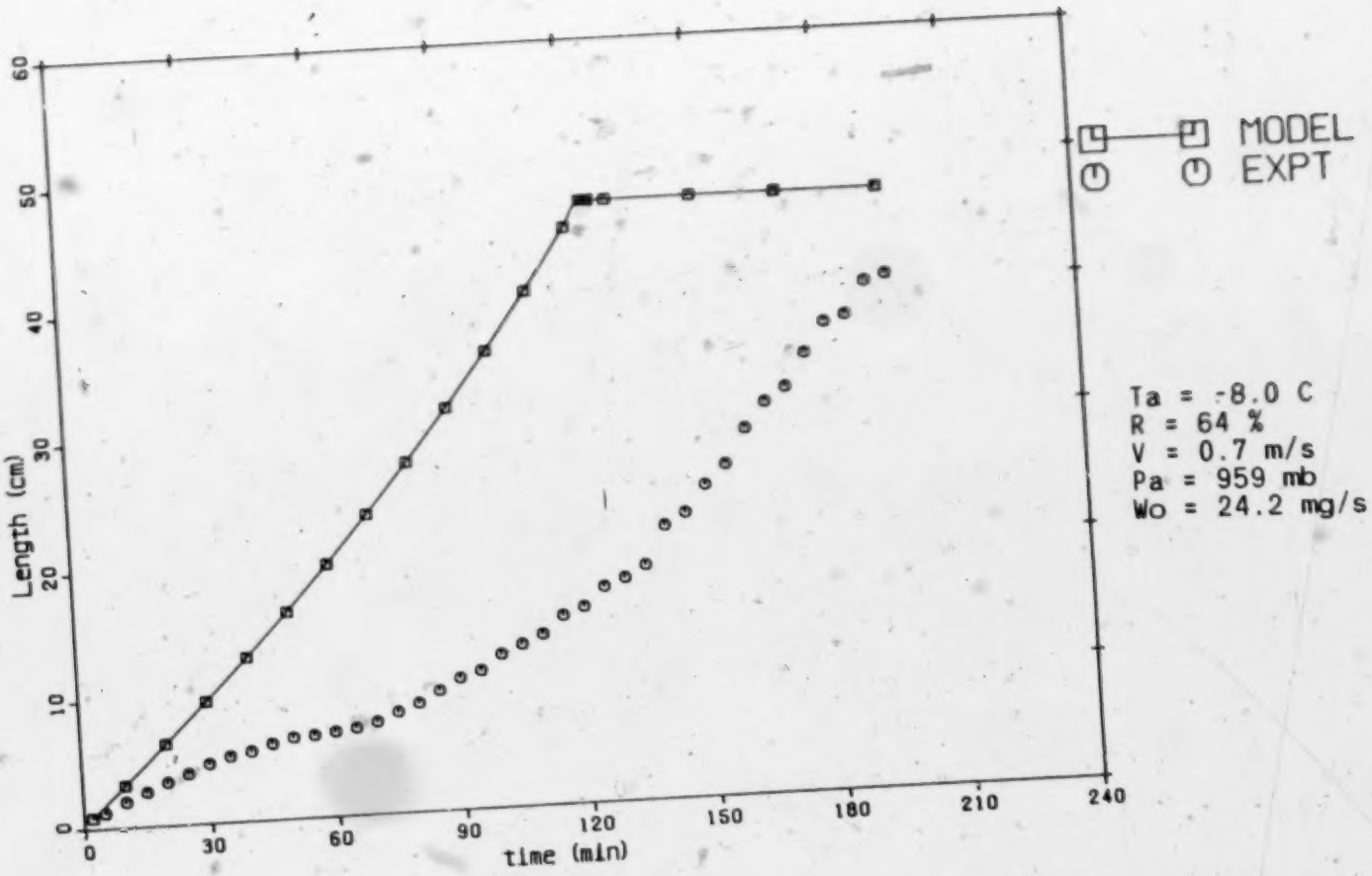

Figure 8.1.6 Icicle length (cm) vs time (min) for pure icicle growth, case #6 in Appendix D.

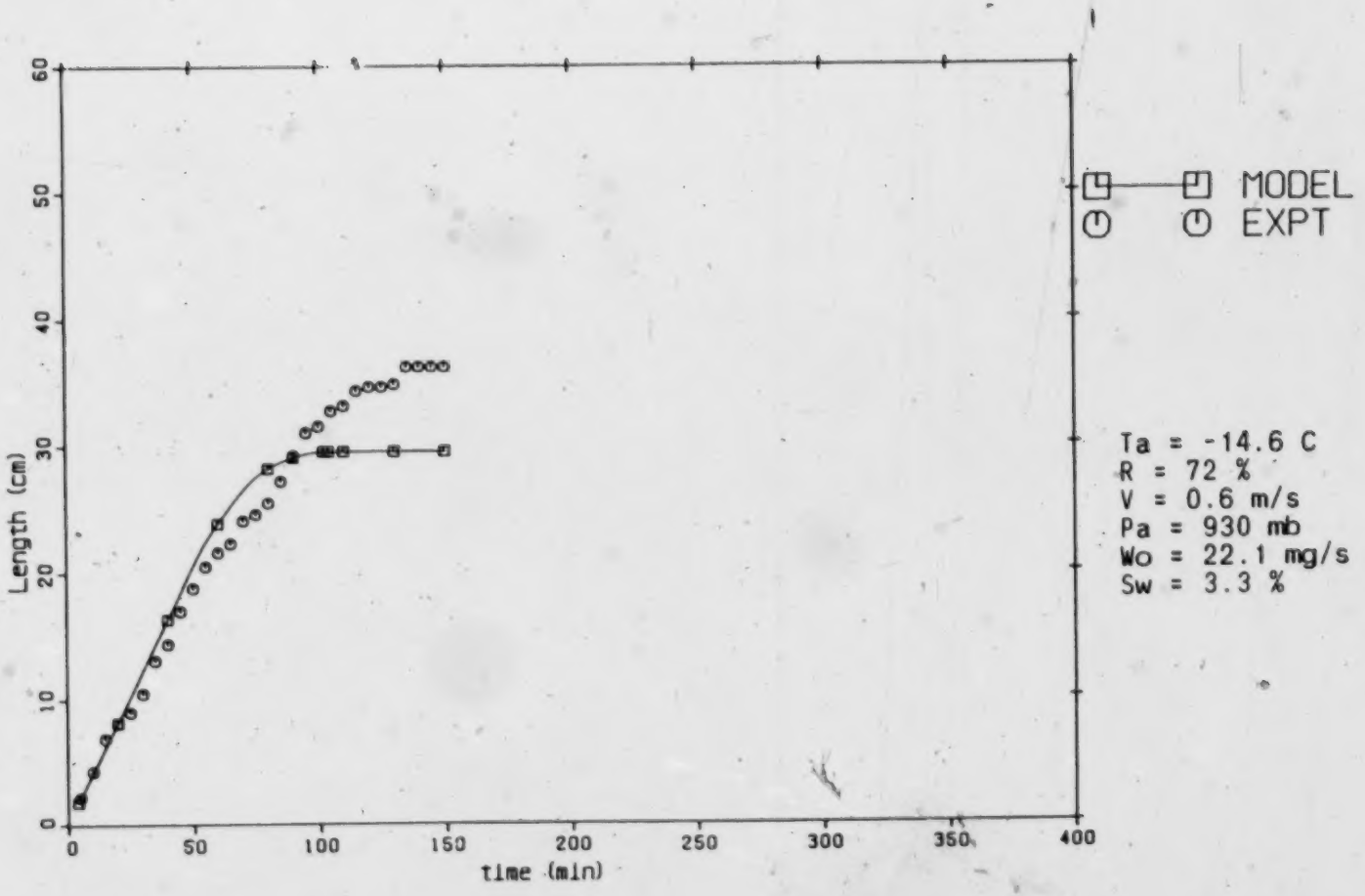

Figure 8.1.7 Icicle length (cm) vs time (min) for saline icicle growth, case #7 in Appendix D.

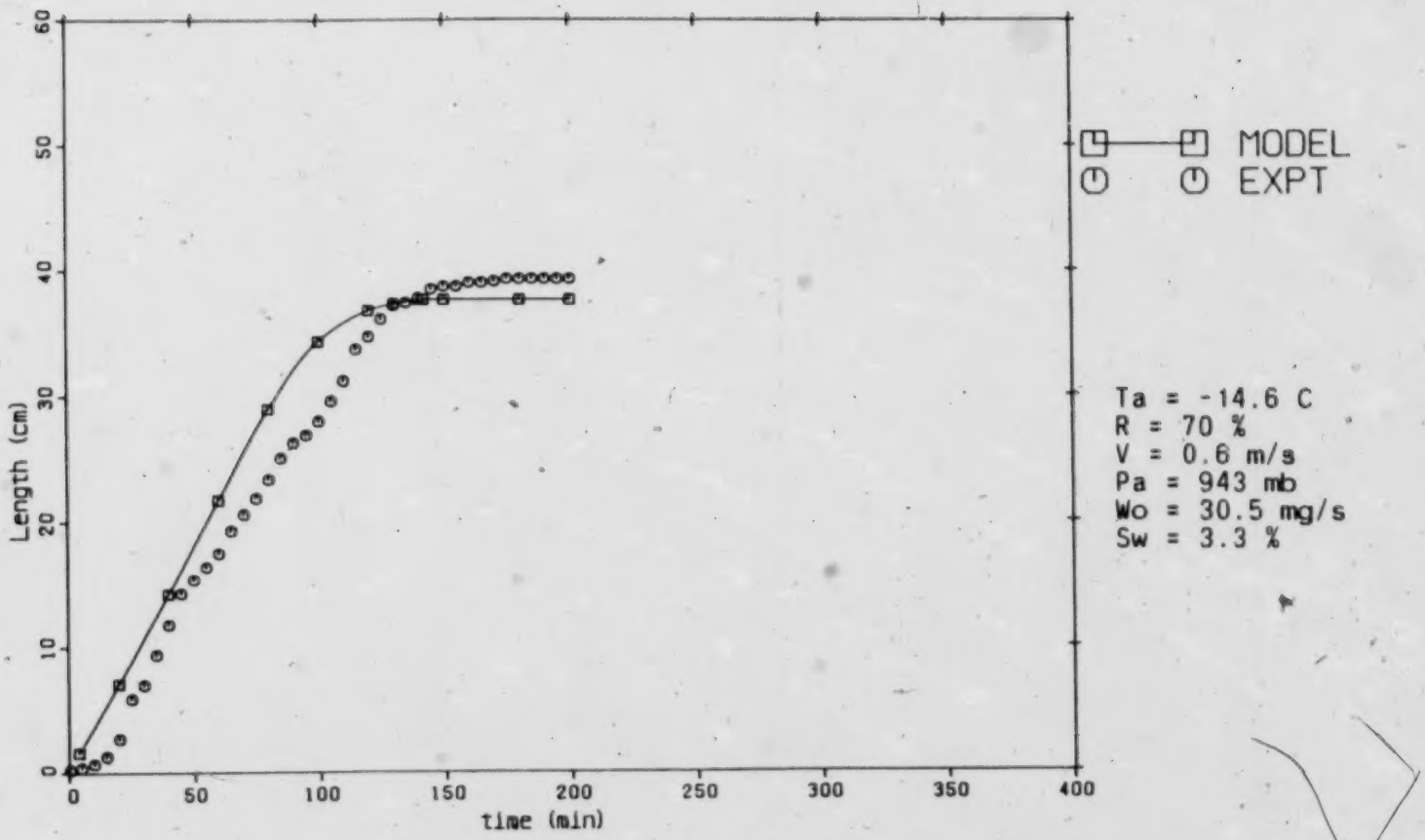

Figure 8.1.8 Icicle length (cm) vs time (min) for saline icicle growth, case #8 in Appendix D.

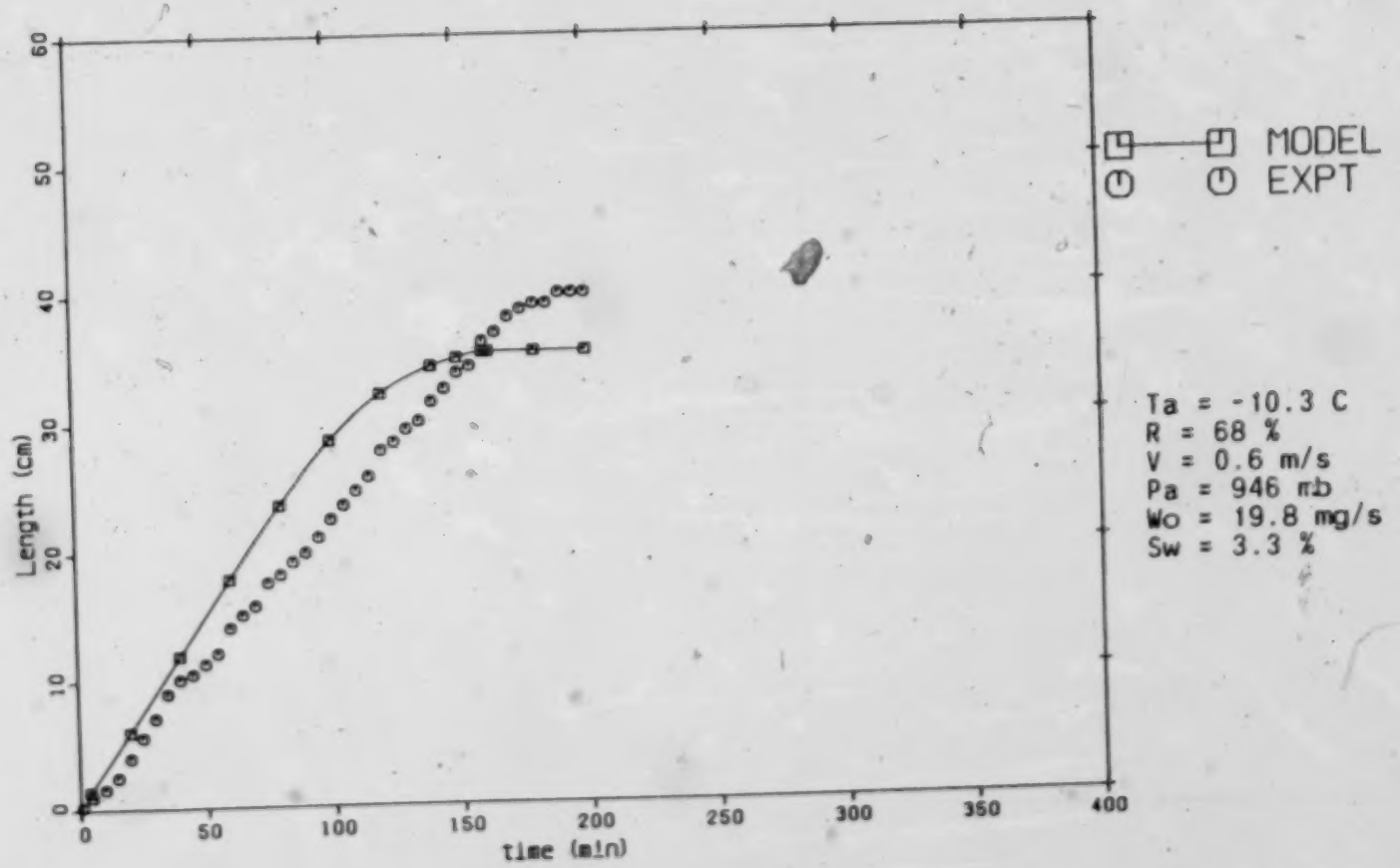

Figure 8.1.9 Icicle length (cm) vs time (min) for saline icicle growth, case #9 in Appendix D.

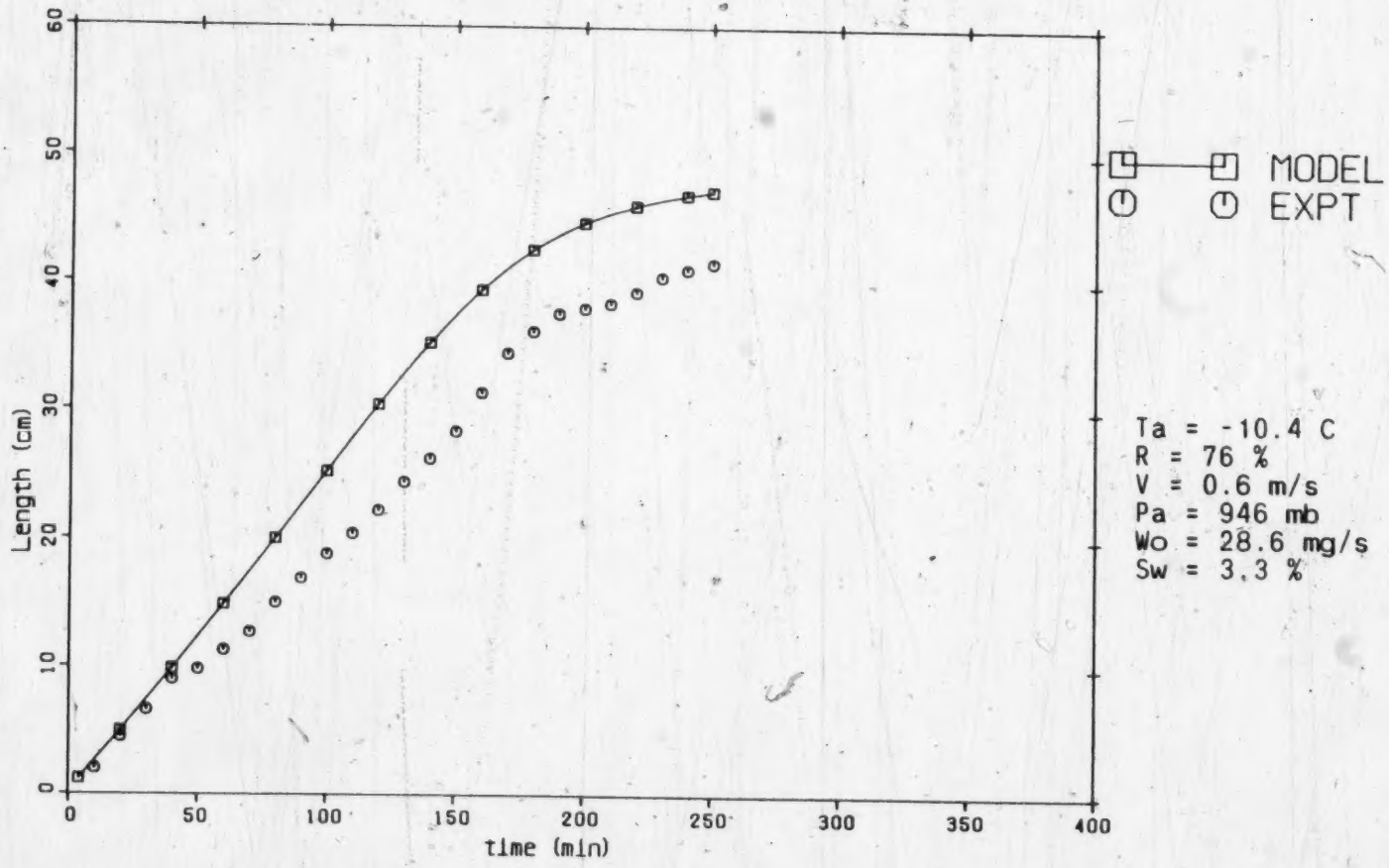

Figure 8.1.10 Icicle length (cm) vs time (min) for saline icicle growth, case #10 in Appendix D.

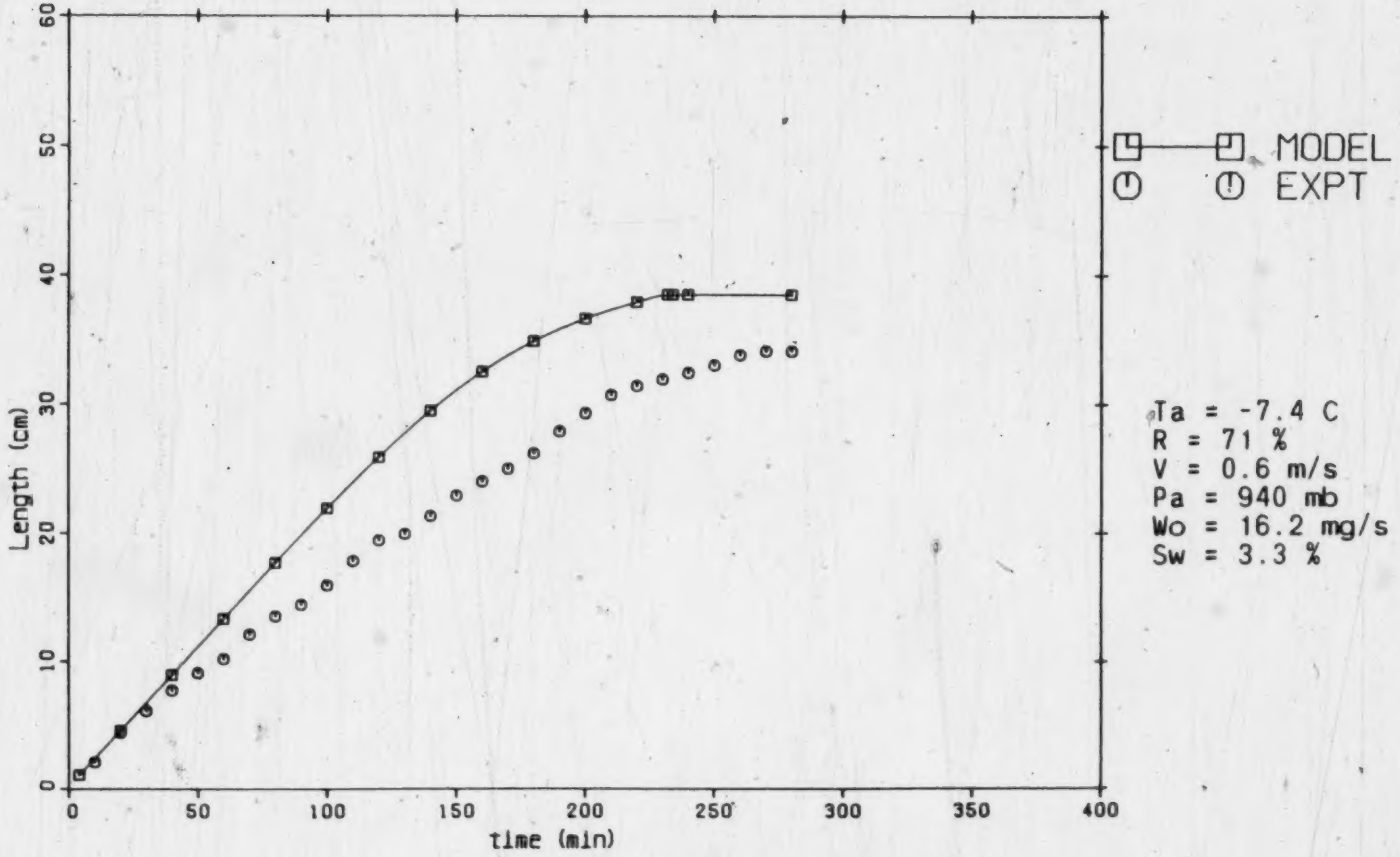

Figure 8.1.11 Icicle length (cm) vs time (min) for saline icicle growth, case #11 in Appendix D.

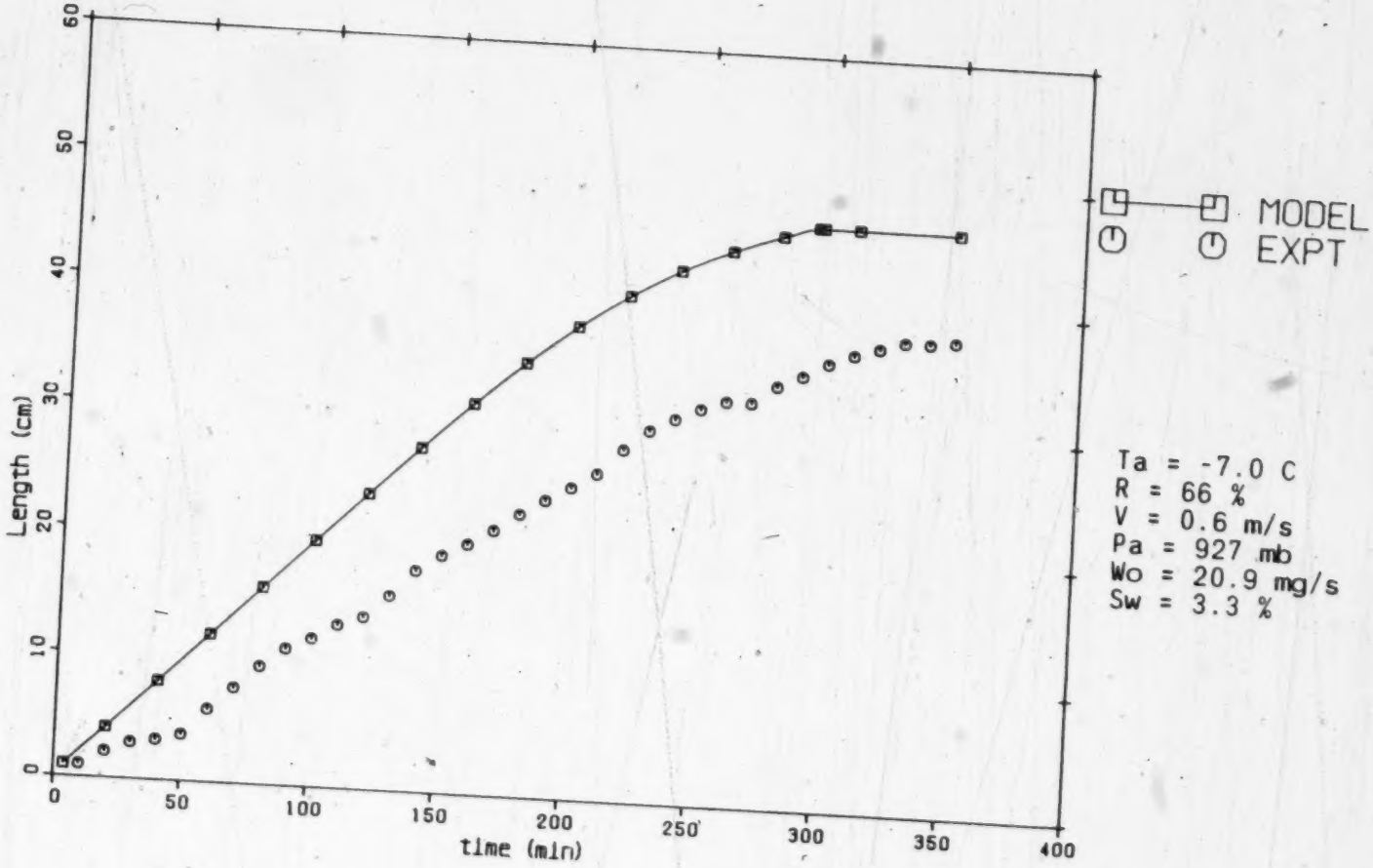

Figure 8.1.12 Icicle length (cm) vs time (min) for saline icicle growth, case #12 in Appendix D.

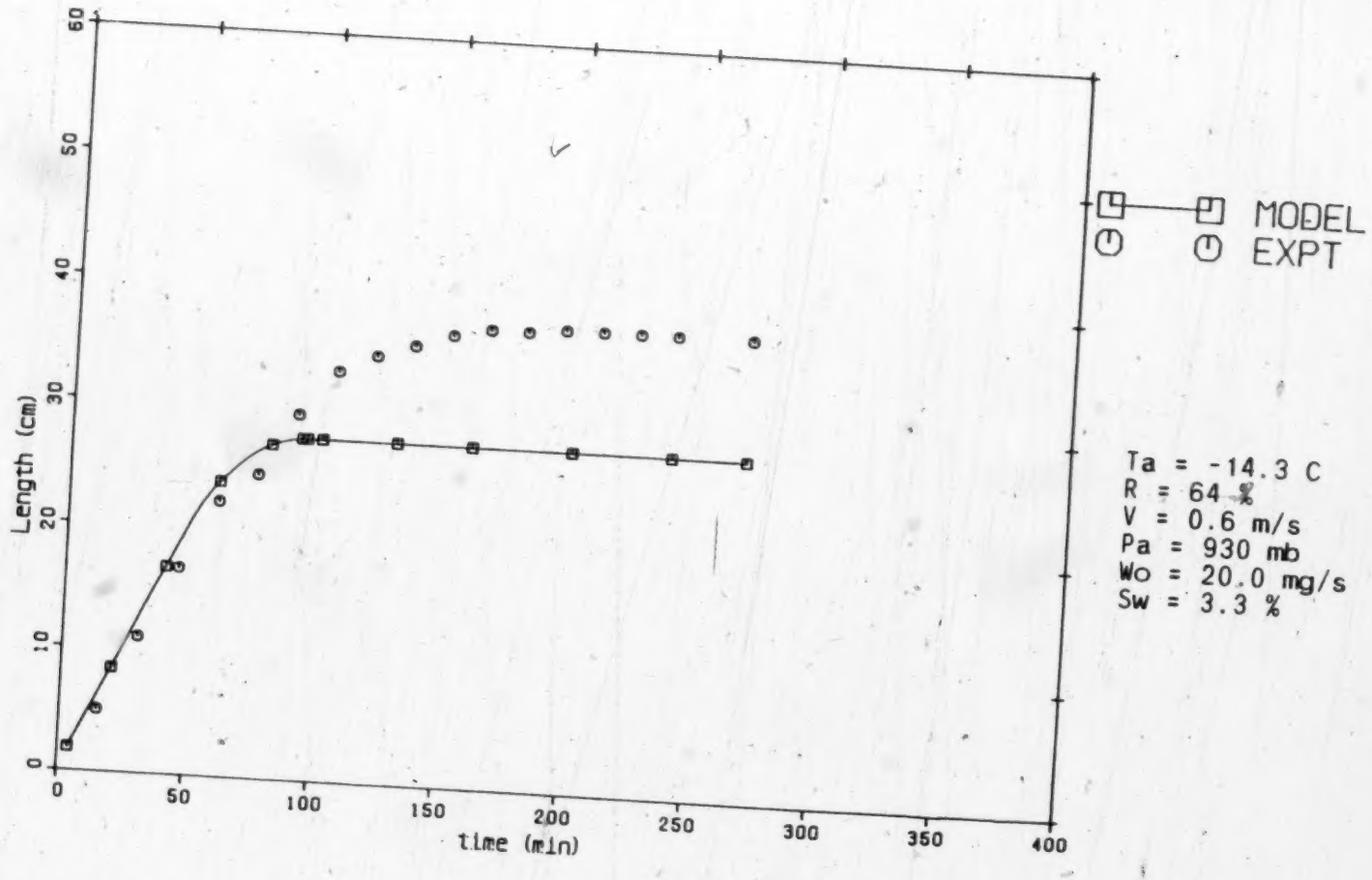

Figure 8.1.13 Icicle length (cm) vs time (min) for saline icicle growth, case #13 in appendix D.

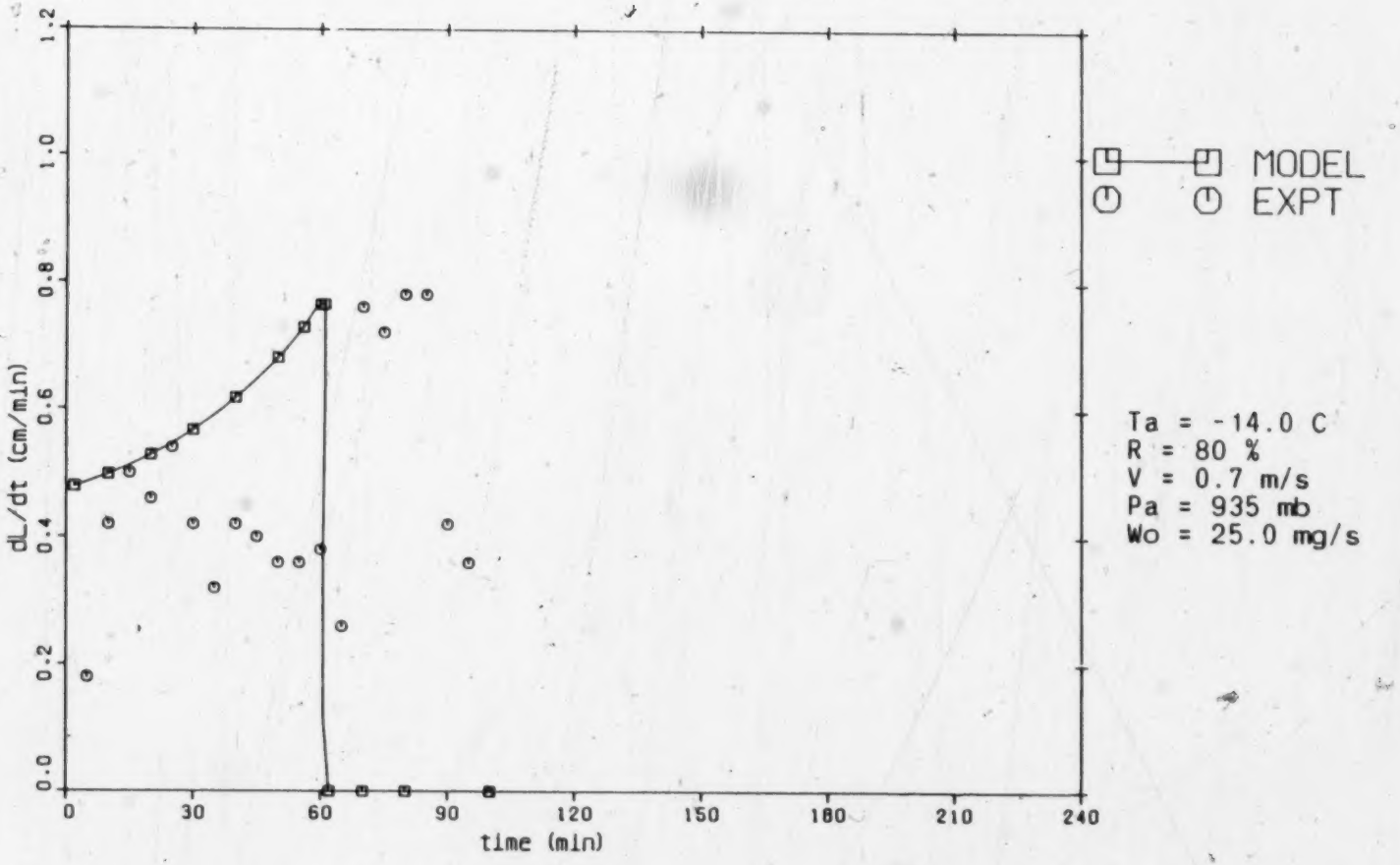

Figure 8.2.1 Icicle length growth rate dL/dt (cm/min) vs time (min) for pure icicle growth, case #1 in Appendix D.

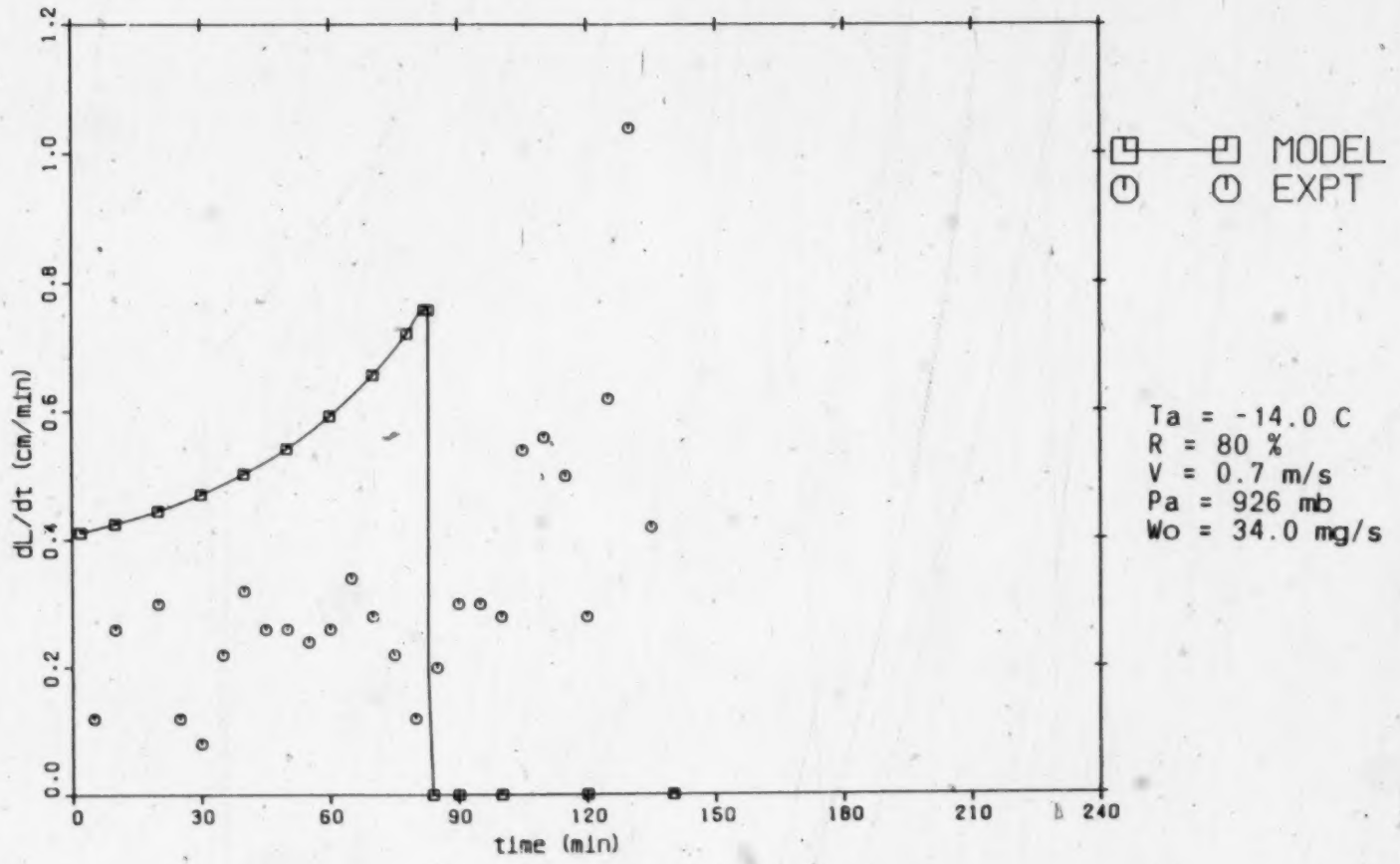

Figure 8.2.2 Icicle length growth rate dL/dt (cm/min) vs time (min) for pure icicle growth, case #2 in Appendix D.

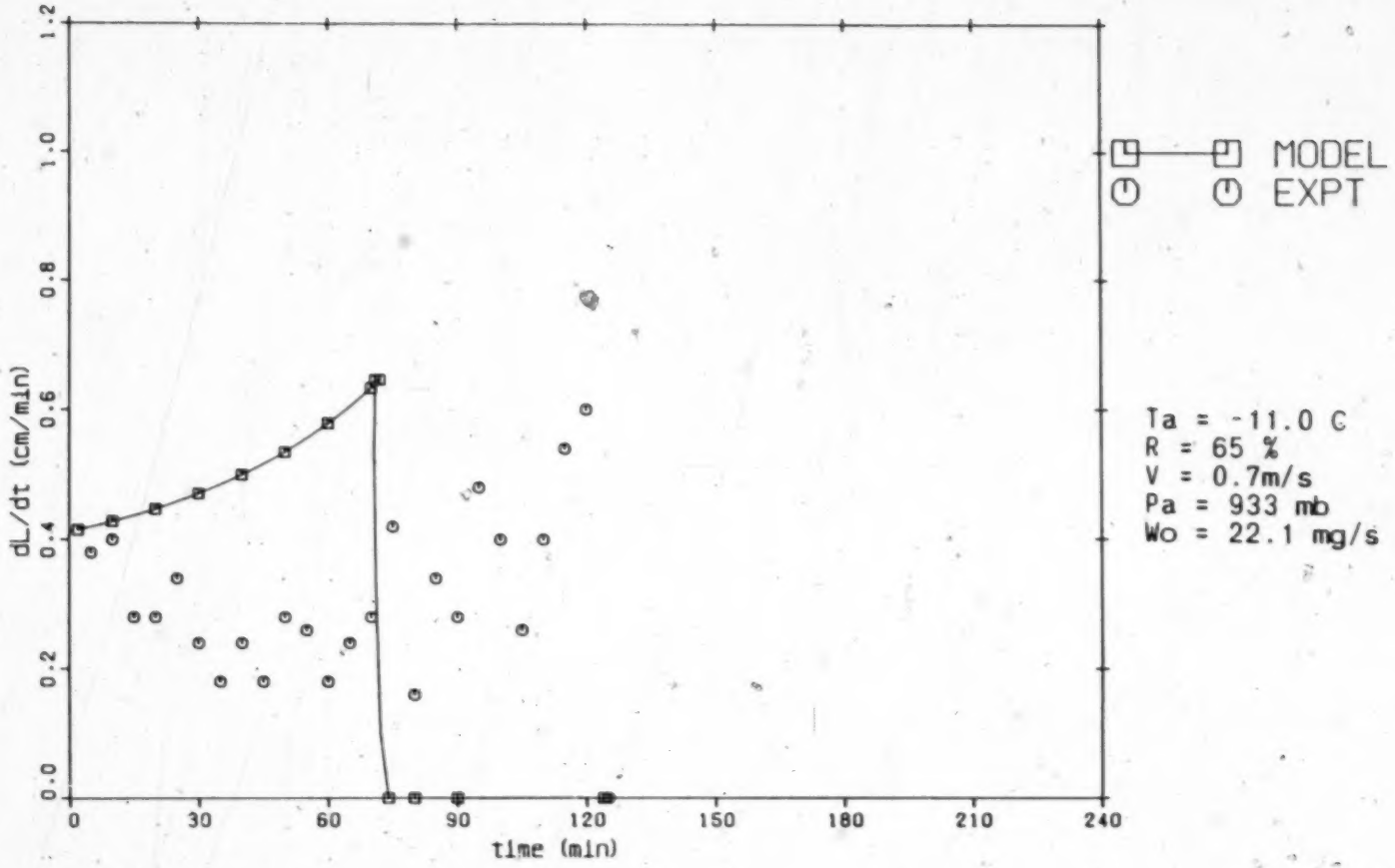

Figure 8.2.3 Icicle length growth rate dL/dt (cm/min) vs time (min) for pure icicle growth, case #3 in Appendix D.

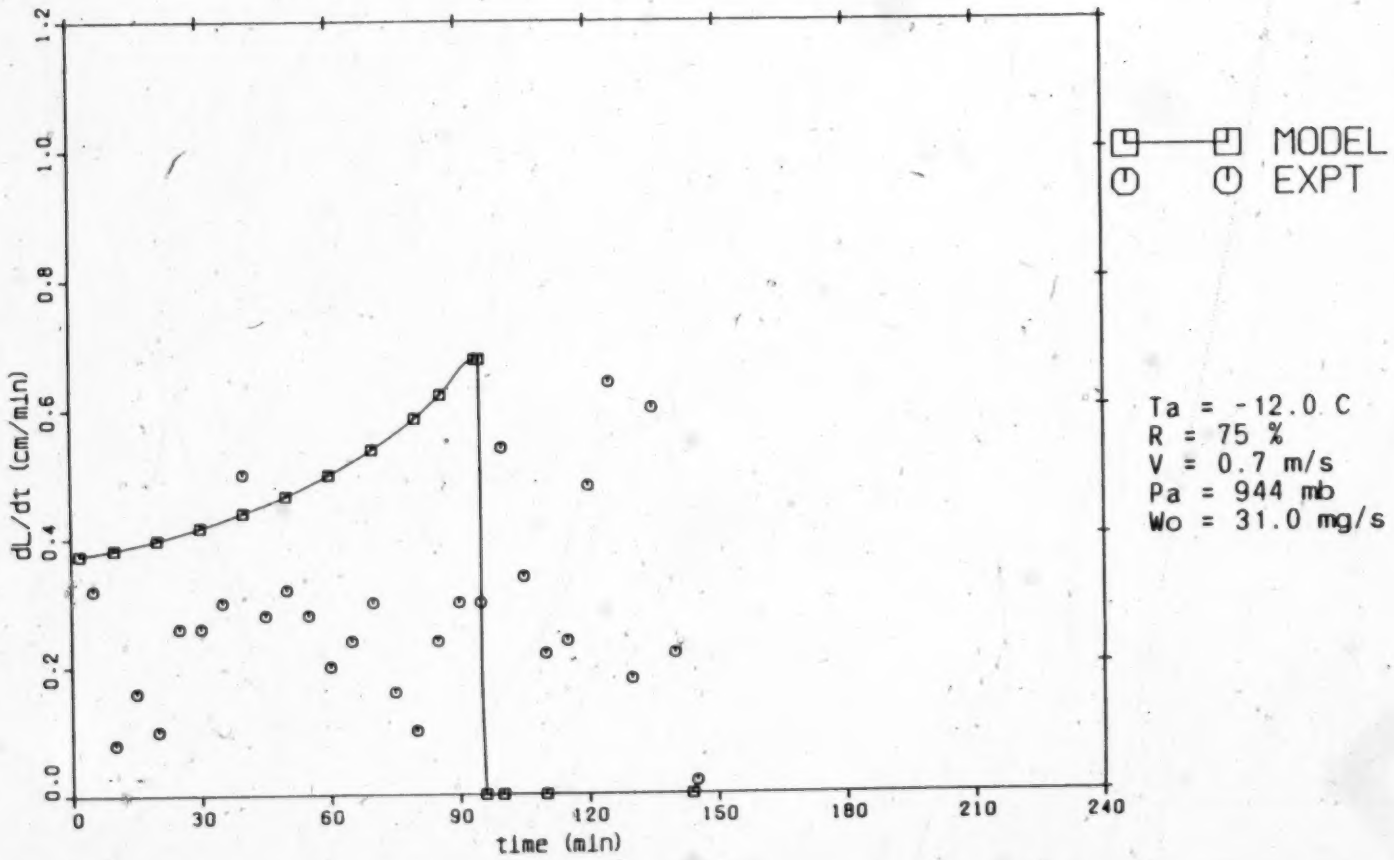

Figure 8.2.4 Icicle length growth rate dL/dt (cm/min) vs time (min) for pure icicle growth, case #4 in Appendix D.

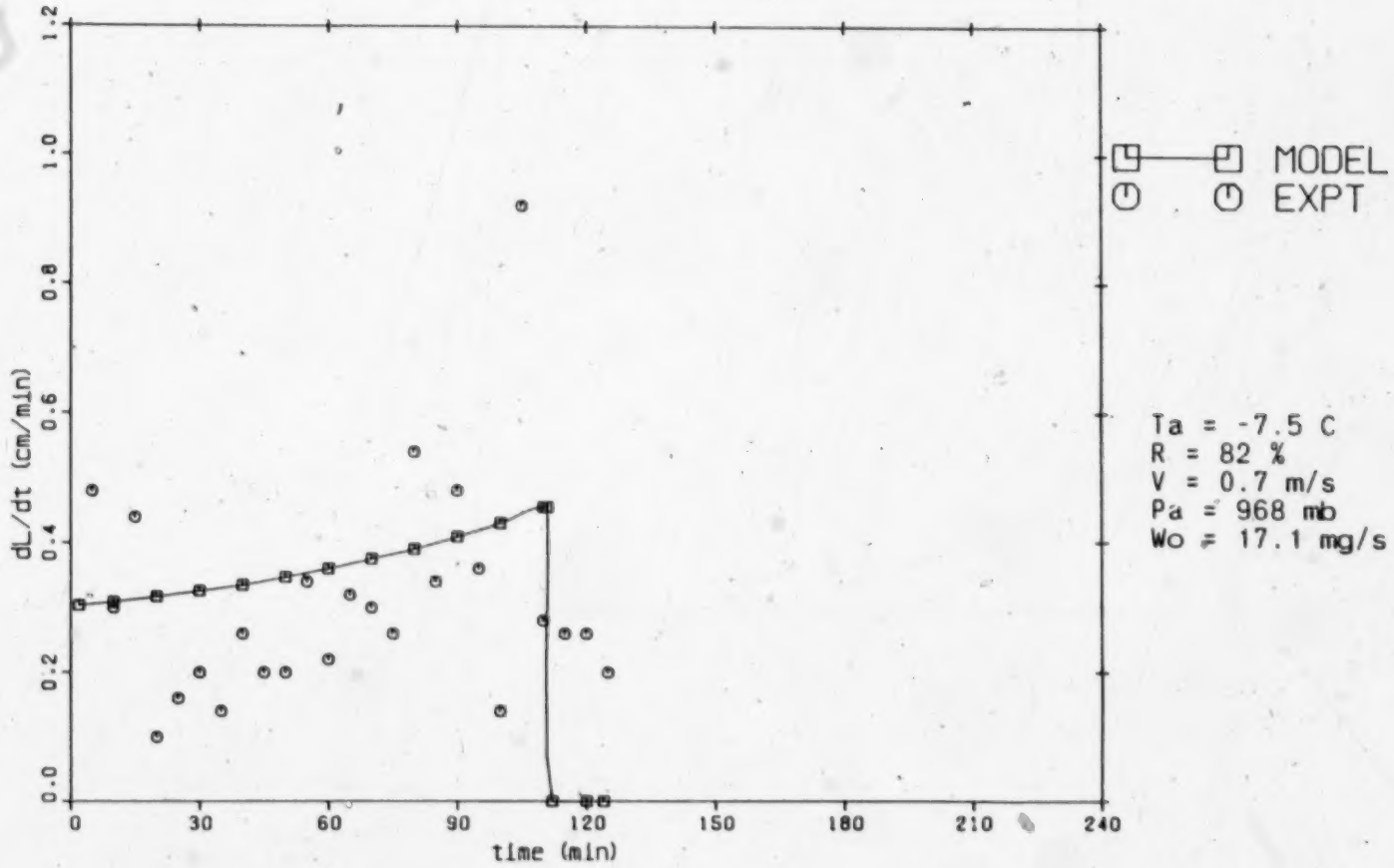

Figure 8.2.5 Icicle length growth rate dL/dt (cm/min) vs time (min) for pure icicle growth, case #5 in Appendix D.

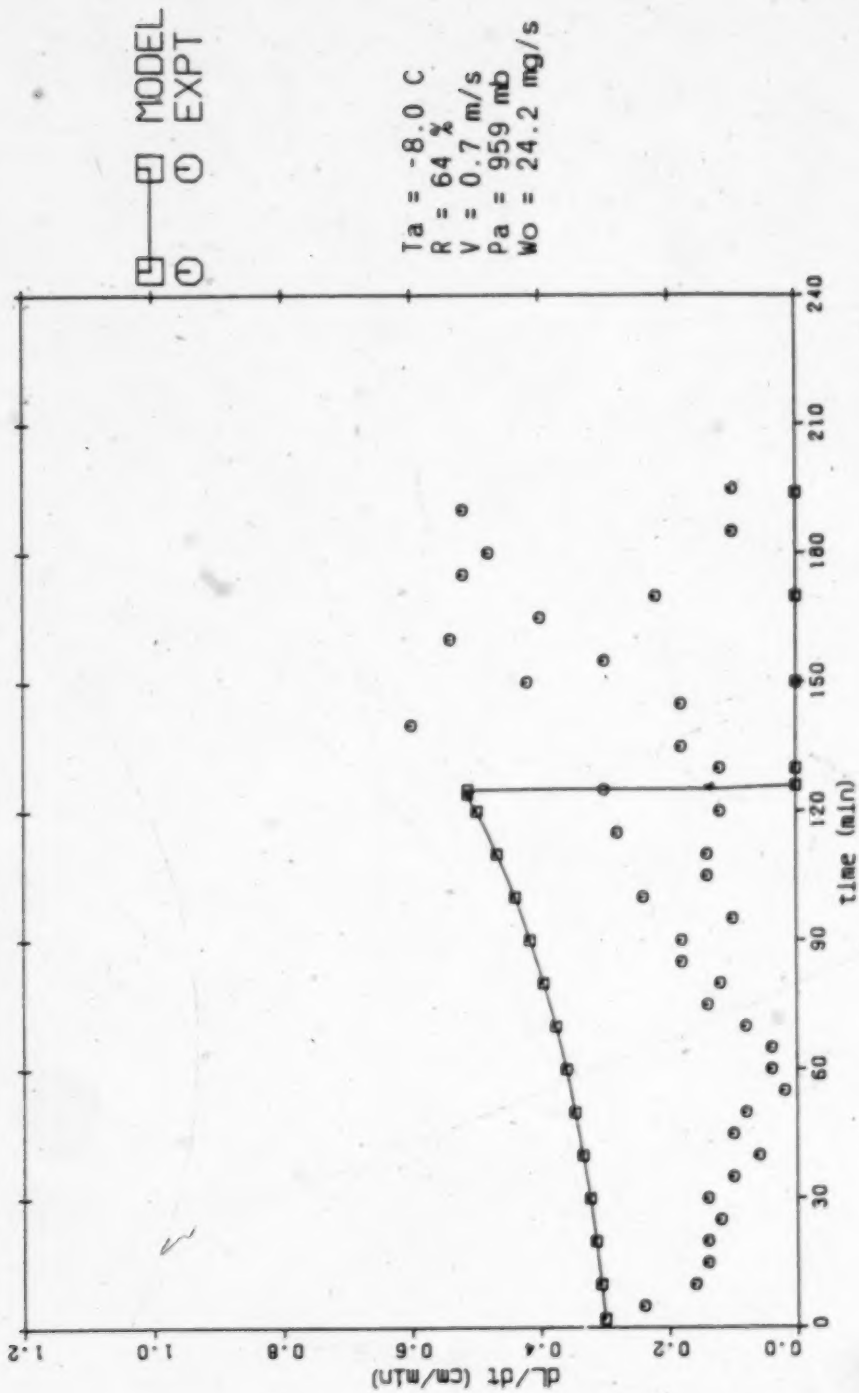

Figure 8.2.6 Icicle length growth rate dL/dt (cm/min) vs time (min) for pure icicle growth, case #6 in Appendix D.

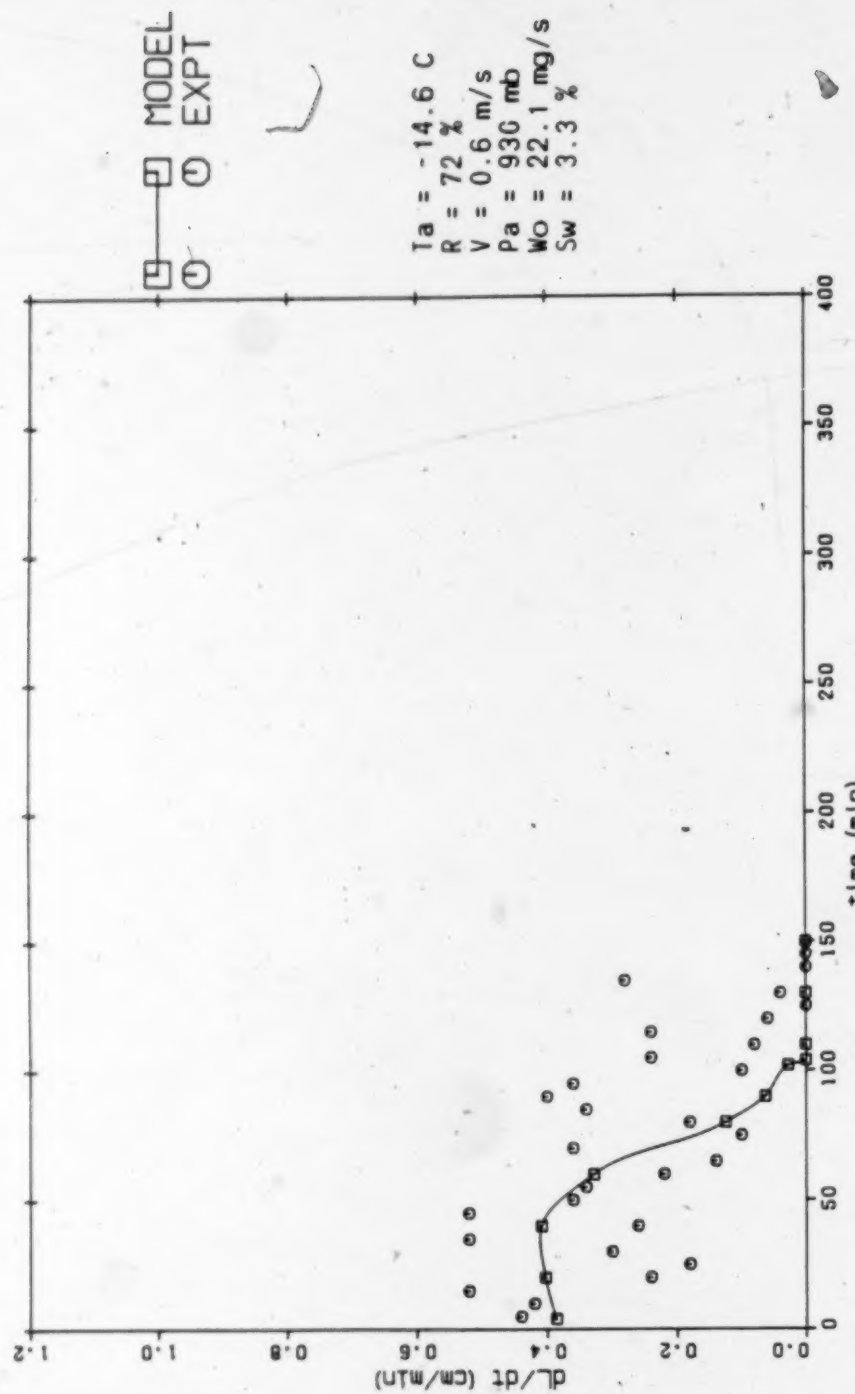

Figure 8.2.7 Icicle length growth rate dL/dt (cm/min) vs time (min) for saline icicle growth, case #7 in Appendix D.

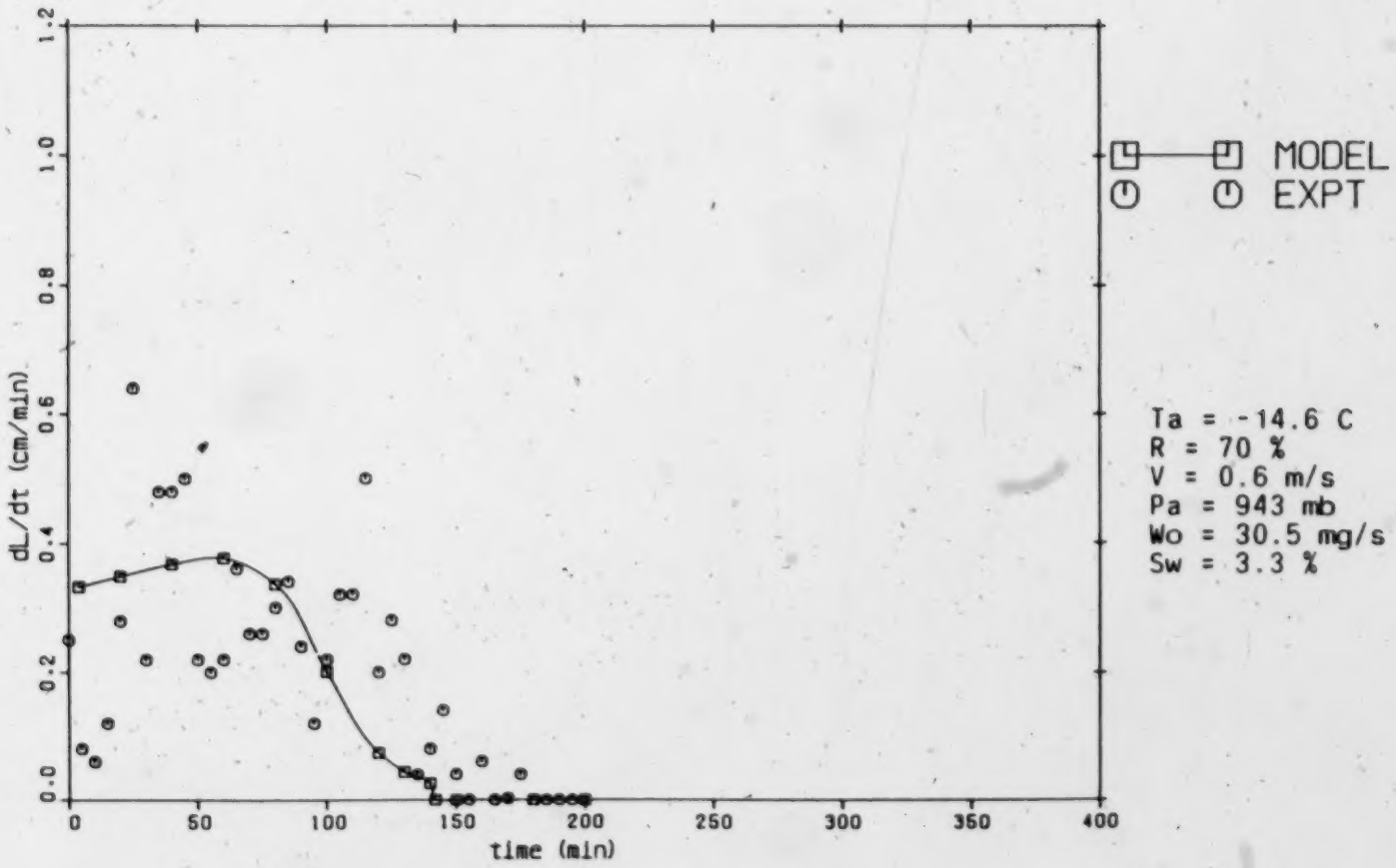

Figure 8.2.8 Icicle length growth rate dL/dt (cm/min) vs time (min) for saline icicle growth, case #8 in Appendix D.

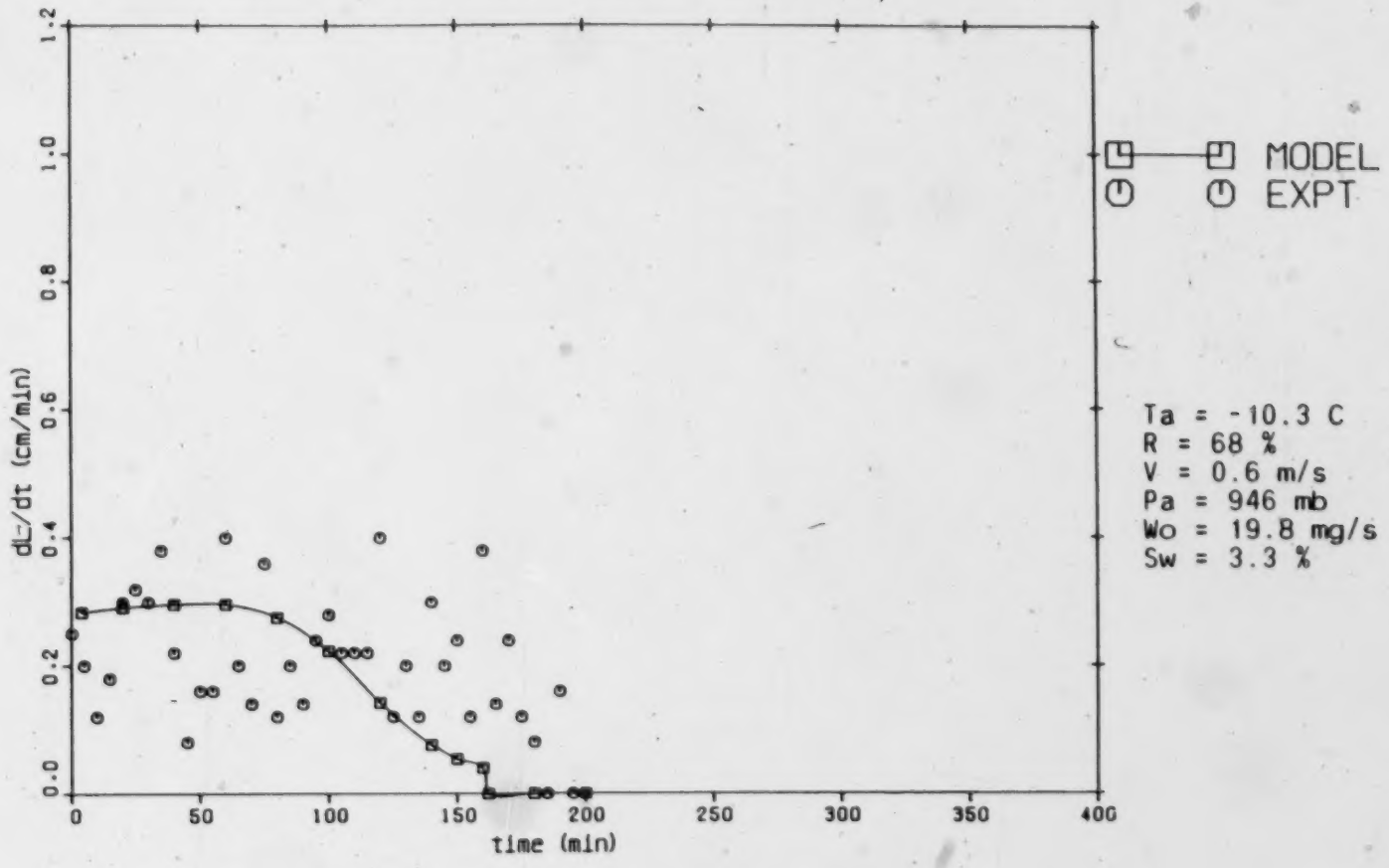

Figure 8.2.9 Icicle length growth rate dL/dt (cm/min) vs time (min) for saline icicle growth, case #9 in Appendix D.

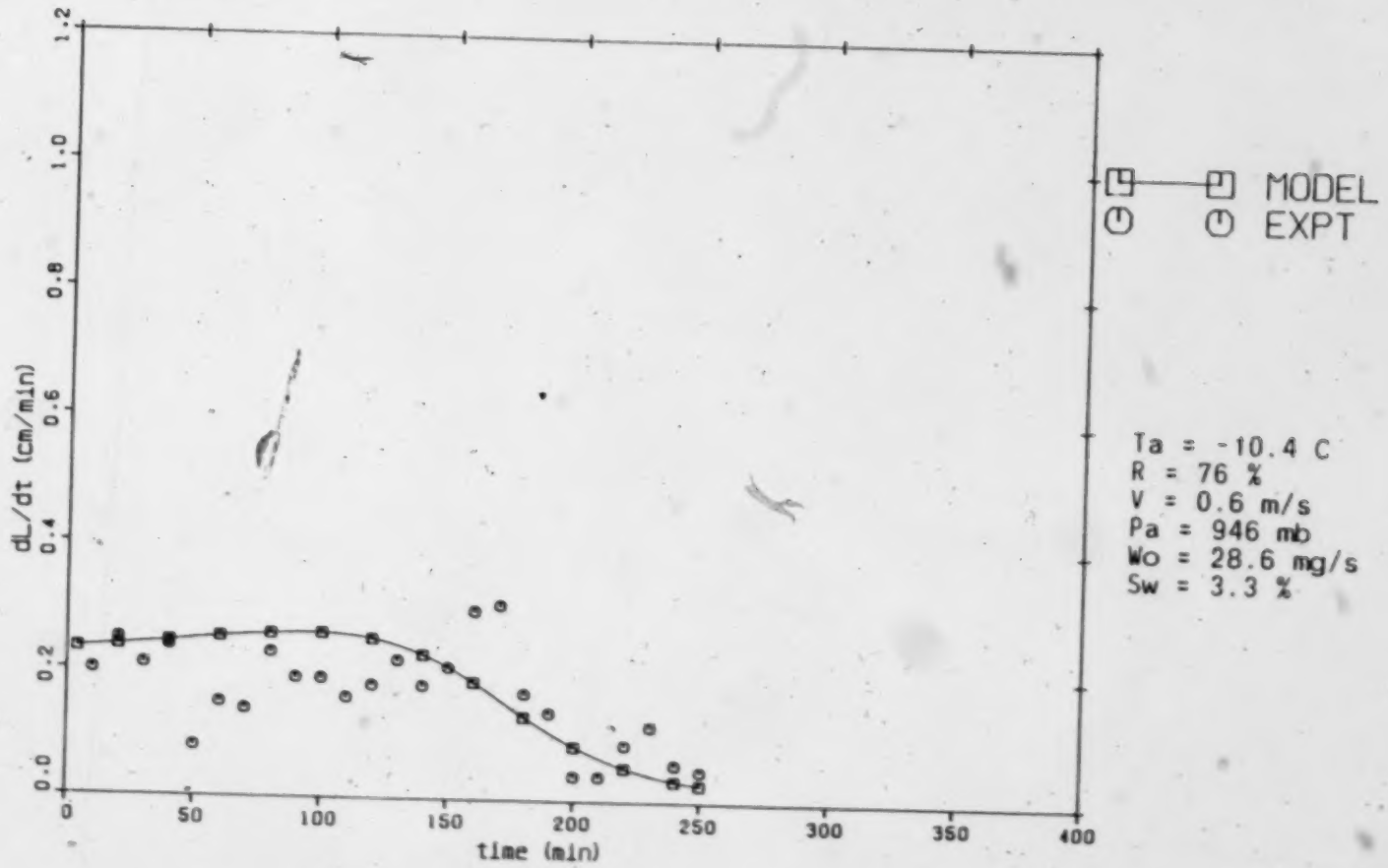

Figure 8.2.10 Icicle length growth rate dL/dt (cm/min) vs time (min) for saline icicle growth, case #10 in Appendix D.

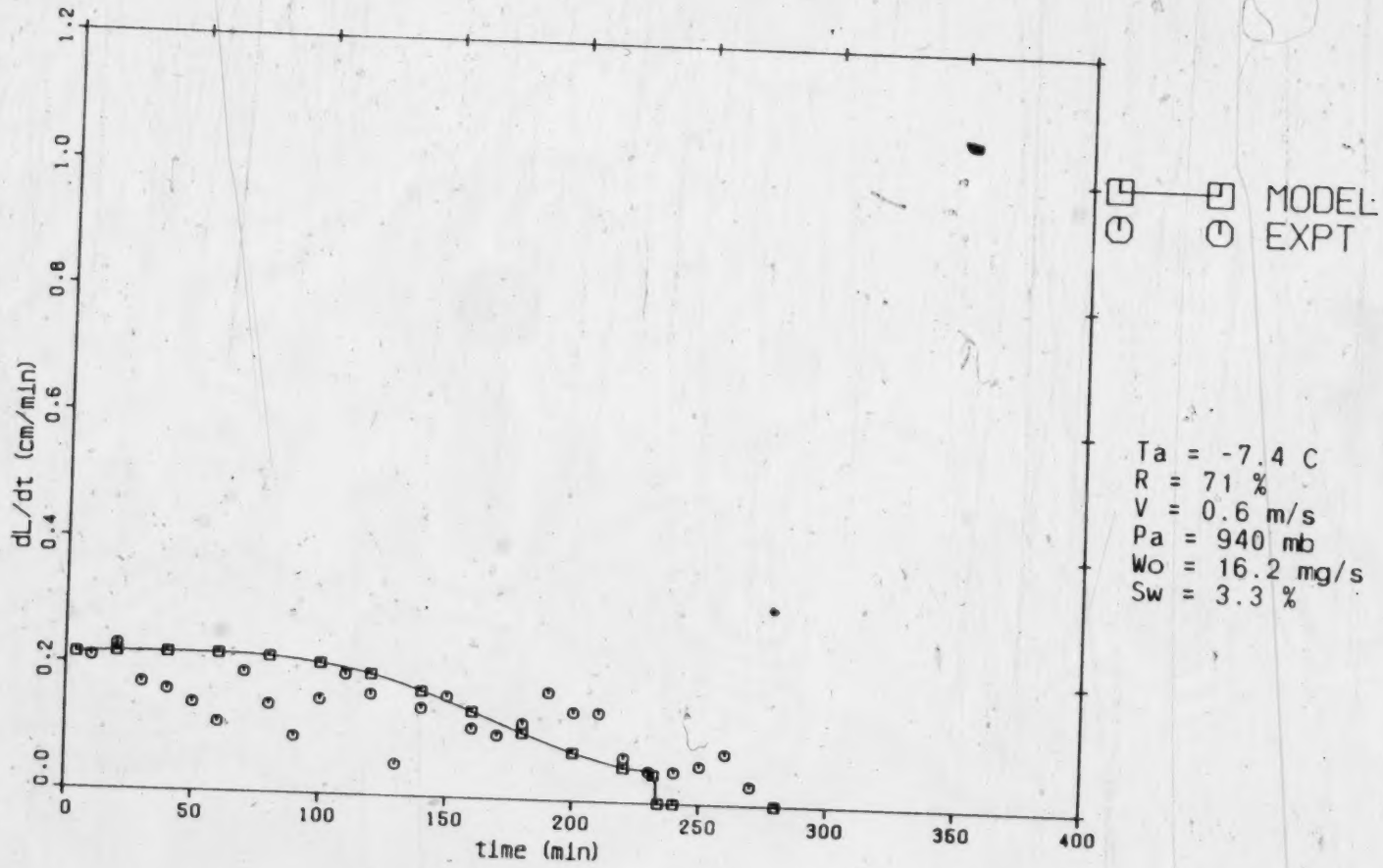

Figure 8.2.11 Icicle length growth rate dL/dt (cm/min) vs time (min) for saline icicle growth, case #11 in Appendix D.

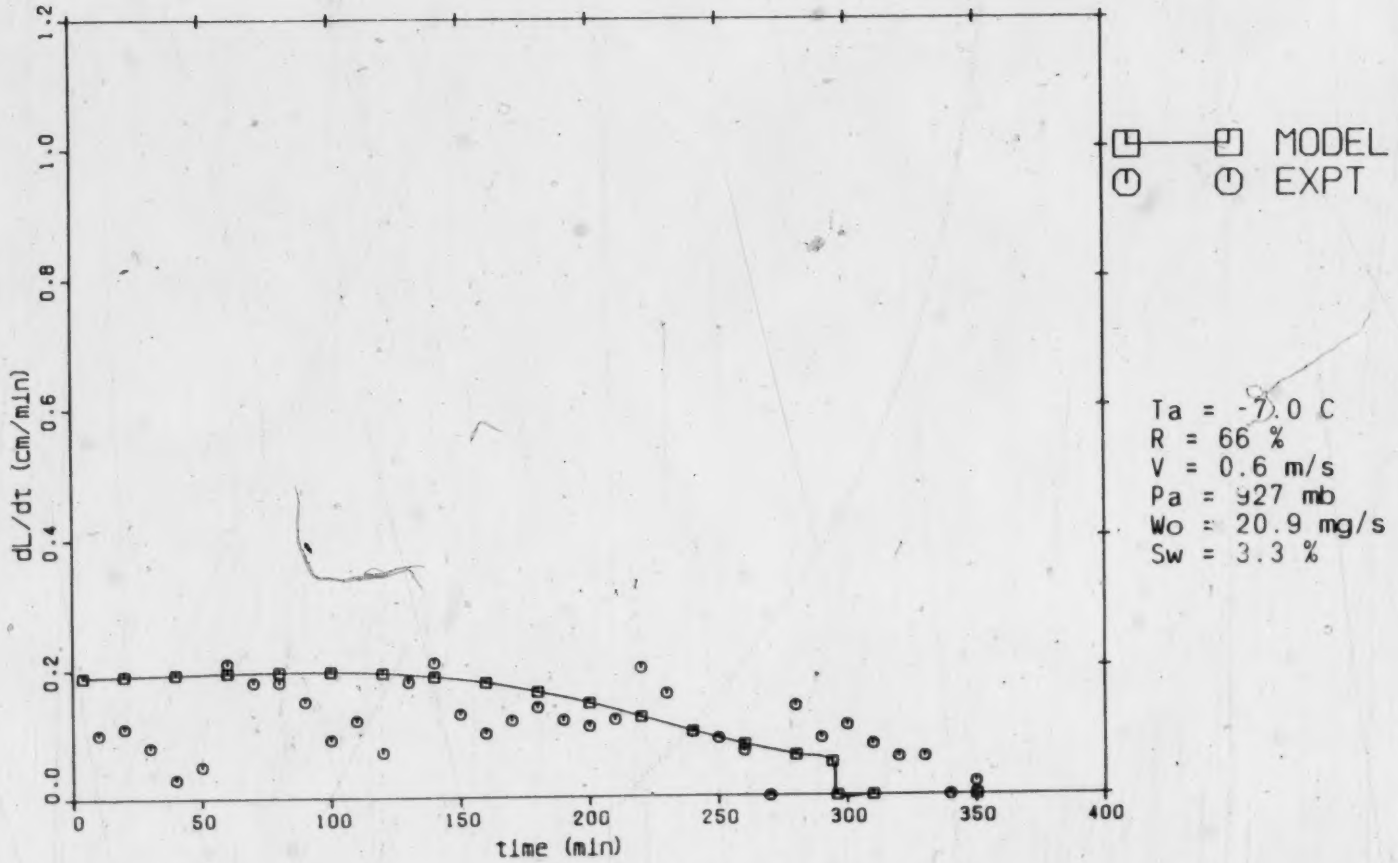

Figure 8.2.12 Icicle length growth rate dL/dt (cm/min) vs time (min) for saline icicle growth, case #12 in Appendix D.

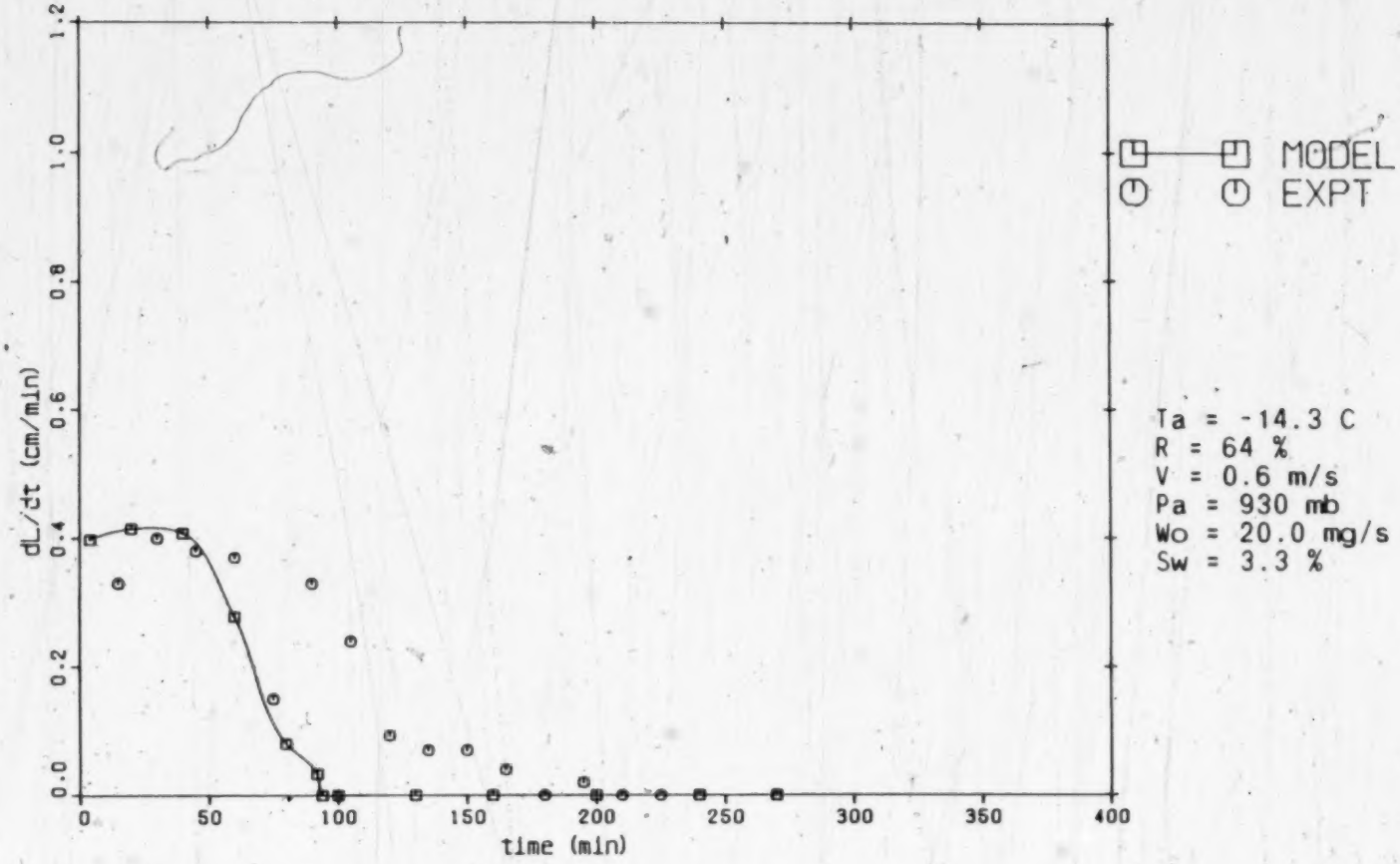

Figure 8.2.13 Icicle length growth rate dL/dt (cm/min) vs time (min) for saline icicle growth, case #13 in Appendix D.

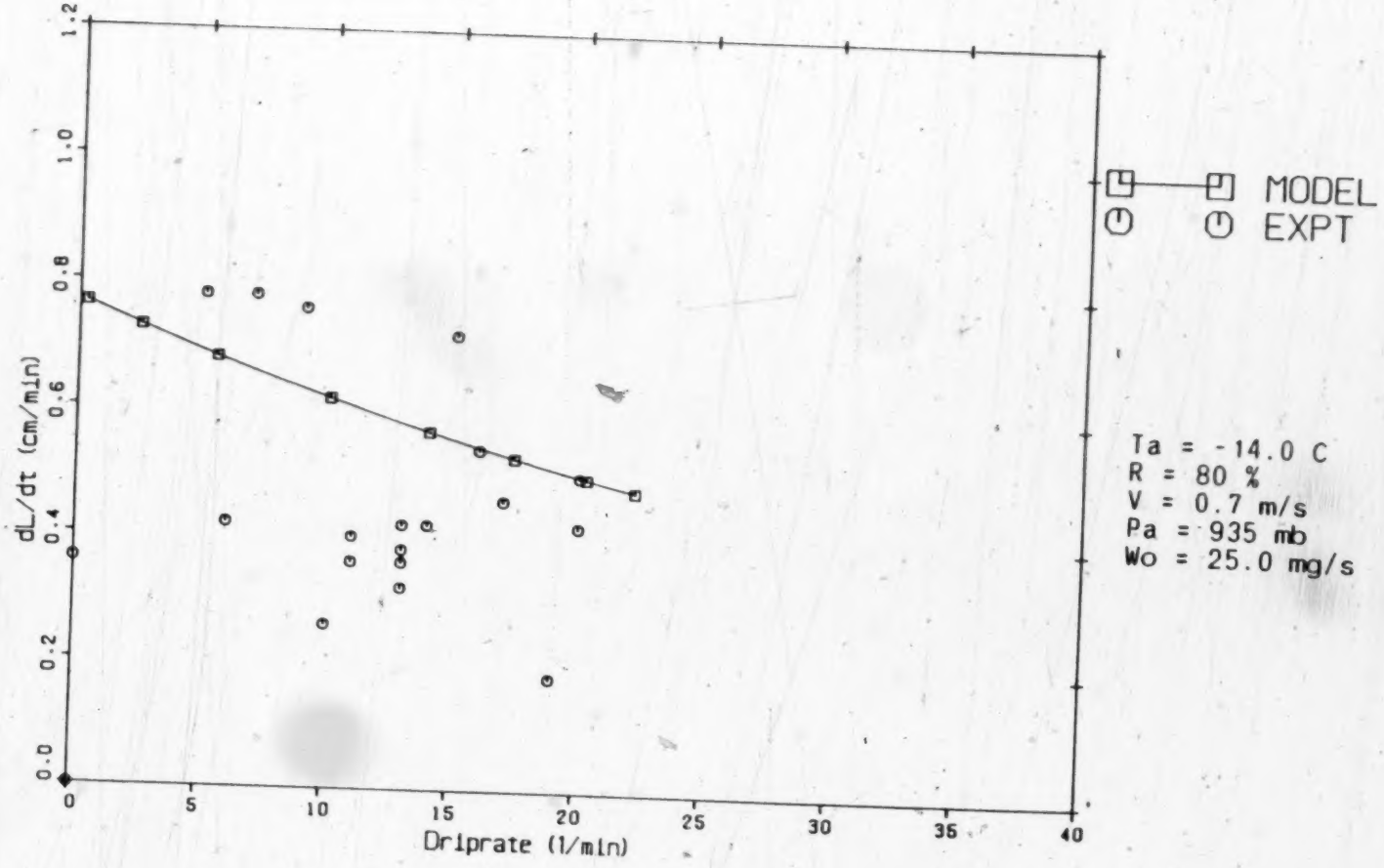

Figure 8.3.1 Icicle length growth rate dL/dt (cm/min) vs drip rate (1/min) for pure icicle growth, case #1 in Appendix D.

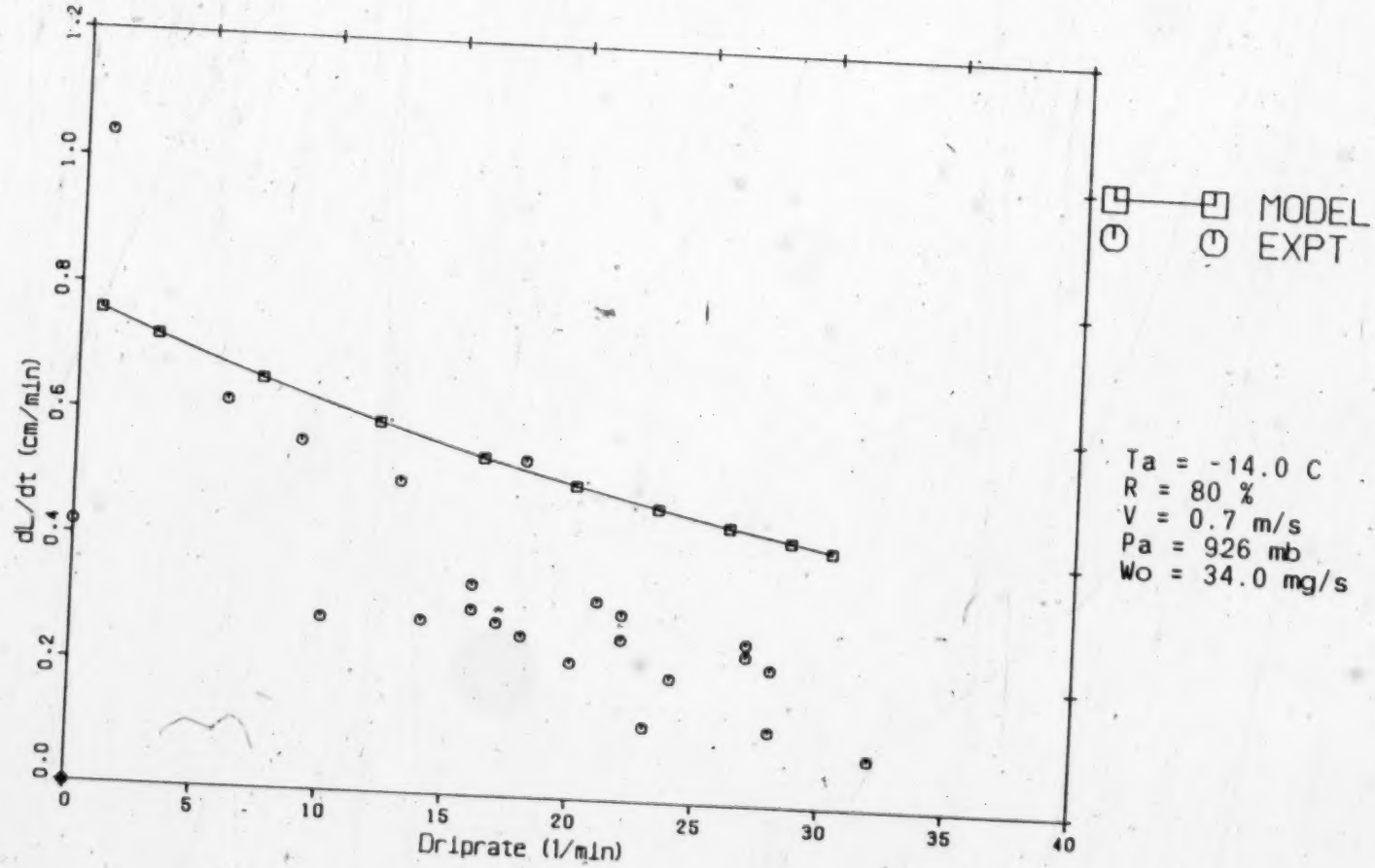

Figure 8.3.2 Icicle length growth rate dL/dt (cm/min) vs drip rate (1/min) for pure icicle growth, case #2 in Appendix D.

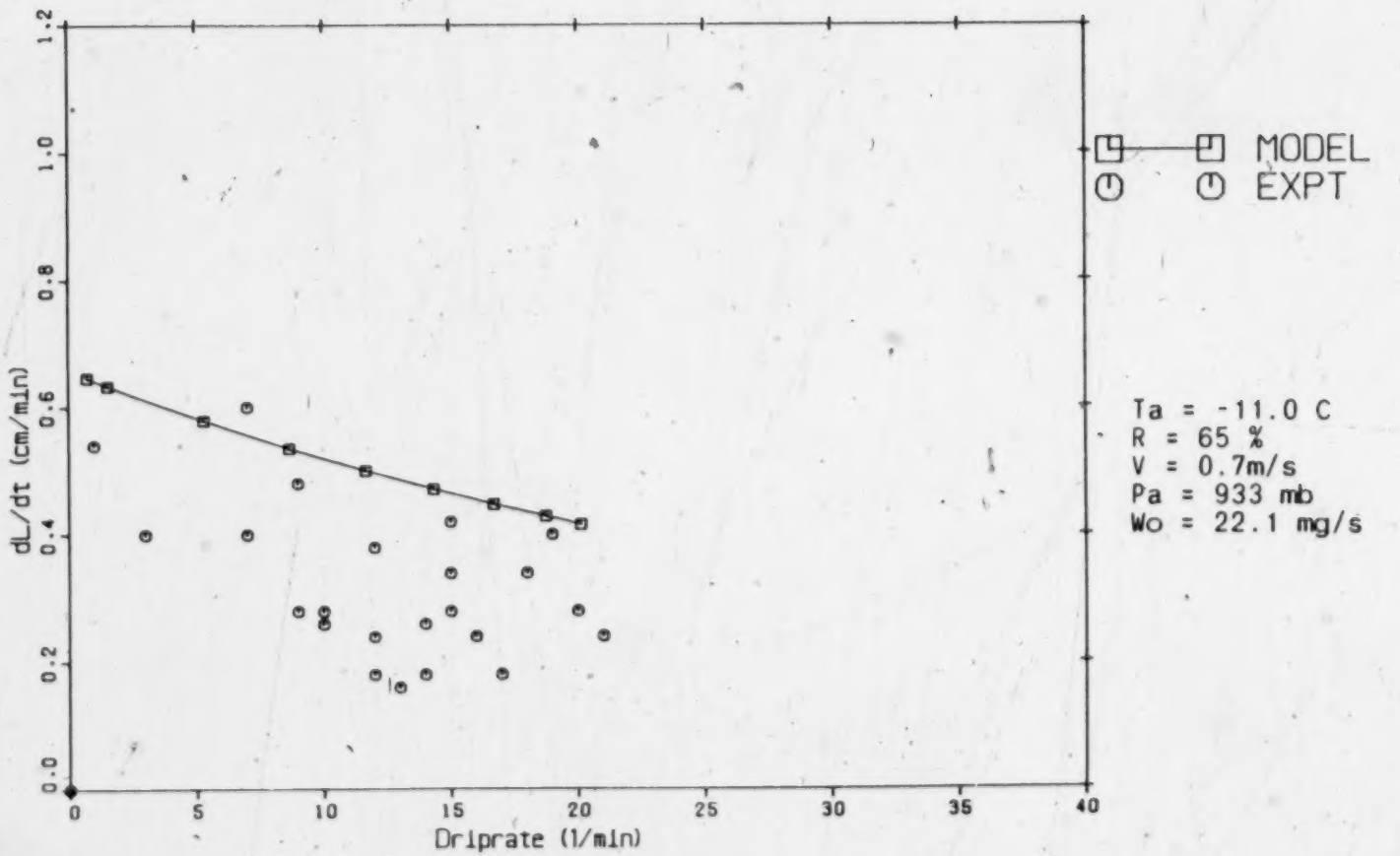

Figure 8.3.3 Icicle length growth rate dL/dt (cm/min) vs drip rate (1/min) for pure icicle growth, case #3 in Appendix D.

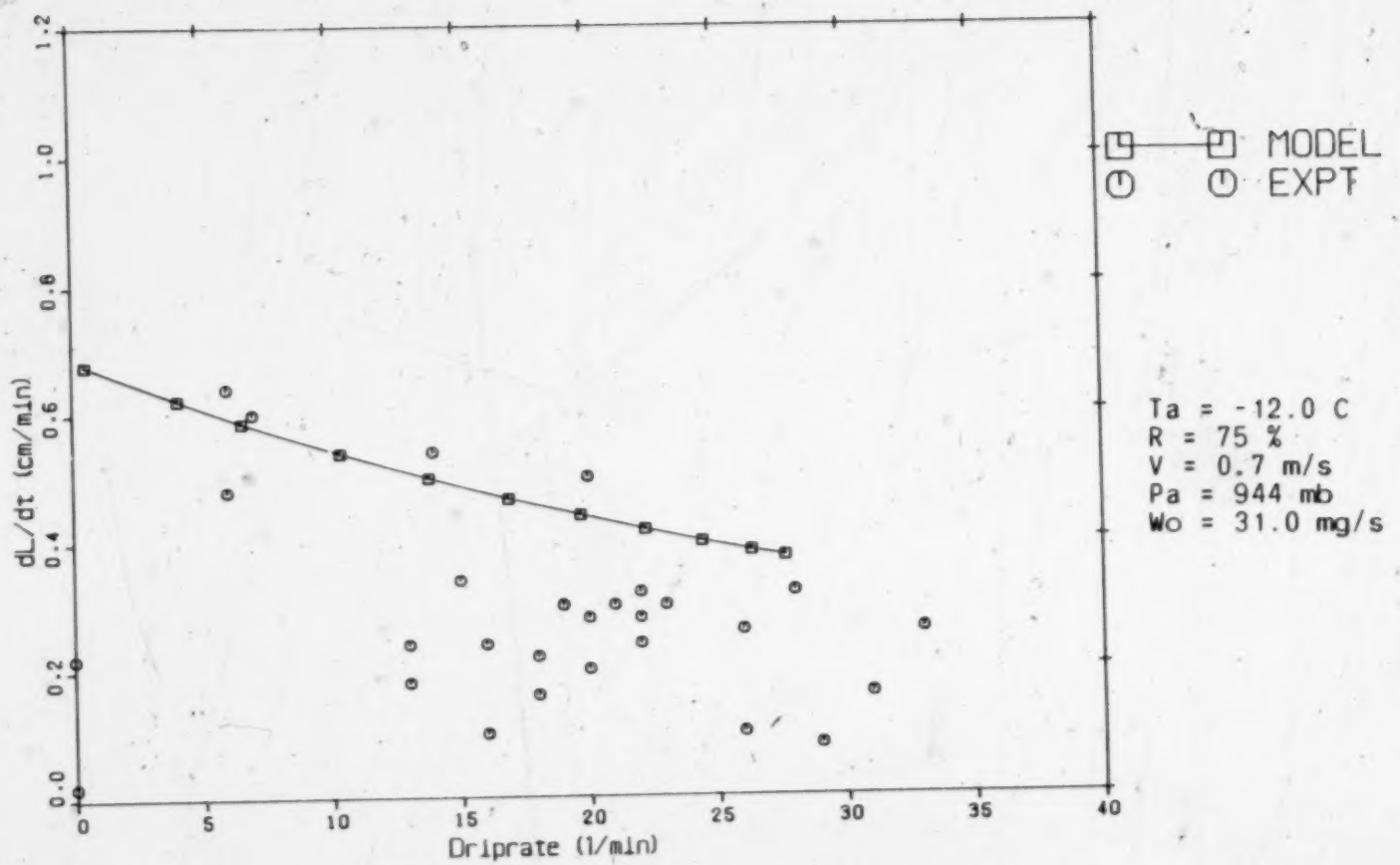

Figure 8.3.4 Icicle length growth rate dL/dt (cm/min) vs drip rate (1/min) for pure icicle growth, case #4 in Appendix D.

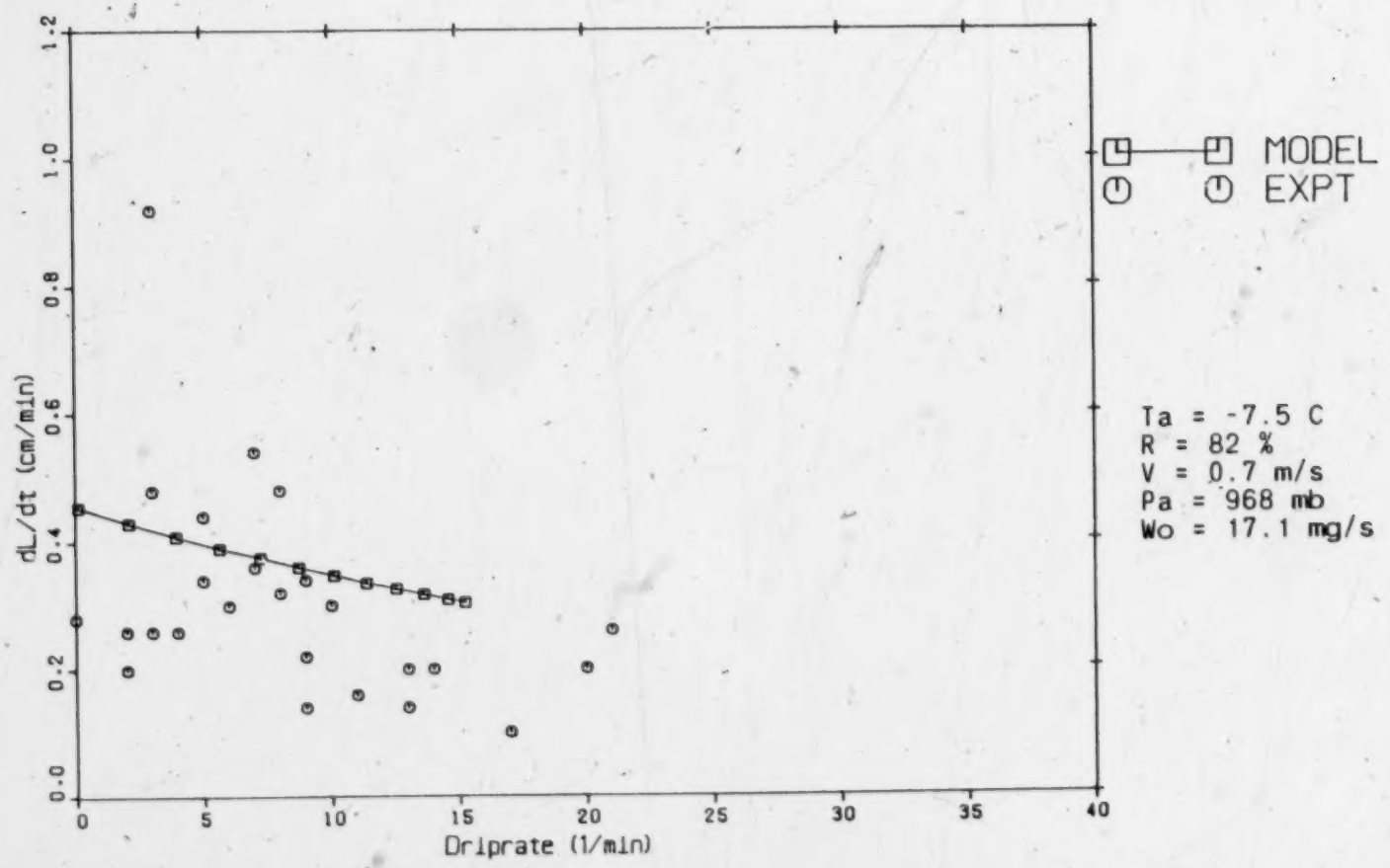

Figure 8.3.5 Icicle length growth rate dL/dt (cm/min) vs drip rate (1/min) for pure icicle growth, case #5 in Appendix D.

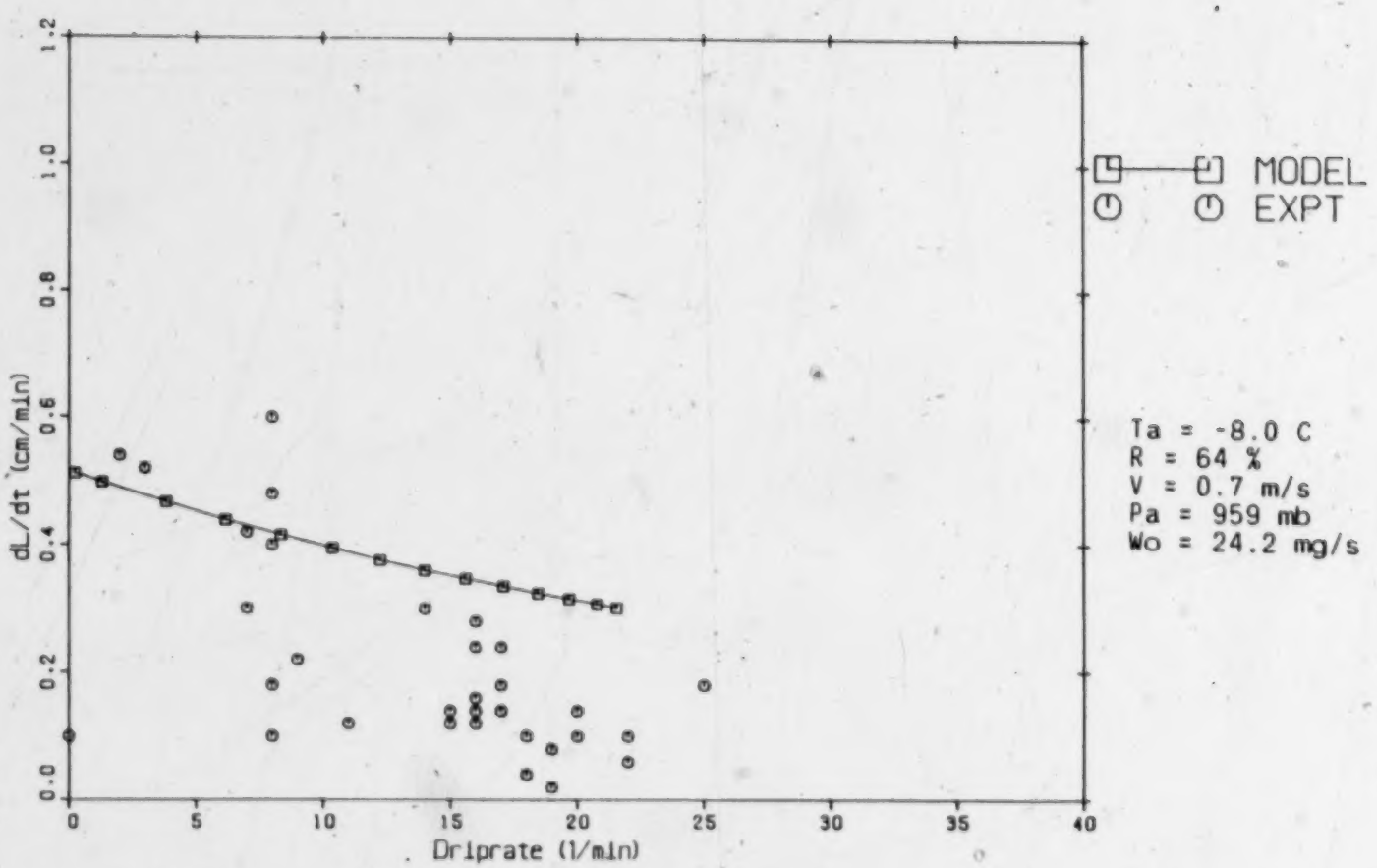

Figure 8.3.6 Icicle length growth rate dL/dt (cm/min) vs drip rate (1/min) for pure icicle growth, case #6 in Appendix D.

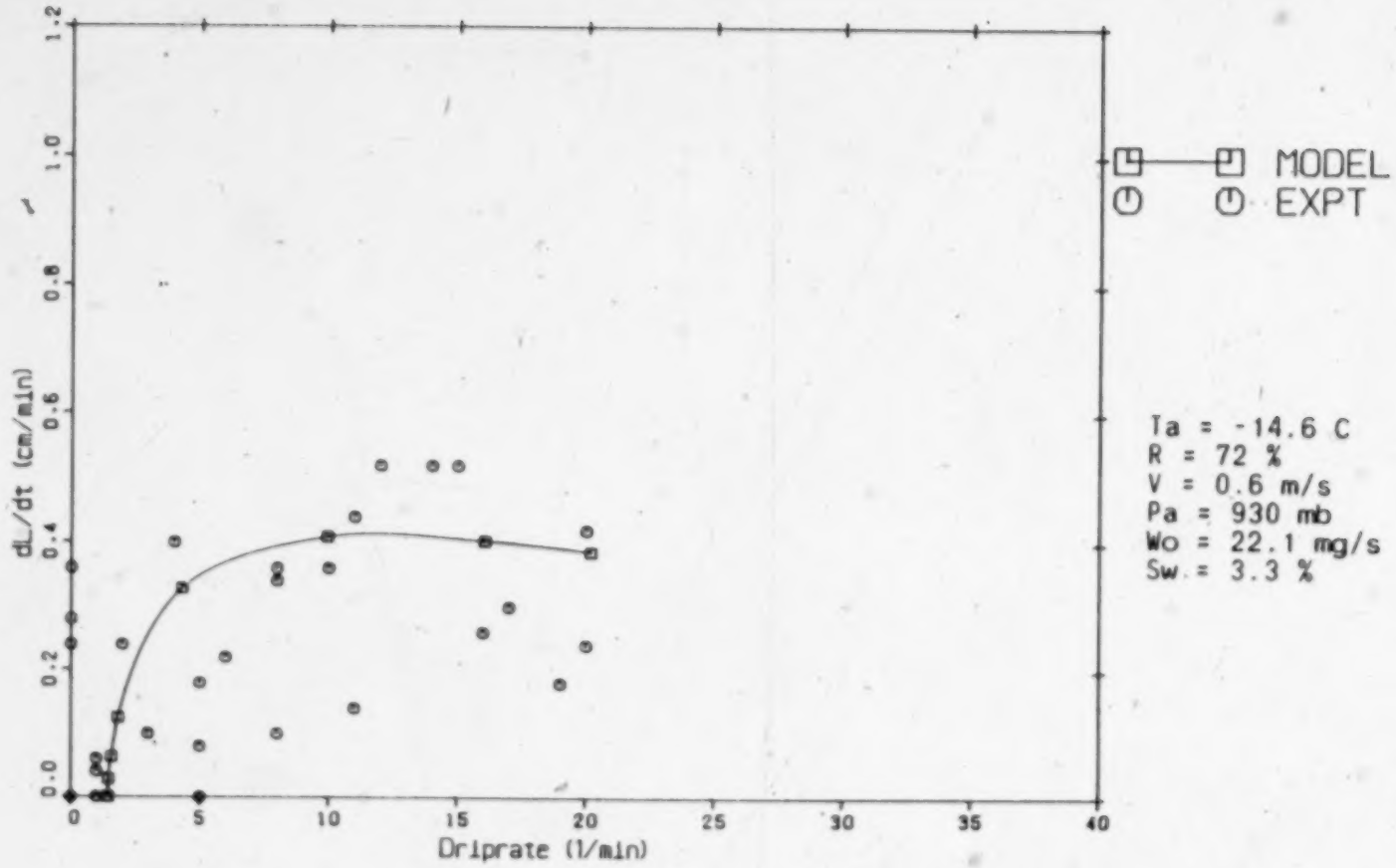

Figure 8.3.7 Icicle length growth rate dL/dt (cm/min) vs drip rate (1/min) for saline icicle growth, case #7 in Appendix D.

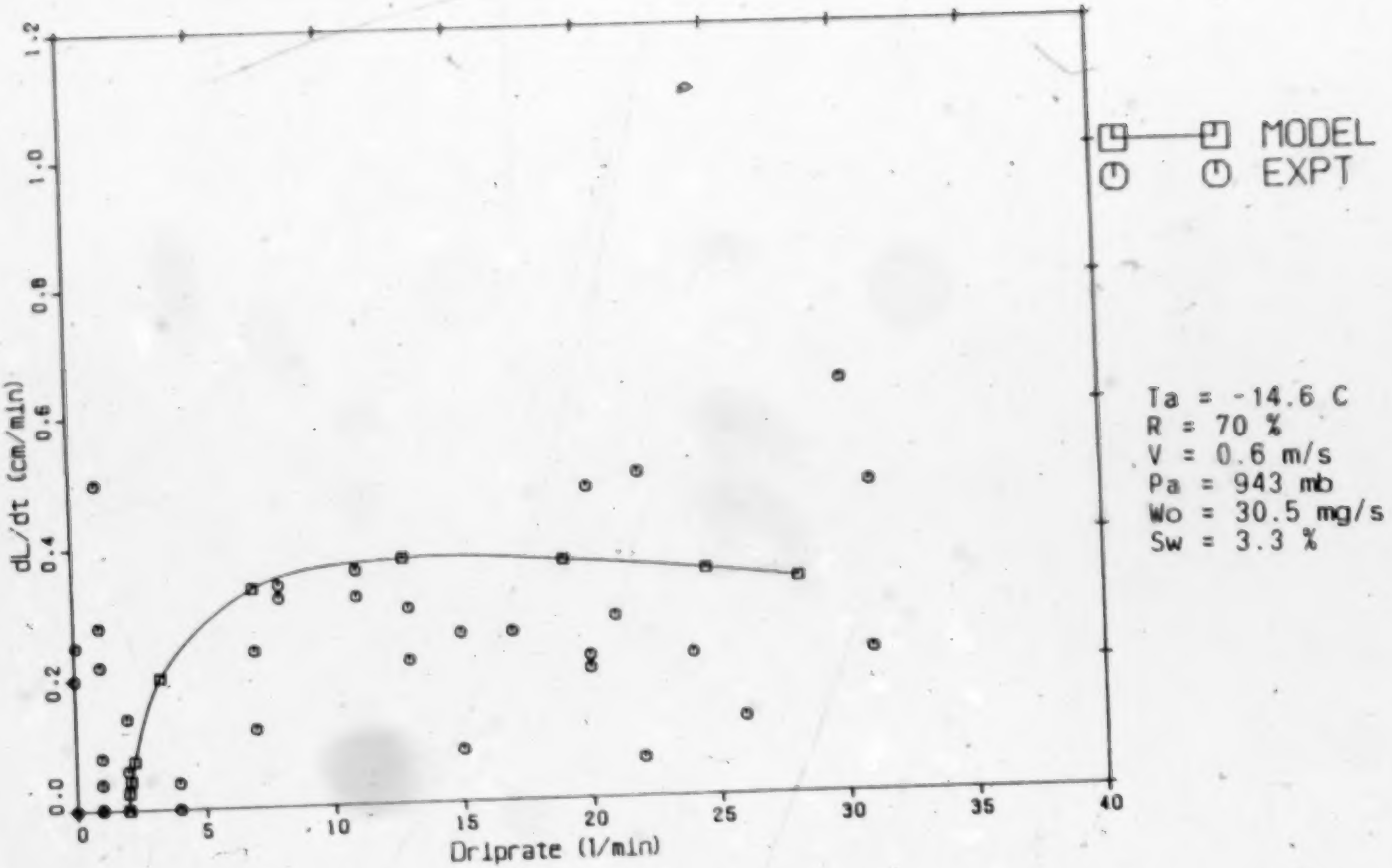

Figure 8.3.8 Icicle length growth rate dL/dt (cm/min) vs drip rate (1/min) for saline icicle growth, case #8 in Appendix D.

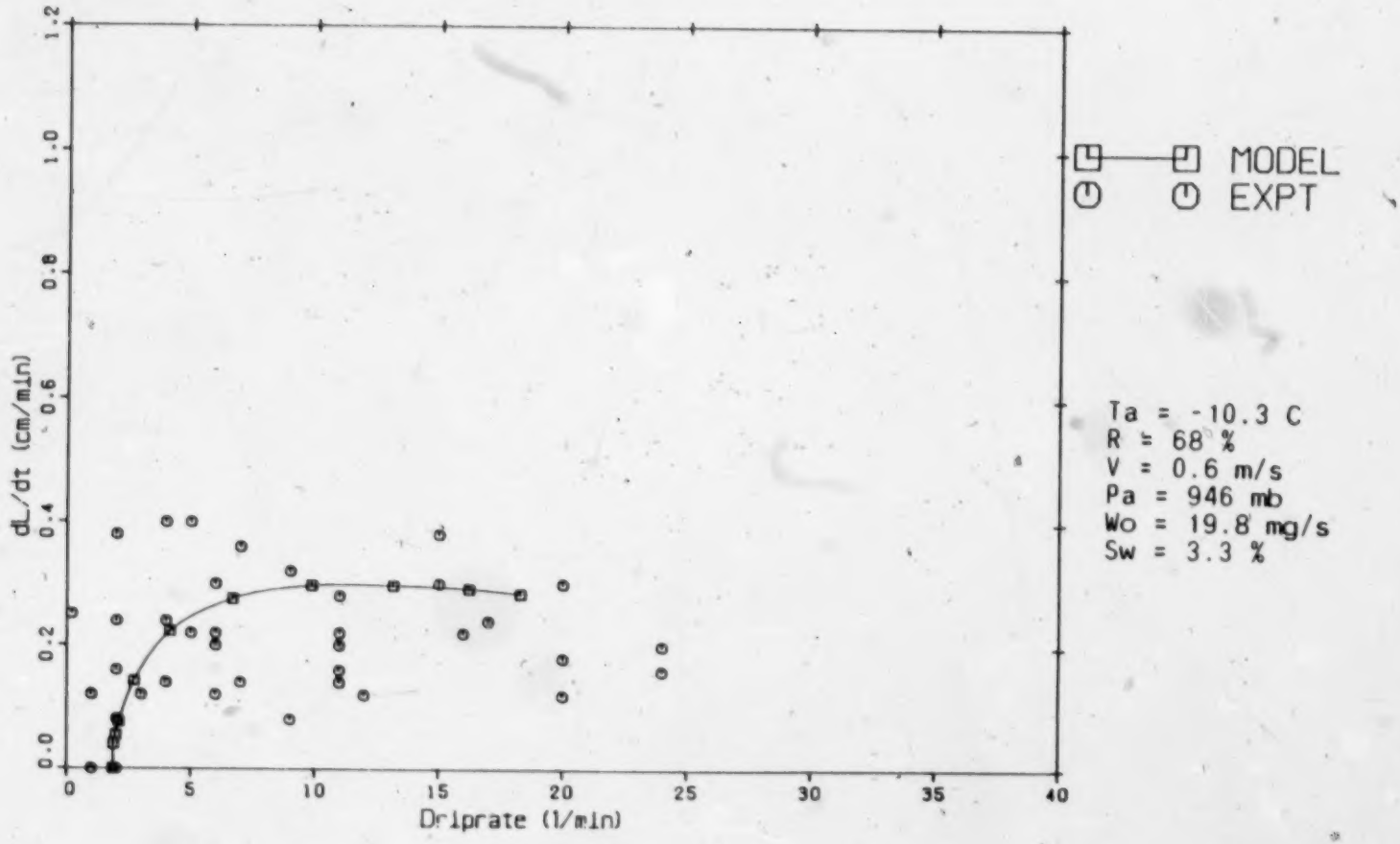

Figure 8.3.9 Icicle length growth rate dL/dt (cm/min) vs drip rate (1/min) for saline icicle growth, case #9 in Appendix D.

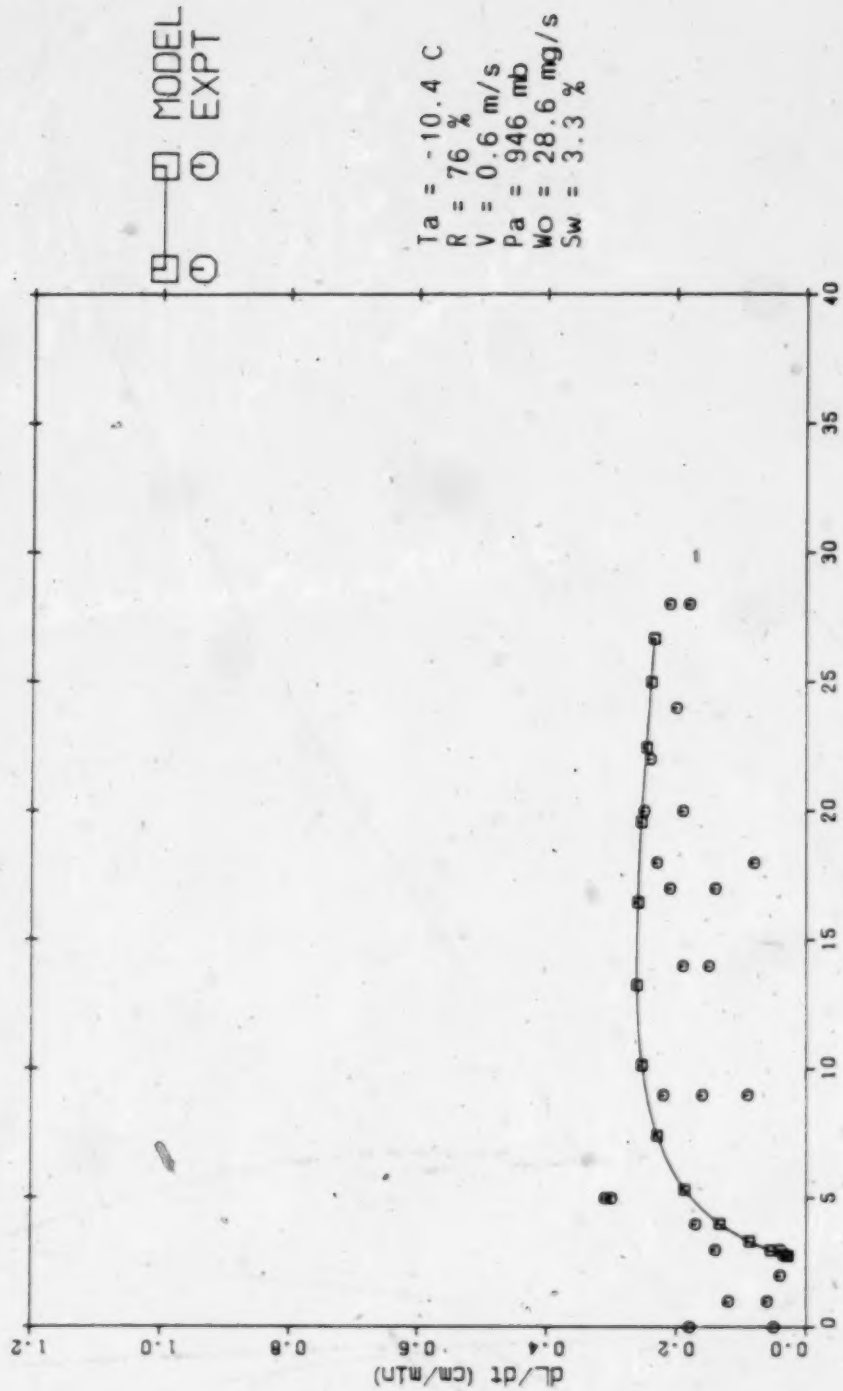

Figure 8.3.10 Icicle length growth rate dL/dt (cm/min) vs drip rate (1/min) for saline icicle growth, case #10 in Appendix D.

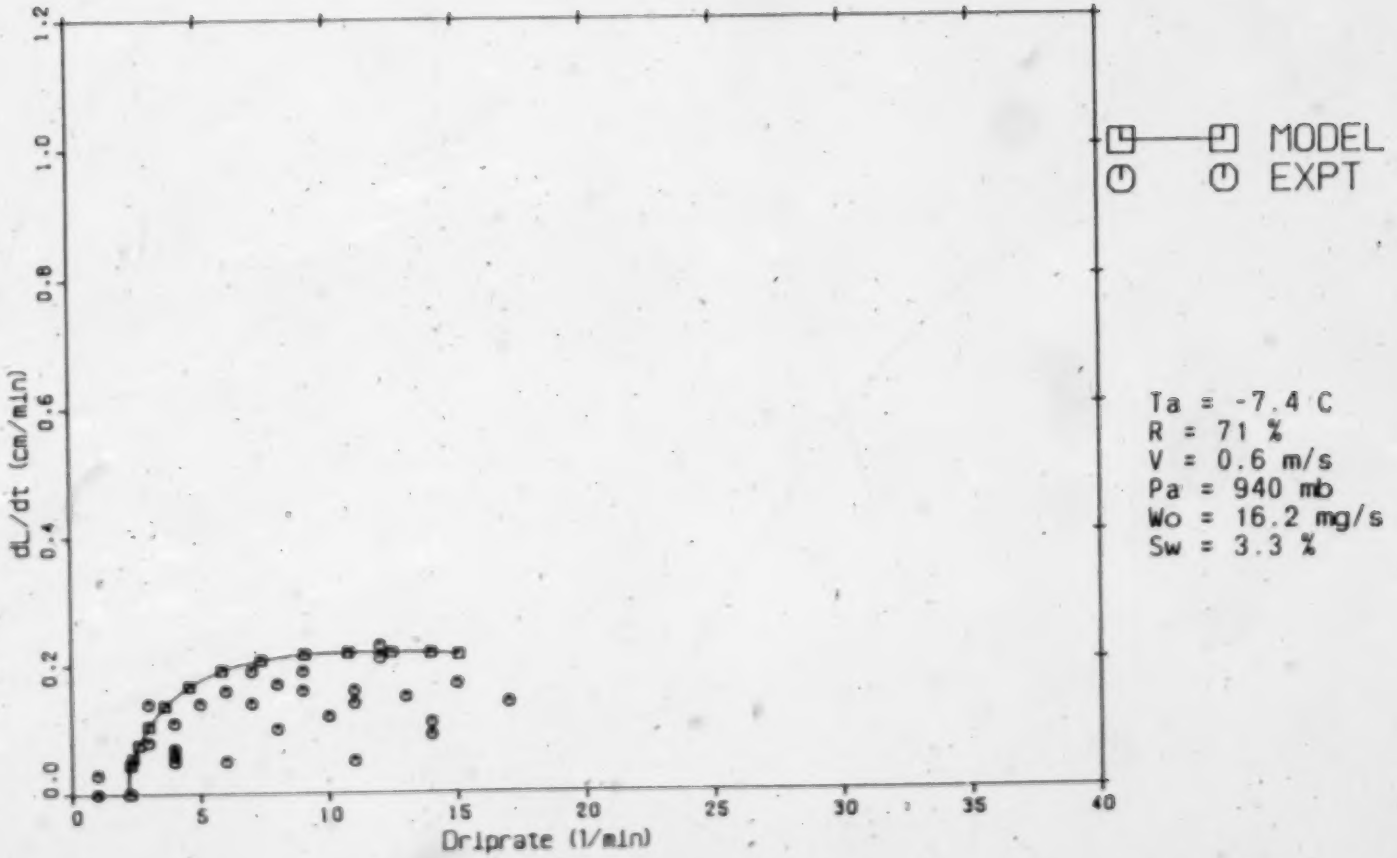

Figure 8.3.11 Icicle length growth rate dL/dt (cm/min) vs drip rate (1/min) for saline icicle growth, case #11 in Appendix D.

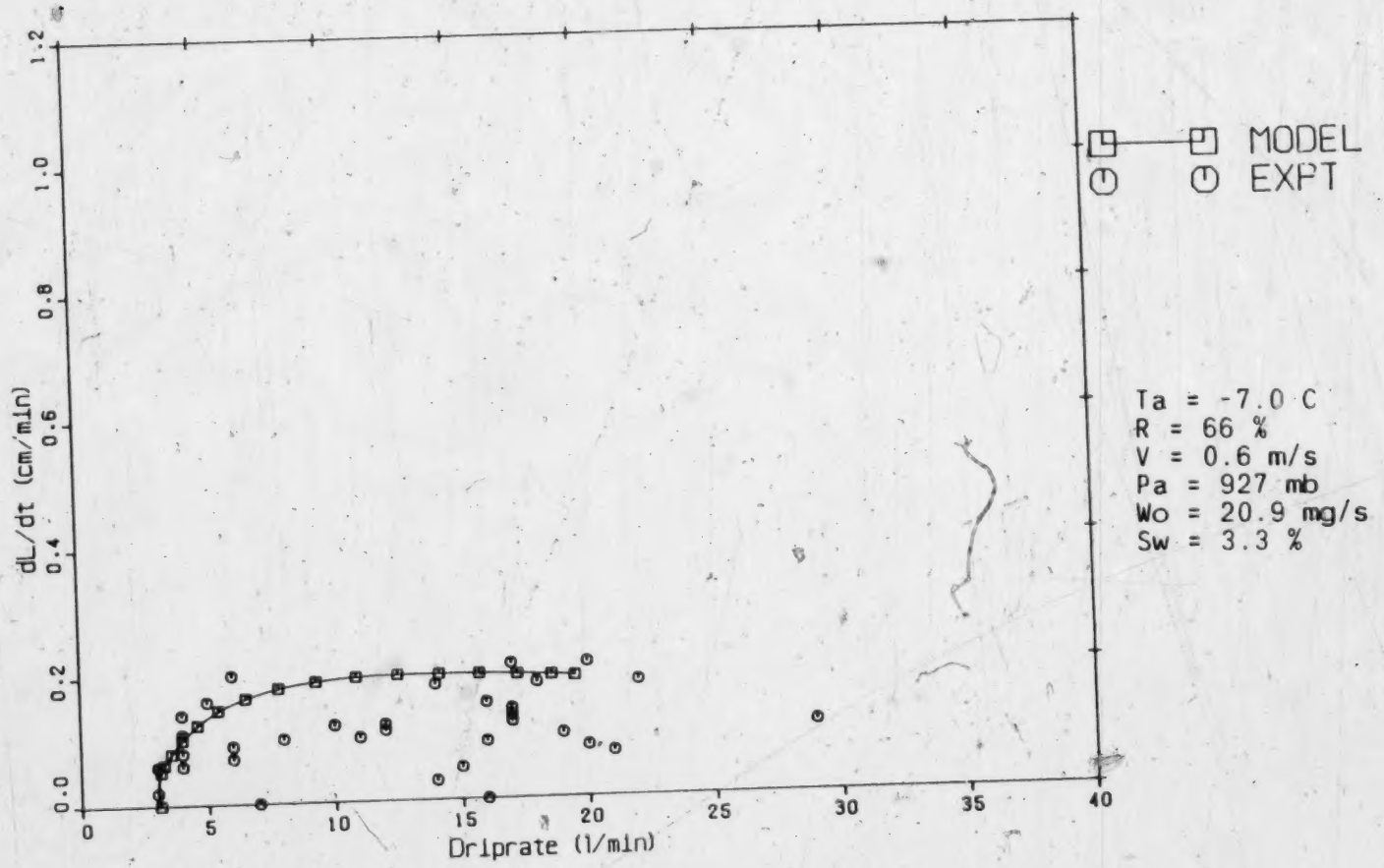

Figure 8.3.12 Icicle length growth rate dL/dt (cm/min) vs drip rate (1/min) for saline icicle growth, case #12 in Appendix D.

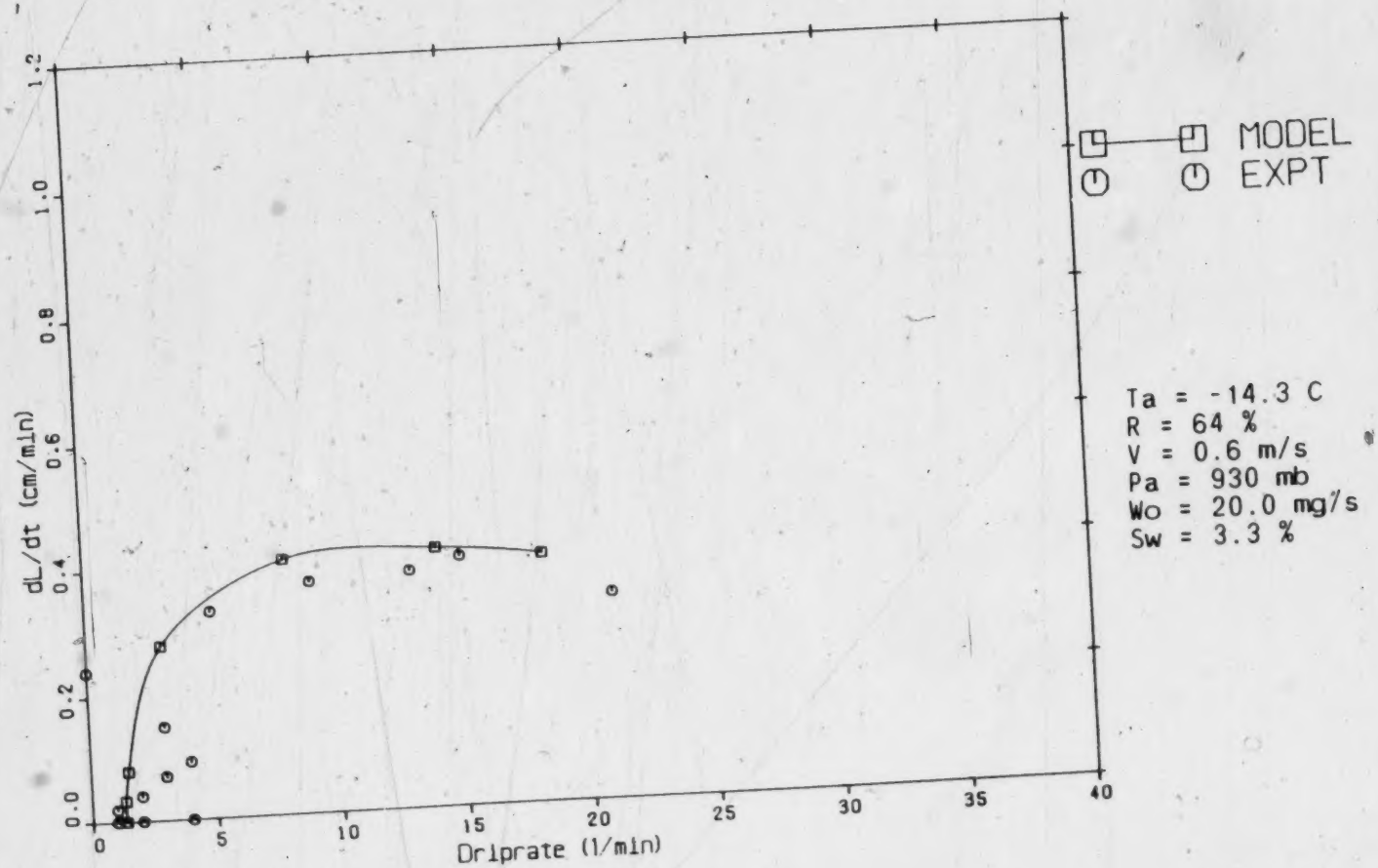

Figure 8.3.13 Icicle length growth rate dL/dt (cm/min) vs drip rate (1/min) for saline icicle growth, case #13 in Appendix D.

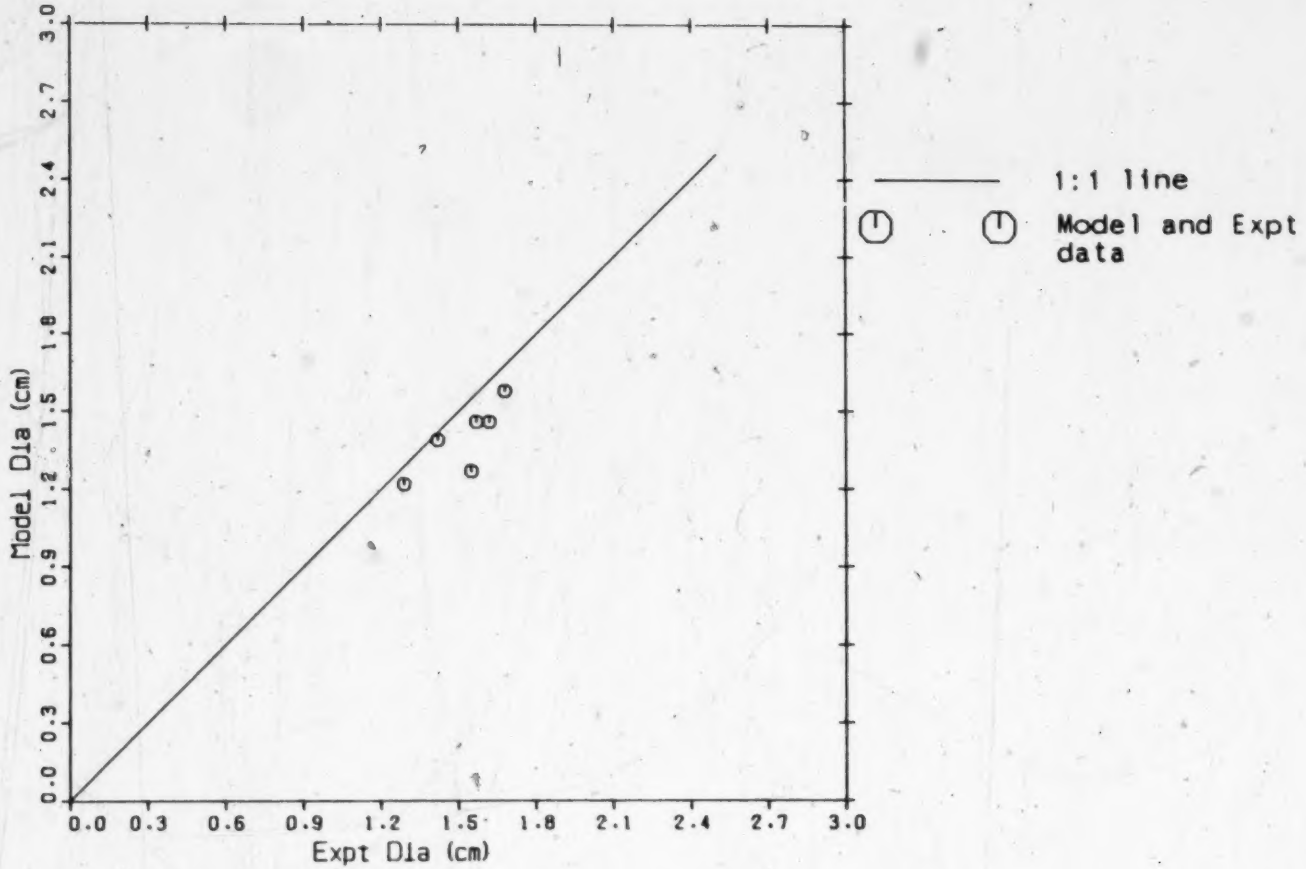

Figure 8.4.1 Model mean diameter (cm) at adjusted model growth termination time (MGTT) vs experimental mean diameter (cm) at experiment termination time (ETT) for pure icicle growth.

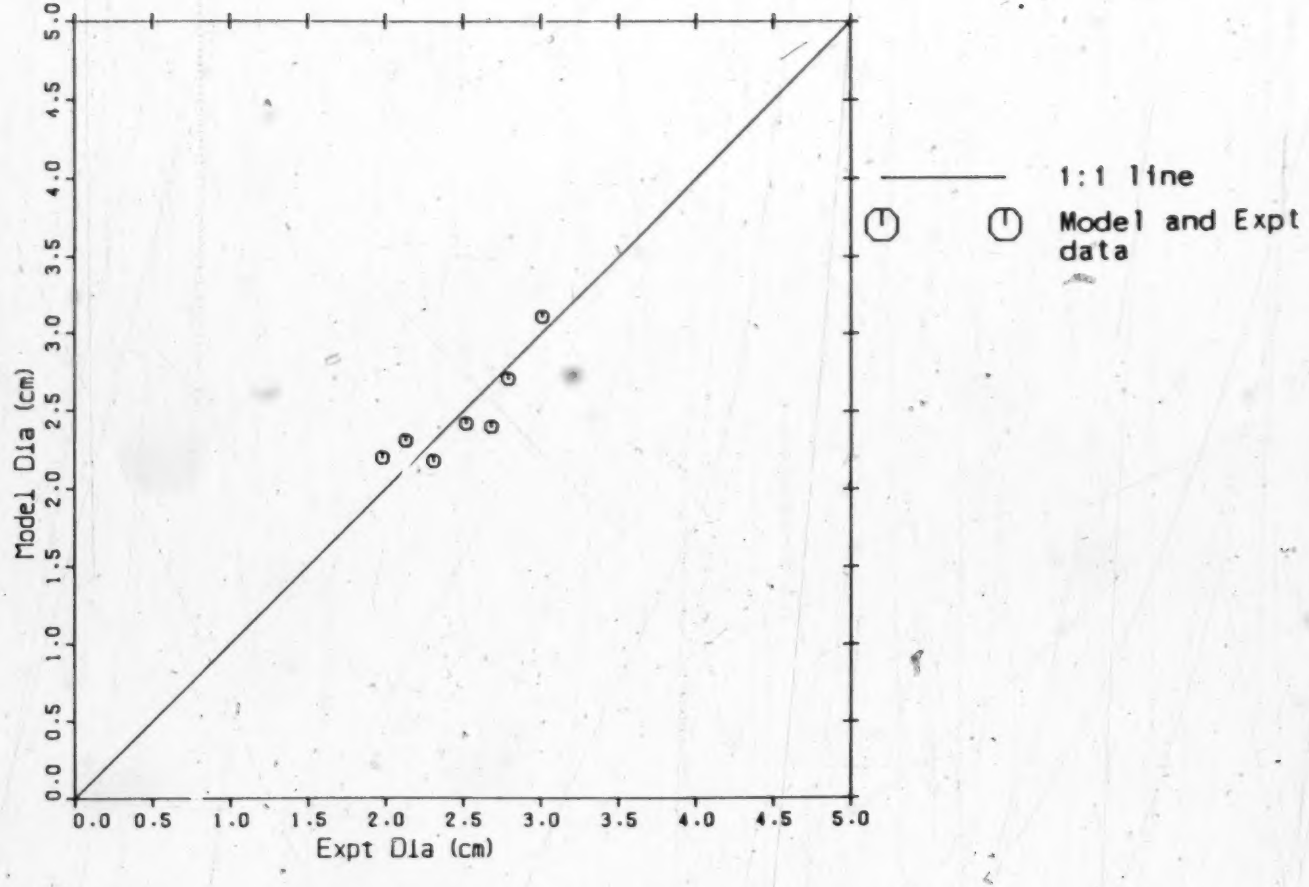

Figure 8.4.2 Model mean diameter (cm) vs experimental mean diameter (cm) at experimental termination time (ETT) for saline icicle growth.

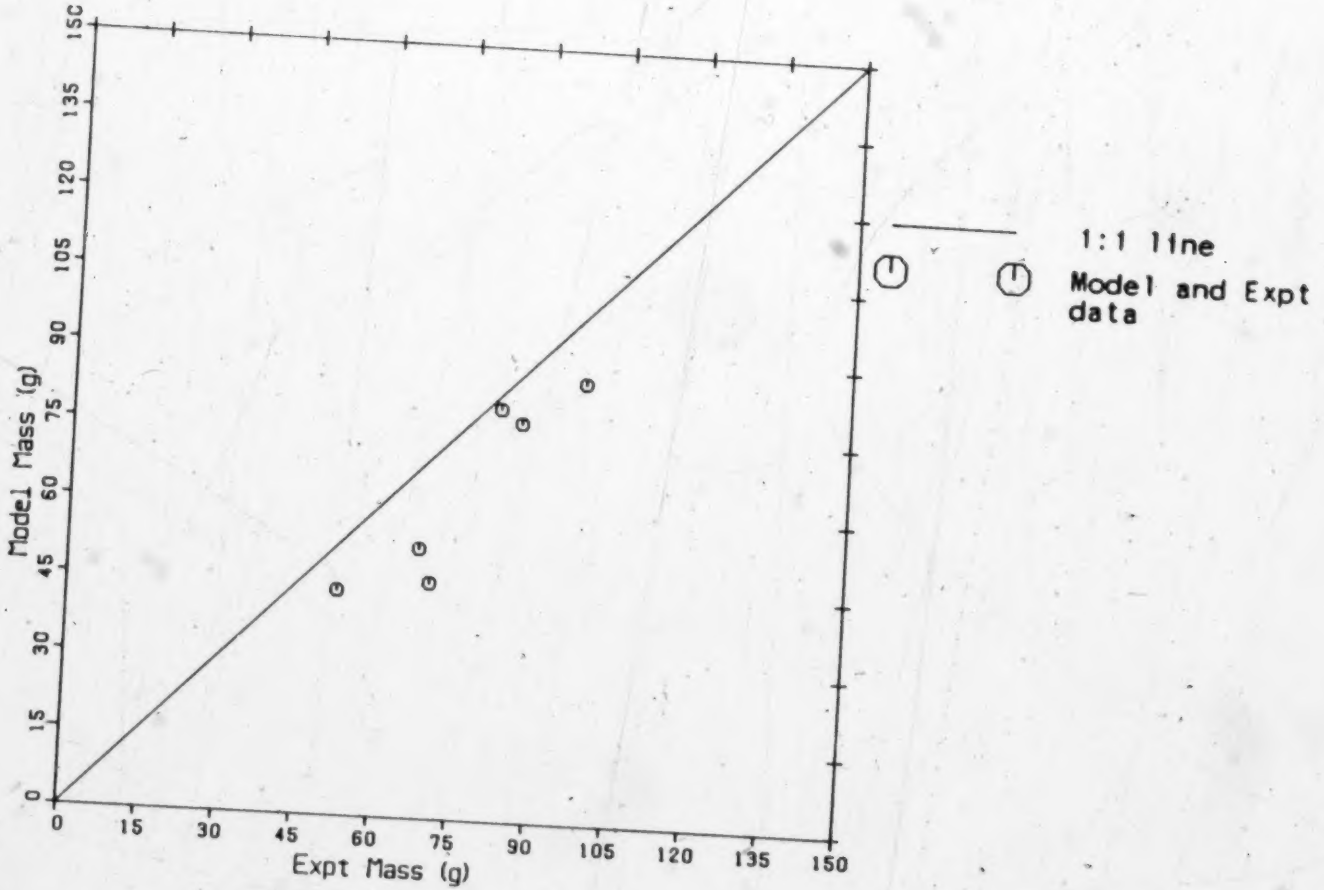

Figure 8.4.3 Model mass (g) at adjusted model growth termination time (MGTT) vs experimental mass (g) at experiment termination time (ETT) for pure icicle growth.

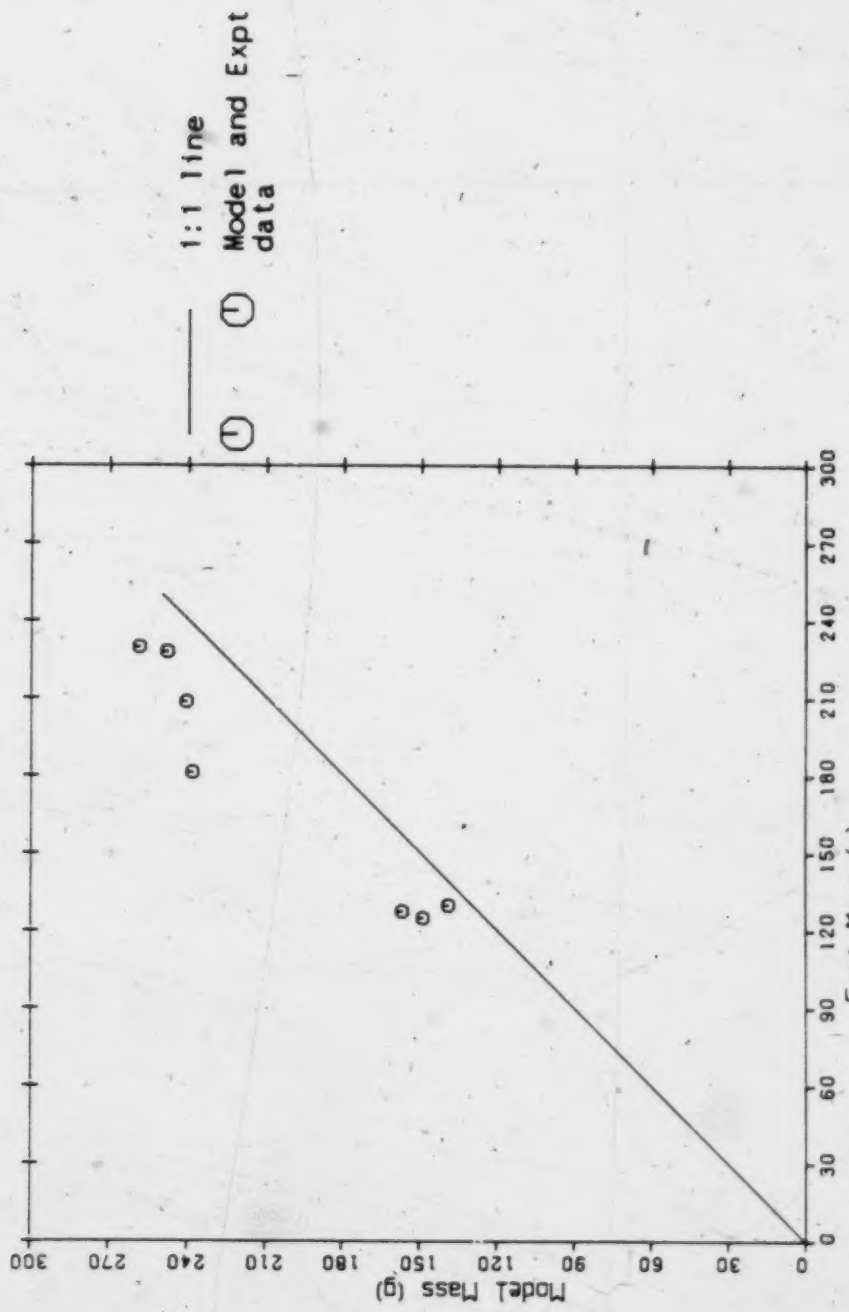

Figure 8.4.4 Model mass (g) vs experimental mass (g) at experiment termination time (ETT) for saline icicle growth.

9. Summary, discussion, and recommendations

9.1 Summary and discussion

The growth mechanism for the formation of pure icicles and the heat balance equations controlling the growth of pure icicles, which were proposed by Makkonen (1988), have been reviewed. This suggested growth mechanism and the heat balance equations have been extended and applied to discuss the formation and growth of saline icicles. Two heat balance equations, with consideration of the effects of salinity, for the growth in diameter and in length have been derived. These two equations form the basis of a model which was designed to simulate the growth process of saline icicles. This new model is based on a time dependent finite element method which is quite different from the method used by Makkonen (1988). The present model can also be used to simulate the growth of pure icicles. Three major assumptions are made in this model:

1. The icicles have a homogeneous liquid film thickness.
2. The icicles have a circular cross section.
3. The liquid fraction of the saline icicles is assumed to be 0.26 while that of the pure icicles is assumed to be 0.

The sensitivity tests have shown that the model for both pure and saline icicles is very sensitive to the air temperatures and wind speeds, especially at low values of wind speed ($<$ 2.5 m/s). It is rather insensitive to relative humidity and pressure.

Two sets of experiments on growing pure and saline icicles, with various air conditions and supply rates, were performed in the coldroom in the Division of Meteorology at the Unverisity of Alberta. The first six experiments were on the growth of pure icicles while the remaining seven experiments were on the growth of saline icicles. The length, length growth rates, and the driprates, were all measured (or calculated) as a function of time. The diameter as a function of distance from the root, the mean diameter, and the mass, were measured after the experiments. The experimental results were then compared with the model's prediction so that the performance of the model could be evaluated and discussed. It was

found, after all the comparisons, that the model overpredicts the icing rates, especially for the case of pure icicles. There are three suggested reasons for the overprediction of the icing rates:

1. The unevenly distributed liquid film creates a preferred flowing path which causes the icicles to develop an ellipitical rather than a circular cross section. Therefore, the calculation of the heat transfer coefficients for the walls based on a circular cylindrical geometry and a uniform distribution of the liquid film around the perimeter is not valid.
2. With the evenly distributed liquid film assumption, the model overestimates the mass accretion on the wall of the icicles.
3. It was observed during the experiments that very often the preferred flowing path is on the downwind side of the icicle. As a result, the rate of heat transfer from the wall to the air may be diminished (Kreith, 1973).

Although, quantitatively speaking, the model does not perform very well, especially for the case of pure icicles, it does seem to give a good qualitative description of what is going on in nature for the growth of both pure and saline icicles. The model successfully predicts that the length growth rates of saline icicles will eventually stop, even with a continuous supply of brine to the tip. It is the author's hope that these studies on the growth of pure and saline icicles will provide helpful insight for further research on icicle growth.

9.2 Recommendations

The experiments performed in the coldroom were not very precise and the experimental apparatus need a lot of modifications. For example, the experiments could be done in the icing wind tunnel in order to obtain a more accurate and steady air temperature and wind speed. In addition, a more sophisticated valve or pump could be used to get a more constant supply rate. By controlling the above three factors better, more precise experimental results could be achieved. The model also needs to be modified further. There are a few areas in the model that can be improved:

1) Since the cross sections of the icicles (pure and saline) are elliptical rather than circular, and in fact, change with time, incorporating this time varing shape in the model could give a more accurate estimate of the heat transfer coefficient for the walls. However, this is a very complicated task and will require detailed studies of heat transfer.

2) Since the thickness of the liquid film is not homogeneous around the wall perimeter, this should also be put into the model.

3) The supercooling of the walls of the icicles should also be incorporated into the model.

Finally, there follow a few suggestions for further research specific to the growth of saline icicles.

1) The distribution of the temperature and salinity at the surface of the saline icicle should be investigated. Since the model has the ability to calculate these two quantities, it would be worthwhile to measure them during the experiments.

2) The sponginess of saline icicles can also be studied through experiments. Special attention should be paid to the dependence of the sponginess on the environmental conditions and supply rate.

3) The crystalline structure of the saline icicles under various conditions should be studied and compared with that of the pure icicles.

4) The reasons offered for the formation of the ribs on the walls of the pure and saline icicles are tentative and they should be investigated in more detail. It would also be interesting to compare the sizes and shapes of the ribs growing on the surface of saline icicles with those growing on the surface of the pure icicles.

5) Instead of growing icicles by dripping liquid onto an overhanging object, it could done by spraying liquid onto the object. This would be more applicable to marine icing, because in marine icing, icicles are formed through the interception of sprayed seawater droplets.

Bibliography

Aksyutin, I.L., 1979: Icing of ships (in Russian). Sudostroyenye Publishing House, Leningrad, 126 pp.

Apytynnyen, N.Kh., Grigoryen, S.S., and Haymov, V.Z., 1988: Growth of an icicle. *Prikledneye Matemetike i Mekhanike (Applied Mathematics & Mechanics)*, special issue, 52(2), 252-263.

Blackmore, R.Z., 1988: Spongy ice formation. *M. Sc. Thesis*, Univerisity of Alberta.

Burt, S.D., 1982: The curious case of the horizontal icicles. *Meteorological Magazine*, 111(1320), 183-184.

Clift, R., Grace, J.R., and Weber, M.E., 1978: *Bubbles, drops, and particles*. New York, Academic press.

Finstad, K.J., Lozowski, E.P., and Gates, E.M., 1988: A computational investigation of water droplet trajectories. *Journal of Atmospheric and Oceanic Technology*, 5(1), 160-161.

Gates, E.M., Liu, A., and Lozowski, E.P., 1988: A stochastic model of atmospheric rime icing. *Journal of Glaciology*, 34(116), 26-29.

Geer, I.W., 1981: The not-so-ordinary icicle. *Weatherwise*, 34(6), 257-259.

Hillig, W.B., and Turnbull, D., 1956: Theory of crystal growth in undercooled pure liquids. *Journal of Chemistry and Physics*, 24(9), 914.

Incropera, F.P., and Dewitt, D.P., 1985: *Introduction to heat transfer*. New York, Wiley & Sons.

Iribarne, J.V., and Godson, W.L., 1985: *Atmospheric thermodynamics*. Dordrecht, D. Reidel.

Johnson, K., 1987: An investigation of the growth of icicle. *M. Sc. Thesis*, University of Alberta.

Knight, C.A., 1967: *The freezing of supercooled liquids*. New Jersey, D. Van Nostrand Company, INC.

Knight, C.A., 1968: On the mechanism of spongy hailstone growth. *Journal of the Atmospheric Sciences*, 25(3), 440-444.

Knight, C.A., 1980: Icicles as crystallization phenomena. *Journal of Crystal Growth*, 49, 193-198.

Knudsen, J.G., and Katz, D.L., 1985: *Fluid dynamics and heat transfer*. New York, Mc Graw-Hill.

Kreith, F., 1973: *Principles of heat transfer*. New York and London, Intext Educational Publishers.

Laudise, R.A., and Barns, R.L., 1979: Are icicles single crystals? *Journal of Crystal Growth*,

46, 379-386.

Lozowski, E.P., Gates, E.M., and Makkonen, L., 1986: Towards estimation of the icing hazard for mobile offshore drilling units. *Fifth Int. Offshore Mechanics and Arctic Engineering Symp.* (OMAE), 4, 175-182.

Lozowski, E.P., Stallabrass, J.R., and Hearty, P.F., 1983: The icing of an unheated, nonrotating cylinder. Part I: A simulation model. *Journal of Climate and Applied Meteorology*, 22, 2053-2062.

Maeno, N., and Takahashi, T., 1984(a): Studies on icicles. I. General aspects of the structure and growth of an icicle. *Low Temperature Science*, Ser. A, 43, 125-138. (In Japanese.)

Maeno, N., and Takahashi, T., 1984(b): Studies on icieles. II. Wave-forms, spikes and bent icicles. *Low Temperature Science*, Ser. A, 43, 139-147. (In Japanese.)

Makkonen, L., 1984: Modeling of ice accretion on wires. *Journal of Climate and Applied Meteorology*, 23(6), 929-939.

Makkonen, L., 1987: Salinity and growth rate of ice formed by sea spray. *Cold Regions Science and Technology*, 14(2), 163-171.

Makkonen, L., 1988: A model of icicle growth. *Journal of Glaciology*, 34(116).

Millero, F.J., Perron, G., and Desnoyers, J.E., 1973: Heat capacity of seawater solution from 5° to 35°C and 0.5 to 22 o/oo chlorinity. *Journal of Geophysical Research*, 78(21), 4499-4506.

Obreiter, E., 1987: Physics of the marine ice accretion process. *M. Sc. Thesis*, University of Alberta.

Schlichting, H., 1979: *Boundary-layer theory*. New York, McGraw-Hill.

Shellard, H.C., 1974: The meteorological aspects of ice accretion on ships. World Meteorological Organization. *Marine Science Affairs Report* No. 10 (WMO, No. 397), Geneva, 34 pp.

Smithsonian Institution, 1963: *Smithsonian Meteorological Tables*. Prepared by R. J. List, Smithsonian Institution, Washington.

Terwileger, J.P., and Dizio, S.F., 1970: Salt rejection phenomena in the freezing of saline solutions. *Chemical Engineering Science*, 25, 1331-1349.

Unterberg, W., 1966: Thermal properties of salt solutions. *Journal of British Chemical Engineering*, 11, 494-495.

Walker, J., 1988: Icicles ensheathe a number of puzzles: Just how does the water freeze? *Scientific American*, 114-117.

Weeks, W.F., and Ackley, S.F., 1982: The growth, structure, and properties of sea ice. *CRREL Monograph*, 82-1.

Yin, C.Y., 1981: Review of thermal properties of snow, ice and sea ice. *CRREL Report*, 81-10.

Zakrzewski, W.P., 1986: Icing of ships. Part 1: Splashing a ship with spray. *NOAA Technical Memorandum EPL PMEL-66*, 74pp.

Zakrzewski, W.P., Blackmore, R., and Lozowski, E.P., 1988: Mapping icing rates on sea-going ships. *Journal of the Meteorological Society of Japan*, 66(5), 661-675.

Appendix A Calculation of the heat-transfer coefficient for the cylindrical sections of the icicle

The heat-transfer coefficient, h_w, for a cylinder segment is given by:

$$h_w = \frac{kN_{uw}}{D} \tag{1}$$

where k is the thermal conductivity of air which is calculated by (Makkonen, 1988):

$$k = 0.0242 + 0.000073T_a \tag{2}$$

and D is the diameter of any cylindrical segment of the icicle.

N_{uw} is the Nusselt number. For free convection, it is calculated by (Makkonen 1988):

$$N_{uw} = 0.478G_{rw}^{0.25} \tag{3}$$

where G_{rw} is the Grashof number:

$$G_{rw} = \frac{gD^3(T_s - T_a)}{N_y^2(T_a + 273.15)} \tag{4}$$

where

g is the gravitational constant.

T_s is the surface temperature of the cylinder.

N_y is the kinematic viscosity .

N_y is defined to be:

$$N_y = \frac{M_y}{\rho_{air}} \tag{5}$$

where M_y is the dynamic viscosity of air, which is calculated by (Makkonen, 1988):

$$M_y = 1.719\times10^{-5} + 5.1\times10^{-8}T_a \tag{6}$$

ρ_{air} is the density of air which is calculated by:

$$\rho_{air} = \frac{352.6}{T_a + 273.15}. \tag{7}$$

For forced convection, the Nusselt number is calculated in terms of the Reynolds number, R_{ew}, for a cylinder as follow (Makkonen, 1988):

$$N_{uw} = 0.881R_{ew}^{0.330} \qquad (0.4 < R_{ew} \leq 4)$$
$$N_{uw} = 0.811R_{ew}^{0.385} \qquad (4 < R_{ew} \leq 40)$$
$$N_{uw} = 0.608R_{ew}^{0.466} \qquad (40 < R_{ew} \leq 4000)$$
$$N_{uw} = 0.172R_{ew}^{0.618} \qquad (4000 < R_{ew} \leq 40000)$$
$$N_{uw} = 0.024R_{ew}^{0.805} \qquad (40000 < R_{ew} \leq 400000).$$

The Reynolds number for the cylinder is defined to be:

$$R_{ew} = \frac{vD}{N_y} \tag{8}$$

where v is the wind speed.

The Nusselt numbers for both free and forced convection are calculated and the larger one is used to calculate h_w. In the present model simulations for both pure and saline icicles, the applied wind speeds are 0.7 m/s and 0.6 m/s, respectively. As a result, the forced convcection parameterizations are actually used in the model when making comparisons with the present experiments.

Appendix B Calculation of the heat-transfer coefficient for the tip of the icicle

The heat transfer ceofficient for the tip is calculated from:

$$h_t = \frac{kN_{ut}}{d} \tag{1}$$

where d is the diameter of the pendant drop.

For free convection, the Nusselt number, N_{ut}, is estimated to be that of a sphere (Makkonen, 1988):

$$N_{ut} = 1.83 + 0.398G_{rt}^{0.252} \tag{2}$$

The Grashof number, G_{rt}, is:

$$G_{rt} = \frac{gd^3(T_s - T_a)}{N_y^2(T_a + 273.15)} \tag{3}$$

where T_s is the surface temperature of the pendant drop.

For forced convection, the Nusselt number is estimated by:

$$N_{ut} = 2.0 + 0.538R_{ed}^{0.5} \tag{4}$$

where R_{ed} is the Reynolds number for the pendant drop:

$$R_{ed} = \frac{vd}{N_y} \tag{5}$$

The Nusselt numbers for both free and forced convection are calculated, and the larger one is used to calculate h_t. Once agin, the Nusselt number for forced covection is actually used when comparisons with the present experiments are made.

Appendix C A Fortran program to compute the growth of a pure or saline icicle.

Definitions of variables :

```
A       - Upper limit of dL/dt(RL).
B       - Lower limit of dL/dt(RL).
CW      - Specific heat capacity of water at 0 C.
CP      - Specific heat capacity of air at constant pressure.
C1      - 1.87*CB(I)/DD**2.
C2      - (LF*ROOI)/RA1.
C3      - 0.64*CB(I)/DD**2
CS      - Specific heat capacity of sea salt.
CB(I)   - Specific heat capacity of the brine on the Ith cylinder.
DD      - Pendant drop diameter.
DEL     - Wall thickness of the ice shell at the tip of the
          of the icicle.
DM(I)   - The diameter of the Ith cylinder(m).
DMO(I)  - The diameter of the Ith cylinder(cm).
ES      - Saturation vapor pressure of water over a flat water
          surface at TAK.
E(I)    - (R/100)*ES of the Ith cylinder.
EO      - Saturation vapor pressure of water over a flat water
          surface at TSF.
EOS(I)  - Saturation vapor pressure of water over a flat saline
          water surface of the Ith cylinder at TSF.
F       - Driprate (1/s).
FX      - A function used in the bisection method.
FO      - Driprate (1/min).
FR      - Accretion fraction.
G       - Gravitational constants.
GRD     - Grashof number with respect to the wall of the icicle.
GR      - Grashof number with respect to the length of the icicle.
HT      - Heat transfer coefficient with respect to the pendant
          drop.
HW      - Heat transfer coefficient with respect to different
          cylinders of the icicle.
I       - Loop counter.
J       - Timer.
K       - Thermal conductivity of the air.
KK      - Constant = 0.622.
LAM     - Liquid fraction.
L       - Length of the icicle(m).
LO      - Length of the icicle(cm).
LL(I)   - Length of the Ith ice cylinder (m).
LOSS    - Water loss to the icicle wall due to the freezing and
          evaporation.
LE      - Latent heat of water evaporation.
LF      - Latent heat of fusion for water.
LFS     - Latent heat of fusion for ice accretion.
MYY     - Dynamic viscosity of air.
M       - Mass of the icicle(Kg).
MWALL   - The mass increment at the wall of the icicle at a given
          time step (Kg).
MTIP    - The mass increment at the tip of the icicle at a given
          time step (Kg).
MO      - Mass of the icicle (g).
MINCR   - The total mass increment at a given time step.
```

```
MED     - The volume mean diameter of the icicle.
NS      - Number of time step.
N       - A loop counter.
NYY     - Kinematic viscosity of the air.
NUN     - Mean Nusselt number of pendant drop for free convection.
NUF     - Mean Nusselt number of pendant drop for forced convection.
NUWN    - Mean Nusselt number of different cylinders of the icicle
          for free convection.
NUWF    - Mean Nusselt number of different cylinders of the icicle
          for forced convection.
NU      - The adopted Nusselt number.
PA      - Air pressure in mb.
QT      - Heat transfered to the air from the pendant drop.
QD      - Heat transfered to the air from different cylinders of
          of the icicle.
QTT     - QT - C3*WT*(TS(NS-1) - TS(NS))
R       - Relative humidity in %.
ROOW    - Density of water.
ROOI    - Density of ice.
ROOA    - Density of the air.
ROOSS(I)- Accretion density for saline ice on the Ith cylinder.
RED     - Reynolds number with respect to the tip of the icicle.
REW     - Reynolds number with respect to different cylinders of
          the icicle.
RL      - Growth rate in length (m/s).(dL/dt)
RLO     - Growth rate in length (cm/s).
RRAD(I)- Radial growth rate(m/s) on the Ith cylinder.(dR/dt)
RAD(I)  - Growth rate in diameter(m/s) on the Ith cylinder.(dD/dt)
RAT     - DD/(2*DEL).
ROOWS   - Density of the brine on different cylinders.
S       - The simulation time in hour.
SIGA    - Solar radiation constant.
SI(I)   - Salinity of the accretion on the Ith cylinder.
SB(I)   - Salinity of the brine on the Ith cylinder.
SW      - Salinity of the influx saline water.
TA      - Air temperature in <degree>C.
TS(I)   - Surface temperature of the Ith ice cylinder.
TSK     - 273.15 + TS(I).
TAK     - 273.15 + TA.
TCH     - TS(I) - TS(I+1)
V       - Wind speed (m/s).
W       - Water flux from the root (mg/s).
WO      - Water flux from the root (kg/s).
WT      - Mass flux of water flowing from one cylinder to another.
X       - (A + B)/2

*-------------------------------------------------------*
*     VARIABLE TYPE SPECIFICATION AND PARAMETER         *
*-------------------------------------------------------*

      INTEGER ROOW, LE, PA, CW, ROOI, LF, R, J, NS, I, N
      REAL A, B, C3, CP, C1, C2, CB(200), DD, DEL, DMO(200), DM(200)
      REAL E(200), ES, EO, EOS(200), F, FO, FX, FR, G, GRD, GR
      REAL HT, HW, K, KK, LAM, L, LO, LL(200), LOSS, LFS, MYY
      REAL M, MWALL, MTIP, MINCR, MO, MED, NYY, NUN, NUF, NUWN
      REAL NUWF, NU, QT, QD, QTT, ROOA, ROOSS(200), RED, RRAD(200)
      REAL RAD(200), RL, RLO, RAT, ROOWS, REW, S, SIGA, SW, SI(200)
      REAL SB(200), SUMD, TA, TS(200), TSK, TCH, TAK, V, W, WO, WT
      REAL X
      LOGICAL SWITCH
```

```
      PARAMETER (SIGA=4.6, ROOW=1000, KK=0.622, CW=4218, LE=2500000)
      PARAMETER ( ROOI=917, G=9.810001)
      PARAMETER (PI=3.141593)

*-----------------------------*
*     INPUT PARAMETERS        *
*-----------------------------*

      PRINT *, 'ENTER AIR TEMPERATURE (C) (1 DECIMAL), TA = '
      READ (5, *), TA
      PRINT *, 'ENTER RELATIVE HUMIDITY (%), R = '
      READ (5, *), R
      PRINT *, 'ENTER AIR PRESSURE (mb), PA ='
      READ (5, *), PA
      PRINT *, 'ENTER WATER FLUX (mg/s) (2 DECIMAL), W = '
      READ (5, *), W
      PRINT *, 'ENTER SALINITY OF WATER (3 DECIMAL), SW = '
      READ (5, *), SW
      PRINT *, 'ENTER WIND SPEED (m/s) (2 DECIMAL), V = '
      READ (5, *), V
      PRINT *, 'ENTER SIMULATION TIME (HR) (1 DECIMAL), S = '
      READ (5, *), S
      WRITE (6, 400) TA, R, PA, W, SW, V, S
      WRITE (6, 450)

*-----------------------------------------------*
*     ASSUMPTIONS AND INITIAL CONDITIONS        *
*-----------------------------------------------*

      LAM = 0.26
      DD = 0.00490
      DEL = 7.500001E-05
      WO = 0.000001*W
      J = 0
      L = 0.00245
      LL(1) = 0.00245
      N = 0
      LOSS = 0.0
      WT = WO
      SB(1) = SW
      SI(1) = 0.26*SB(1)

*-------------------------------------------------------*
*     ATMOSPHERIC AND THERMODYNAMIC PROPERTIES          *
*     WITH INITIAL SALINITY                             *
*-------------------------------------------------------*

      TS(1) = -54.0*SB(1) - 600*SB(1)**3
      TSK = 273.15 + TS(1)
      TAK = 273.15 + TA
      ROOA = 352.6/TAK
      MYY = (1.719E-05) + (5.1E-08)*TA
      NYY = MYY/ROOA
      K = 0.0242 + 0.000073*TA
      CP = 1004 + 0.046*TA
      ES = EXP(-6763.6/TAK - 4.9283*ALOG(TAK) + 54.23)
      EO = EXP(-6763.6/TSK - 4.9283*ALOG(TSK) + 54.23)
      EOS(1) = (1 - 0.537*SB(1))*EO
      ESS = (R/100.0)*ES
      ROOWS = ROOW*(1 + SB(1))/(1 - SB(1))
```

```
      ROOSS(1) = (ROOI*ROOWS)/((1-LAM)*ROOWS + LAM*ROOI)
      CB(1) = (1 - SB(1))*CW
      LF = 2240*TS(1) + .333400
      LFS = 0.74*LF
      M = PI/4*(DD**2)*L*ROOSS(1)

*-------------------------*
*     GROWTH IN WIDTH     *
*-------------------------*

      NS = 1
110   LOSS = 0.0
      MWALL = 0.0
      TCH = 0.0
      DM(NS) = DD
      DMO(NS) = 100*DM(NS)
      WT = WO
      DO 5 I = 1, NS
         CALL HWALL (G, DM , TS , TA, TAK, I, NYY, V, K, HW, SWITCH)
         IF ( .NOT. SWITCH) THEN
            PRINT *, '*** BOUNDARY LAYER TURBULENCE. NO RESULT ***'
            GOTO 10
         ENDIF
         QD = HW*(TS(I) - TA) + HW*KK*LE*(EOS(I) - E(I))/(PA*CP)
     +       + SIGA*(TS(I) - TA) - WT*CB(I)*TCH/(DM(I)*PI*LL(I))
         RRAD(I) = QD/(LFS*ROOSS(I))
         RAD(I) = 2*RRAD(I)
         DM(I) = DM(I) + 120*RAD(I)
         DMO(I) = 100*DM(I)
         FR = (LL(I)*PI*DM(I)*ROOSS(I)*RRAD(I))/WT
         LOSS = LOSS + LL(I)*PI*DM(I)*(ROOSS(I)*RRAD(I)
     +             + HW*KK*(EOS(I) - E(I))/(PA*CP))
         WT = WO - LOSS
         MWALL = MWALL + LL(I)*PI*DM(I)*ROOSS(I)*RRAD(I)*120

*-------------------------------------------------------------------*
*     RE-CALCULATION OF THE ATMOSPHERIC AND THERMODYNAMIC           *
*     PROPERTIES WITH THE NEWLY CALCULATED SALINITY                 *
*-------------------------------------------------------------------*

         SB(I+1) = SB(I)/(1 - 0.74*FR)
         SI(I+1) = 0.26*SB(I+1)
         TS(I+1) = -54.0*SB(I+1) - 600*SB(I+1)**3
         TSK = 273.15 + TS(I+1)
         TAK = 273.15 + TA
         ROOA = 352.6/TAK
         MYY = (1.719E-05) + (5.1E-08)*TA
         NYY = MYY/ROOA
         K = 0.0242 + 0.000073*TA
         CP = 1004 + 0.046*TA
         TCH = TS(I) - TS(I+1)
         IF (TS(I+1) .LT. TA) THEN
            RL = 0.0
            GOTO 25
         ENDIF
         ES = EXP(-6763.6/TAK - 4.9283*ALOG(TAK) +54.23)
         EO = EXP(-6763.6/TSK - 4.9283*ALOG(TSK) + 54.23)
         EOS(I+1) = (1 - 0.537*SB(I+1))*EO
         E(I+1) = (R/100.0)*ESS
         ROOWS = ROOW*(1 + SB(I+1)/(1 - SB(I+1)))
```

```
      ROOSS(I+1) = (ROOI*ROOWS)/((1-LAM)*ROOWS + LAM*ROOI)
      CB(I+1) = (1-SB(I+1))*CW
      LF = 2240*TS(I+1) + 333400
      LFS = 0.74*LF
5     CONTINUE
      NS = NS + 1

*-----------------------------*
*     GROWTH IN LENGTH        *
*-----------------------------*

      IF (WT .LE. 0.0) GOTO 10
      CALL HTIP (G, DD, TS, TA, TAK, NS, NYY, V, K, HT)
      QT = HT*(TS(NS) - TA) + HT*KK*LE*(EOS(NS) - E(NS))/(CP*PA)
     +     + SIGA*(TS(NS) - TA)
      RAT = DD/(2*DEL)
      C1 = 1.87*CB(NS)/DD**2
      C2 = (LF*ROOI)/RAT
      C3 = 0.64*CB(NS)/DD**2
      QTT = QT - C3*WT*(TS(NS-1) - TS(NS))
      IF (QTT .LE. 0.0) THEN
         PRINT *, '*** GROWTH STOP ***'
         GOTO 10
      ENDIF
      A = QTT/C2
      B = RRAD(NS-1)
30    X = (A + B)/2.0
      IF (X .LE. RRAD(NS-1)) THEN
         PRINT *, '*** GROWTH RATE IN LENGTH IS LESS THAN GROWTH'
         PRINT *, '    RATE IN WIDTH. ASSUME dL/dt = ZERO ***'
         PRINT *, ' ---- GROWTH IN LENGTH STOP! ----'
         GOTO 10
      ENDIF
      FX = QTT - C1*WT*(100*(X - RRAD(NS-1)))**0.588 - C2*X
      N = N + 1
      IF (N .LE. 5000) THEN
         IF (ABS(FX) .LE. 1.0) THEN
            RL = X
            GOTO 20
         ELSE
            IF (FX .LT. 0.0) THEN
               A = X
            ELSE
               B = X
            ENDIF
            GOTO 30
         ENDIF
      ELSE
         PRINT *, 'OVER 5000 LOOPS! PLEASE ADJUST N.'
         GOTO 10
      ENDIF
20    LL(NS) = 120*RL
25    RLO = RL*60*100
      L = L + 120*RL
      LO = L*100
      MTIP = PI/4*(DD**2)*RL*ROOSS(NS)*120
      MINCR = MWALL + MTIP
      M = M + MINCR
      MO = M*1000
      F = 6*WT/(PI*DD**3*ROOWS)
```

```
      FO = F*60

C-----------------------------
C     THE RESULT IS LISTED     C
C-----------------------------

      J = J + 2
      IF (J/60.0 .LE. S .AND. F .GE. 0.0) THEN
         WRITE (6, 500) J, FO, RLO, LO, MO
      ELSE
         GOTO 10
      ENDIF
      IF (F .GT. 0.0) THEN
         GOTO 110
      ELSE
         GOTO 10
      ENDIF
400   FORMAT ('0', 'THE AIR TEMPERATURE TA = ',F5.1, 'C'/
     +        ' ', 'THE RELATIVE HUMIDITY R = ',I3, '%'/
     +        ' ', 'THE AIR PRESSURE PA = ',I4, 'mb'/
     +        ' ', 'THE WATER FLUX W = ',F9.2, 'mg/s'/
     +        ' ', 'THE SALINITY IS SW = ',F6.3, 'ppt'/
     +        ' ', 'THE WIND SPEED V = ',F4.1, 'm/s'/
     +        ' ', 'THE SIMULATION TIME S = ', F5.2, 'HRS')
450   FORMAT ('0', 'TIME',6X, 'DRIP',5X, 'GROWTH IN',5X,
     +          'LENGTH',5X, 'MASS'/
     +        ' ', '(min)',3X, 'FREQUENCY',2X, 'LENGTH',8X,/
     +        ' ',8X, '(1/min)',4X, '(cm/min)',6X, '(cm)',7X, '(g)')
500   FORMAT (' ',I3,3X, F7.2,3X, F8.3,6X, F7.2,2X, F10.3)
10    CONTINUE
      WRITE (6, 550)
      J = -2
      SUMD = 0.0
      DO 40 I = 1, NS
         J = J + 2
         LL(I) = LL(I)*100
         SUMD = SUMD + LL(I)*DMO(I)
         WRITE (6, 600) J, LL(I), DMO(I)
40    CONTINUE
      MED = SUMD/LO
      PRINT *, '  *** THE MEAN DIAMETER OF THE ICICLE IS ***'
      WRITE (6, 650) MED
550   FORMAT('0', 'TIME STEP(min) SECTION LENGTH (cm)  DIAMETER (cm)'
     +)
600   FORMAT(' ',I3,12X,F7.3,14X,F6.3)
650   FORMAT(' ','   MED = ',F4.2,' cm')
      END
C-----------------------------
C     SUBROUTINE HTIP          C
C-----------------------------
      SUBROUTINE HTIP (G, DD, TS, TA, TAK, NS, NYY, V, K, HT)
C-------------------------------------------------------------C
C     FUNCTION: To calculate the heat-transfer coefficient for C
C               the tip of the icicle.                         C
C     INPUT ARGUMENT: G, DD, TS(NS), TA, TAK, NYY, V, K        C
C     OUTPUT ARGUMENT: HT                                      C
C     OTHER VARIABLES: GR, NUN, RED, NUF, NU                   C
C                                                              C
C                                                              C
C-------------------------------------------------------------C
```

```
      REAL G, DD, TS(200), TA, TAK, NYY, V, K, HT, GR, NUN, RED, NUF
      REAL NU
      INTEGER NS
      GR = (G*DD**3*(TS(NS)-TA))/(NYY**2*TAK)
      NUN = 1.83 + 0.398*GR**0.252
      RED = V*DD/NYY
      IF (RED .LT. 1.0) RED = 0.0
      IF (RED .GT. 50000.0) THEN
         PRINT *, '***WIND SPEED TOO HIGH***'
      ENDIF
      NUF = 2 + 0.538*RED**0.5
      IF (NUN .GT. NUF) THEN
         NU = NUN
      ELSE
         NU = NUF
      ENDIF
      HT = K*NU/DD
      RETURN
      END
*************************************
*     SUBROUTINE HWALL              *
*************************************
      SUBROUTINE HWALL(G, DM, TS, TA, TAK, I, NYY, V, K,
     +                 HW, SWITCH)
*-------------------------------------------------------------------*
*     FUNCTION: To calculate the heat-transfer coefficient for      *
*               the wall of the icicle.                             *
*     INPUT ARGUMENT: G, LL(I), TS(I), TA, NYY, TAK, DM(I), V, K    *
*     OUTPUT ARGUMENT: HW, SWITCH                                   *
*     OTHER VARIABLES: GRD, NUWN, NUWF, REW, NUW                    *
*-------------------------------------------------------------------*

      REAL G, DM(200), TS(200), TA, NYY, TAK, V, K, HW, GRD, REW
      REAL NUWN, NUWF, NUW
      INTEGER I
      LOGICAL SWITCH
      GRD = (G*DM(I)**3*(TS(I) - TA))/(NYY**2*TAK)
      SWITCH = .TRUE.
      IF (0.72*GRD .GT. 10**10) THEN
         SWITCH = .FALSE.
         GOTO 50
      ENDIF
      NUWN = 0.478*GRD**0.25
      REW = V*DM(I)/NYY
      IF (REW .LE. 0.4) THEN
         REW = 0.0
      ELSEIF (REW .LE. 4.0) THEN
         NUWF = 0.881*REW**0.33
      ELSEIF (REW .LE. 40.0) THEN
         NUWF = 0.811*REW**0.385
      ELSEIF (REW .LE. 4000.0) THEN
         NUWF = 0.608*REW**0.466
      ELSEIF (REW .LE. 4.0E04) THEN
         NUWF = 0.172*REW**0.618
      ELSE
         NUWF = 0.024*REW**0.805
      ENDIF
      IF (NUWN .GT. NUWF) THEN
         NUW = NUWN
      ELSE
```

```
      NUW = NUWF
    ENDIF
    HW = K*NUW/DM(I)
50  RETURN
    END
```

A flowchart for the program to compute the growth of a pure or saline icicle.

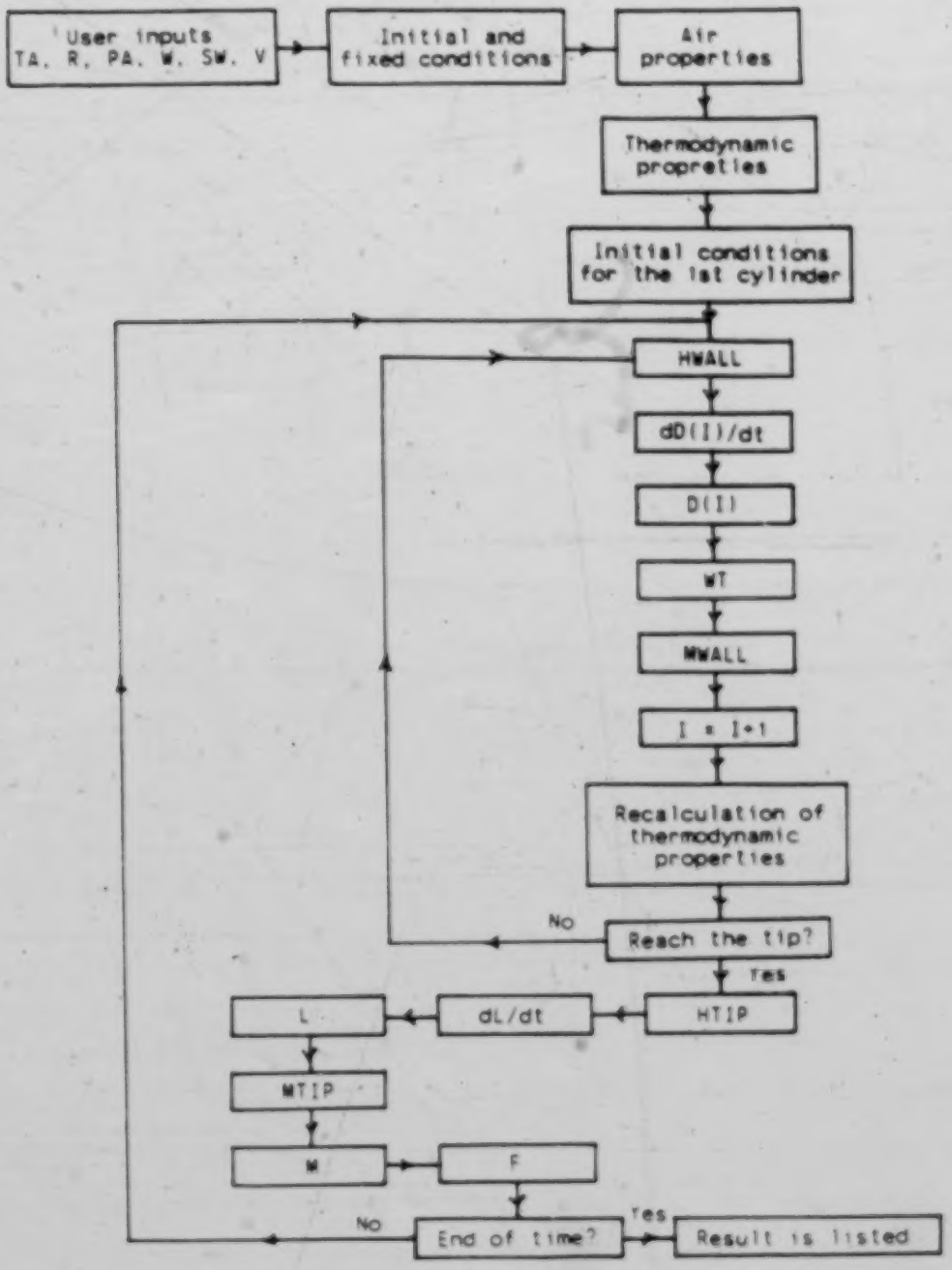

Appendix D The experimental results of pure and saline icicle growth for thirteen different cases

case #1

Ta = -14.0 C v = 0.7 m/s
R = 80 % wo = 25.0 mg/s
Pa = 935 mb

Time (min)	Driprate (1/min)	dL/dt (cm/min)	Length (cm)
5.00	19.00	0.180	0.90
10.00	20.00	0.420	3.00
15.00	20.00	0.500	5.50
20.00	17.00	0.460	7.80
25.00	16.00	0.540	10.50
30.00	14.00	0.420	12.60
35.00	13.00	0.320	14.20
40.00	13.00	0.420	16.20
45.00	11.00	0.400	18.20
50.00	11.00	0.360	20.00
55.00	13.00	0.360	21.80
60.00	13.00	0.380	23.70
65.00	10.00	0.260	25.00
70.00	9.00	0.760	28.80
75.00	15.00	0.720	32.40
80.00	7.00	0.780	36.30
85.00	5.00	0.780	40.20
90.00	6.00	0.420	42.30
95.00	0.00	0.360	44.10

Distance from root (cm)	Diameter (cm)	Variation in supply rates (drops/min)
0.00	2.60	
2.00	1.94	•
4.00	2.00	•
6.00	1.97	•
8.00	1.89	•
10.00	1.83	•
12.00	2.03	Missing
14.00	1.78	•
16.00	1.74	•
18.00	1.74	•
20.00	1.62	•
22.00	1.63	•
24.00	1.46	
26.00	1.37	
28.00	1.23	
30.00	1.07	
32.00	1.04	
34.00	0.89	
36.00	0.82	
38.00	0.66	
40.00	0.52	
42.00	0.49	
44.00	0.51	

Mean diameter = 1.42 cm

Mass of icicle = 67.74 g

Case #2

Ta = -14.0 C
R = 80 %
Pa = 926 mb

v = 0.7 m/s
wo = 34.0 mg/s

Time (min)	Driprate (1/min)	dL/dt (cm/min)	Length (cm)
5.00	28.00	0.120	0.50
10.00	22.00	0.260	1.90
20.00	22.00	0.300	4.90
25.00	23.00	0.120	5.50
30.00	32.00	0.080	5.90
35.00	20.00	0.220	7.00
40.00	21.00	0.320	8.60
45.00	27.00	0.260	9.90
50.00	22.00	0.260	11.20
55.00	27.00	0.240	12.40
60.00	18.00	0.260	13.70
55.00	16.00	0.340	15.40
70.00	17.00	0.280	16.80
75.00	28.00	0.220	17.90
80.00	23.00	0.120	18.50
85.00	24.00	0.200	19.50
90.00	22.00	0.300	21.00
95.00	16.00	0.300	22.50
100.00	14.00	0.280	23.90
105.00	18.00	0.540	26.60
110.00	9.00	0.560	29.40
115.00	13.00	0.500	31.90
120.00	10.00	0.280	33.30
125.00	6.00	0.620	36.40
130.00	1.00	1.040	41.60
135.00	0.00	0.420	43.70
140.00	0.00	0.000	43.70

Distance from root (cm)	Diameter (cm)	Variation in supply rates drops/min
0.00	3.24	24
2.00	2.69	28
4.00	2.63	32
6.00	2.49	24
8.00	2.53	20
10.00	2.48	24
12.00	2.36	16
14.00	2.25	25
16.00	2.16	23
18.00	1.93	21
20.00	1.82	16
22.00	1.67	17
24.00	1.42	16
26.00	1.38	17
28.00	1.30	
30.00	1.04	
32.00	0.94	
34.00	0.76	
36.00	0.57	
38.00	0.52	
40.00	0.42	
42.00	0.47	

Mean diameter = 1.68 cm

Mass of icicle = 98.48 g

Case #3

Ta = -11.0 C v = 0.7 m/s
R = 65 % wo = 22.6 mg/s
Pa = 933 mb

Time (min)	Driprate (/min)	dL/dt (cm/min)	Length (cm)
5.00	12.00	0.380	1.90
10.00	19.00	0.400	3.90
15.00	20.00	0.280	5.30
20.00	20.00	0.280	6.70
25.00	18.00	0.340	8.40
30.00	16.00	0.240	9.60
35.00	14.00	0.180	10.50
40.00	21.00	0.240	11.70
45.00	12.00	0.180	12.60
50.00	10.00	0.280	14.00
55.00	14.00	0.260	15.30
60.00	17.00	0.180	16.20
65.00	12.00	0.240	17.40
70.00	15.00	0.280	18.80
75.00	15.00	0.420	20.90
80.00	13.00	0.160	21.70
85.00	15.00	0.340	23.40
90.00	9.00	0.280	24.80
95.00	9.00	0.480	27.20
100.00	7.00	0.400	29.20
105.00	10.00	0.260	30.50
110.00	3.00	0.400	32.50
115.00	1.00	0.540	35.20
120.00	7.00	0.800	38.20
125.00	0.00	0.000	38.20

Distance from root (cm)	Diameter (cm)	Variation in supply rates (drops/min)
0.00	3.23	
2.00	2.56	14
4.00	2.38	16
6.00	2.06	15
8.00	2.18	16
10.00	2.25	17
12.00	2.26	17
14.00	1.95	11
16.00	1.80	15
18.00	1.62	19
20.00	1.41	10
22.00	1.36	17
24.00	1.14	12
26.00	1.07	21
28.00	1.02	19
30.00	0.80	18
32.00	0.64	17
34.00	0.66	
36.00	0.45	
38.00	0.41	

Mean diameter = 1.55 cm

Mass of icicle = 70.00 g

Case #4

Ta = -12.0 C v = 0.7 m/s
θ = 75 % w_o = 31.0 mg/s
Pa = 944 mb

Time (min)	Driprate (1/min)	dL/dt (cm/min)	Length (cm)
5.00	28.00	0.320	1.60
10.00	29.00	0.080	2.00
15.00	31.00	0.160	2.80
20.00	26.00	0.100	3.30
25.00	26.00	0.260	4.60
30.00	33.00	0.260	5.90
35.00	23.00	0.300	7.40
40.00	20.00	0.500	9.90
45.00	22.00	0.280	11.30
50.00	22.00	0.320	12.90
55.00	20.00	0.280	14.30
60.00	20.00	0.200	15.30
65.00	22.00	0.240	16.50
70.00	21.00	0.300	18.00
75.00	18.00	0.160	18.80
80.00	16.00	0.100	19.30
85.00	16.00	0.240	20.50
90.00	19.00	0.300	22.00
95.00	19.00	0.300	23.50
100.00	14.00	0.540	26.20
105.00	15.00	0.340	27.90
110.00	18.00	0.220	29.00
115.00	13.00	0.240	30.20
120.00	6.00	0.480	32.60
125.00	6.00	0.640	35.80
130.00	13.00	0.180	38.70
135.00	7.00	0.600	39.70
140.00	0.00	0.220	40.80
145.00	0.00	0.020	40.90

Distance from root (cm)	Diameter (cm)	Variation in supply rates (drops/min)
0.00	3.10	
2.00	2.81	
4.00	2.26	
6.00	2.48	
8.00	2.47	
10.00	2.22	
12.00	2.15	Missing
14.00	2.11	
16.00	1.72	
18.00	1.74	
20.00	1.60	
22.00	1.43	
24.00	1.25	
26.00	1.21	
28.00	1.21	
30.00	0.96	
32.00	0.88	
34.00	0.81	
36.00	0.85	
38.00	0.44	
40.00	0.44	

Mean diameter = 1.62 cm

Mass of icicle = 86.45 g

Case #5

Ta = -7.5 C V = 0.7 m/s
R = 82 % Wo = 17.1 mg/s
Pa = 968 mb

Time (min)	Driprate (1/min)	dL/dt (cm/min)	Length (cm)
5.00	8.00	0.480	2.40
10.00	10.00	0.300	3.90
15.00	5.00	0.440	6.10
20.00	17.00	0.100	6.60
25.00	11.00	0.160	7.40
30.00	14.00	0.200	8.40
35.00	13.00	0.140	9.10
40.00	21.00	0.260	10.40
45.00	20.00	0.200	11.40
50.00	13.00	0.200	12.40
55.00	9.00	0.340	14.10
60.00	9.00	0.220	15.20
65.00	8.00	0.320	16.80
70.00	6.00	0.300	18.30
75.00	4.00	0.260	19.60
80.00	7.00	0.540	22.30
85.00	5.00	0.340	24.00
90.00	3.00	0.480	26.40
95.00	7.00	0.360	28.20
100.00	9.00	0.140	28.90
105.00	3.00	0.920	33.50
110.00	0.00	0.280	34.90
115.00	2.00	0.260	36.20
120.00	3.00	0.260	37.50
125.00	2.00	0.200	38.50

Distance from root (cm)	Diameter (cm)	Variation in supply rates (drops/min)
0.00	2.71	12
2.00	2.11	17
4.00	2.22	14
6.00	1.96	13
8.00	1.87	15
10.00	1.61	13
12.00	1.59	12
14.00	1.42	11
16.00	1.34	12
18.00	1.21	14
20.00	1.11	13
22.00	1.04	13
24.00	1.04	12
26.00	0.94	15
28.00	0.86	9
30.00	0.68	13
32.00	0.70	11
34.00	0.60	15
36.00	0.52	7
38.00	0.48	

Mean diameter = 1.29 cm

Mass of icicle = 52.27 g

Case #6

Ta = -8.0 C V = 0.7 m/s
R = 64 % Wo = 24.2 mg/s
Pa = 959 mb

Time (min)	Driprate (1/min)	dL/dt (cm/min)	Length (cm)
5.00	16.00	0.240	1.20
10.00	16.00	0.160	2.00
15.00	15.00	0.140	2.70
20.00	16.00	0.140	3.40
25.00	16.00	0.120	4.00
30.00	20.00	0.140	4.70
35.00	22.00	0.100	5.20
40.00	22.00	0.060	5.50
45.00	20.00	0.100	6.00
50.00	19.00	0.080	6.40
55.00	19.00	0.020	6.50
60.00	18.00	0.040	6.70
65.00	18.00	0.040	6.90
70.00	19.00	0.080	7.30
75.00	15.00	0.140	8.00
80.00	11.00	0.120	8.60
85.00	17.00	0.180	9.50
90.00	25.00	0.180	10.40
95.00	18.00	0.100	10.90
100.00	17.00	0.240	12.10
105.00	17.00	0.140	12.80
110.00	17.00	0.140	13.50
115.00	16.00	0.280	14.90
120.00	15.00	0.120	15.50
125.00	14.00	0.300	17.00
130.00	15.00	0.120	17.60
135.00	8.00	0.180	18.50
140.00	8.00	0.600	21.50
145.00	8.00	0.180	22.40
150.00	7.00	0.420	24.50
155.00	7.00	0.300	26.00
160.00	2.00	0.540	28.70
165.00	8.00	0.400	30.70
170.00	9.00	0.220	31.80
175.00	3.00	0.520	34.40
180.00	8.00	0.480	36.80
185.00	8.00	0.400	37.30
190.00	8.00	0.520	39.90
195.00	0.00	0.100	40.40

Distance from root (cm)	Diameter (cm)
0.00	3.75
2.00	3.10
4.00	2.26
6.00	2.52
8.00	2.30
10.00	2.08
12.00	2.03
14.00	1.88
16.00	1.63
18.00	1.57
20.00	1.46
22.00	1.34
24.00	1.22
26.00	1.05
28.00	1.06
30.00	1.00
32.00	0.86
34.00	0.78
36.00	0.55
38.00	0.49
40.00	0.47

Mean diameter = 1.57 cm

Mass of icicle =82.34 g

Variation in supply rates (drops/min)	
21	22
16	19
16	18
27	
20	
19	
20	
23	
22	
17	
19	
17	
15	
20	
17	
17	
17	
15	
14	
14	
14	
15	
15	
15	
11	

Case #7

Ta = -14.6 C
R = 72 %
Pa = 930 mb

V = 0.6 m/s
Wo = 22.1 mg/s
Sw = 3.3 %

Time (min)	Driprate (1/min)	dL/dt (cm/min)	Length (cm)
5.00	11.00	0.440	2.20
10.00	20.00	0.420	4.30
15.00	15.00	0.520	6.90
20.00	20.00	0.240	8.10
25.00	19.00	0.180	9.00
30.00	17.00	0.300	10.50
35.00	14.00	0.520	13.10
40.00	16.00	0.260	14.40
45.00	12.00	0.520	17.00
50.00	10.00	0.360	18.80
55.00	8.00	0.340	20.50
60.00	6.00	0.220	21.60
65.00	11.00	0.140	22.30
70.00	8.00	0.360	24.10
75.00	8.00	0.100	24.60
80.00	5.00	0.180	25.50
85.00	8.00	0.340	27.20
90.00	4.00	0.400	29.20
95.00	0.00	0.360	31.00
100.00	3.00	0.100	31.50
105.00	0.00	0.240	32.70
110.00	5.00	0.080	33.10
115.00	2.00	0.240	34.30
120.00	1.00	0.060	34.60
125.00	5.00	0.000	34.60
130.00	1.00	0.040	34.80
135.00	0.00	0.280	36.20
140.00	0.00	0.000	36.20
145.00	1.00	0.000	36.20
150.00	1.00	0.000	36.20

Distance from root (cm)	Diameter (cm)	Variation in supply rates (drops/min)
0.00	3.42	
2.00	3.29	14
4.00	3.19	14
6.00	3.17	19
8.00	3.38	17
10.00	3.40	19
12.00	3.12	24
14.00	2.42	24
16.00	2.30	24
18.00	2.15	19
20.00	1.92	24
22.00	1.79	21
24.00	1.53	19
26.00	1.28	27
28.00	1.20	27
30.00	1.03	20
32.00	0.80	28
34.00	0.44	20
36.00	0.45	

Mean diameter = 2.13 cm

Mass of icicle = 130.02 g

Case #8

Ta = -14.6 C
R = 70 %
Pa = 943 mb

V = 0.6 m/s
Wo = 30.5 mg/s
Sw = 3.3 %

Time (min)	Driprate (1/min)	dL/dt (cm/min)	Length (cm)
5.00	15.00	0.080	0.40
10.00	22.00	0.060	0.70
15.00	26.00	0.120	1.30
20.00	21.00	0.280	2.70
25.00	30.00	0.640	5.90
30.00	31.00	0.220	7.00
35.00	20.00	0.480	9.40
40.00	31.00	0.480	11.80
45.00	22.00	0.500	14.30
50.00	24.00	0.220	15.40
55.00	20.00	0.200	16.40
60.00	20.00	0.220	17.50
65.00	11.00	0.360	19.30
70.00	15.00	0.260	20.60
75.00	17.00	0.260	21.90
80.00	13.00	0.300	23.40
85.00	8.00	0.340	25.10
90.00	7.00	0.240	26.30
95.00	7.00	0.120	26.90
100.00	13.00	0.220	28.00
105.00	11.00	0.320	29.60
110.00	8.00	0.320	31.20
115.00	1.00	0.500	33.70
120.00	0.00	0.200	34.70
125.00	1.00	0.280	36.10
130.00	1.00	0.220	37.20
135.00	4.00	0.040	37.40
140.00	1.00	0.080	37.80
145.00	2.00	0.140	38.50
150.00	1.00	0.040	38.70
155.00	4.00	0.000	38.70
160.00	2.00	0.060	39.00
165.00	1.00	0.000	39.00
170.00	1.00	0.002	39.10
175.00	1.00	0.040	39.30
180.00	2.00	0.000	39.30
185.00	1.00	0.000	39.30
190.00	1.00	0.000	39.30
195.00	0.00	0.000	39.30
200.00	1.00	0.000	39.30

Distance from root (cm)	Diameter (cm)	Variation in supply rates (drops/min)
0.00	3.99	21
2.00	4.03	25
4.00	4.19	30
6.00	3.71	31
8.00	4.17	33
10.00	3.91	26
12.00	4.24	18
14.00	3.97	35
16.00	3.39	30
18.00	2.97	27
20.00	2.87	29
22.00	2.75	30
24.00	2.00	27
26.00	1.71	29
28.00	1.83	43
30.00	1.54	25
32.00	1.31	26
34.00	1.30	30
36.00	0.90	21
38.00	0.62	32
		28
		30

Mean diameter = 2.79 cm

Mass of icicle = 227.99 g

Case #9

Ta = -10.3 C
R = 68 %
Pa = 946 mb

V = 0.6 m/s
Wo = 19.8 mg/s
Sw = 3.3 %

Time (min)	Driprate (1/min)	dL/dt (cm/min)	Length (cm)
5.00	24.00	0.200	1.00
10.00	20.00	0.120	1.60
15.00	20.00	0.180	2.50
20.00	15.00	0.300	4.00
25.00	9.00	0.320	5.60
30.00	20.00	0.300	7.10
35.00	15.00	0.380	9.00
40.00	11.00	0.220	10.10
45.00	9.00	0.080	10.50
50.00	11.00	0.160	11.30
55.00	24.00	0.160	12.10
60.00	4.00	0.400	14.10
65.00	11.00	0.200	15.10
70.00	11.00	0.140	15.80
75.00	7.00	0.360	17.60
80.00	12.00	0.120	18.20
85.00	11.00	0.200	19.20
90.00	7.00	0.140	19.90
95.00	17.00	0.240	21.10
100.00	11.00	0.280	22.50
105.00	16.00	0.220	23.60
110.00	5.00	0.220	24.70
115.00	6.00	0.220	25.80
120.00	5.00	0.400	27.80
125.00	6.00	0.120	28.40
130.00	6.00	0.200	29.40
135.00	3.00	0.120	30.00
140.00	6.00	0.300	31.50
145.00	6.00	0.200	32.50
150.00	4.00	0.240	33.70
155.00	1.00	0.120	34.20
160.00	2.00	0.380	36.10
165.00	3.00	0.140	36.80
170.00	2.00	0.240	38.00
175.00	1.00	0.120	38.60
180.00	2.00	0.080	39.00
185.00	1.00	0.000	39.00
190.00	2.00	0.160	39.80
195.00	2.00	0.000	39.80
200.00	2.00	0.000	39.80

Distance from root (cm)	Diameter (cm)	Variation in supply rates (drops/min)
0.00	3.40	25 19
2.00	2.82	20 19
4.00	2.85	22 22
6.00	2.97	13 16
8.00	2.85	18 17
10.00	2.87	11 18
12.00	2.54	11 16
14.00	2.42	28
16.00	2.24	9
18.00	2.24	16
20.00	1.97	15
22.00	1.94	23
24.00	1.78	15
26.00	1.64	30
28.00	1.54	20
30.00	1.32	25
32.00	1.23	21
34.00	0.98	21
36.00	0.82	15
38.00	0.59	16
40.00	0.49	16
		20
		20
		16
		20
		19

Mean diameter = 1.98 cm

Mass of icicle = 125.16 g

Case #10

Ta = -10.4 C
R = 75 %
Pa = 946 mb

V = 0.6 m/s
wo = 28.6 mg/s
Sw = 3.3 %

Time (min)	Driprate (1/min)	dL/dt (cm/min)	Length (cm)
10.00	24.00	0.200	2.50
20.00	20.00	0.250	4.50
30.00	28.00	0.210	6.60
40.00	22.00	0.240	9.00
50.00	18.00	0.080	9.80
60.00	14.00	0.150	11.30
70.00	17.00	0.140	12.70
80.00	18.00	0.230	15.00
90.00	20.00	0.190	16.90
100.00	14.00	0.190	18.80
110.00	9.00	0.160	20.40
120.00	28.00	0.180	22.20
130.00	9.00	0.220	24.40
140.00	0.00	0.180	26.20
150.00	17.00	0.210	28.30
160.00	5.00	0.300	31.30
170.00	5.00	0.310	34.40
180.00	4.00	0.170	36.10
190.00	3.00	0.140	37.50
200.00	2.00	0.040	37.90
210.00	3.00	0.040	38.30
220.00	9.00	0.090	39.20
230.00	1.00	0.120	40.40
240.00	1.00	0.060	41.00
250.00	0.00	0.050	41.50

Distance from root (cm)	Diameter (cm)	Variation in supply rates (drops/min)
0.00	4.99	15
2.00	4.24	26
4.00	4.24	40
6.00	3.93	29
8.00	3.86	26
10.00	3.66	22
12.00	3.70	23
14.00	3.48	30
16.00	3.18	27
18.00	3.13	28
20.00	2.61	23
22.00	2.30	23
24.00	2.14	38
26.00	1.99	27
28.00	1.90	23
30.00	1.65	35
32.00	1.58	31
34.00	1.34	31
36.00	1.11	27
38.00	0.86	22
40.00	0.44	27
		23
		25
		23
		31
		28

Mean diameter = 2.68 cm

Mass of icicle = 208.62 g

Case #11

Ta = -7.4 C
φ = 71 %
Pa = 940 mb

V = 0.6 m/s
Wo = 16.2 mg/s
Sw = 3.3 %

Time (min)	Driprate (1/min)	dL/dt (cm/min)	Length (cm)
10.00	12.00	0.210	2.10
20.00	12.00	0.230	4.40
30.00	15.00	0.170	6.10
40.00	9.00	0.160	7.70
50.00	17.00	0.140	9.10
60.00	14.00	0.110	10.20
70.00	9.00	0.190	12.10
80.00	11.00	0.140	13.50
90.00	14.00	0.090	14.40
100.00	13.00	0.150	15.90
110.00	7.00	0.190	17.80
120.00	11.00	0.160	19.40
130.00	11.00	0.050	19.90
140.00	7.00	0.140	21.30
150.00	6.00	0.160	22.90
160.00	4.00	0.110	24.00
170.00	8.00	0.100	25.00
180.00	10.00	0.120	26.20
190.00	8.00	0.170	27.90
200.00	5.00	0.140	29.30
210.00	3.00	0.140	30.70
220.00	4.00	0.070	31.40
230.00	4.00	0.050	31.90
240.00	6.00	0.050	32.40
250.00	4.00	0.060	33.00
260.00	3.00	0.080	33.80
270.00	1.00	0.030	34.10
280.00	1.00	0.000	34.10

Distance from root (cm)	Diameter (cm)
0.00	4.40
2.00	3.32
4.00	3.17
6.00	3.02
8.00	3.15
10.00	3.08
12.00	2.69
14.00	2.76
16.00	2.23
18.00	2.08
20.00	1.94
22.00	1.84
24.00	1.57
26.00	1.36
28.00	1.21
30.00	0.97
32.00	0.69

Mean diameter = 2.31 cm

Mass of icicle = 127.68 g

Variation in supply rates (drops/min)	
13	17
12	14
13	16
17	16
19	11
13	15
16	
16	
17	
15	
14	
11	
16	
15	
13	
20	
14	
19	
22	
16	
16	
15	

Case #12

Ta = -7 C V = 0.6 m/s
R = 66 % Wo = 20.9 mg/s
Pa = 927 mb Sw = 3.3 %

Time (min)	Driprate (...l/min)	dL/dt (cm/min)	Length (cm)
10.00	19.00	0.100	1.00
20.00	29.00	0.110	2.10
30.00	20.00	0.080	2.90
40.00	14.00	0.030	3.20
50.00	15.00	0.050	3.70
60.00	20.00	0.210	5.80
70.00	22.00	0.180	7.60
80.00	24.00	0.180	9.40
90.00	16.00	0.150	10.90
100.00	16.00	0.090	11.80
110.00	12.00	0.120	13.00
120.00	21.00	0.070	13.70
130.00	18.00	0.180	15.50
140.00	17.00	0.210	17.60
150.00	17.00	0.130	18.90
160.00	11.00	0.100	19.90
170.00	17.00	0.120	21.10
180.00	17.00	0.140	22.50
190.00	10.00	0.120	23.70
200.00	12.00	0.110	24.80
210.00	10.00	0.120	26.00
220.00	6.00	0.200	28.00
230.00	5.00	0.160	29.60
240.00	8.00	0.100	30.60
250.00	6.00	0.090	31.50
260.00	6.00	0.070	32.20
270.00	16.00	0.000	32.20
280.00	4.00	0.140	33.60
290.00	6.00	0.090	34.50
300.00	4.00	0.110	35.60
310.00	4.00	0.080	36.40
320.00	4.00	0.060	37.00
330.00	3.00	0.060	37.60
340.00	7.00	0.000	37.60
350.00	3.00	0.020	37.80

Distance from root (cm)	Diameter (cm)
0.00	4.26
2.00	4.07
4.00	3.84
6.00	3.38
8.00	3.48
10.00	3.19
12.00	3.24
14.00	3.39
16.00	2.98
18.00	2.81
20.00	2.71
22.00	2.46
24.00	2.17
26.00	1.76
28.00	1.71
30.00	1.59
32.00	1.14
34.00	0.90
36.00	0.57
38.00	0.47

Mean diameter = 2.52 cm

Mass of icicle = 181.30 g

Variation in supply rates (drops/min):

21	16	23
29	18	17
25	17	23
14	20	10
16	16	20
22	18	19
21	22	17
16	18	19
18	22	19
17	21	16
18	29	18
23	25	17
20	14	20
18	16	16
22	22	18
19	21	22
23	16	18
17	18	22
23	17	
10	18	
20	23	
19	20	
17	18	
19	22	
19	19	

Case #13

Ta = -14.3 C
R = 64 %
Pa = 930 mb

V = 0.6 m/s
Wo = 20.0 mg/s
Sw = 3.3 %

Time (min)	Driprate (1/min)	dL/dt (cm/min)	Length (cm)
15.00	21.00	0.330	5.00
30.00	15.00	0.400	11.00
45.00	13.00	0.380	16.70
60.00	9.00	0.370	22.20
75.00	3.00	0.150	24.50
90.00	5.00	0.330	29.40
105.00	0.00	0.240	33.00
120.00	4.00	0.093	34.40
135.00	3.00	0.070	35.40
150.00	3.00	0.070	36.40
165.00	2.00	0.040	37.00
180.00	4.00	0.000	37.00
195.00	1.00	0.020	37.30
210.00	2.00	0.000	37.30
225.00	1.00	0.000	37.30
240.00	1.00	0.000	37.30
270.00	1.00	0.000	37.30

Distance from root (cm)	Diameter (cm)	Variation in supply rates (drops/min)
0.00	4.85	23
2.00	4.60	22
4.00	5.00	20
6.00	4.79	21
8.00	4.15	15
10.00	3.66	19
12.00	3.96	12
14.00	3.60	22
16.00	3.19	21
18.00	2.72	19
20.00	2.83	19
22.00	2.63	24
24.00	2.35	20
26.00	2.30	20
28.00	2.00	20
30.00	1.67	21
32.00	1.23	
34.00	0.89	
36.00	0.54	

Mean diameter = 3.01 cm

Mass of icicle = 229.84 g

Appendix E Calibration of the salinometer

Brine solution (#)	Salinity (o/oo)	Salinometer reading (o/oo)
1	10	70
2	20	79
3	30	87
4	40	95
5	50	104
6	60	114
7	70	122
8	80	131
9	90	139
10	100	146
11	120	165
12	140	182
13	160	200
14	180	216
15	220	248